PERFORMANCE OF SEATS WITH ACTIVE HEAD RESTRAINTS IN REAR IMPACTS

Liming Voo
Bethany McGee
Andrew Merkle
Michael Kleinberger
Johns Hopkins University Applied Physics Laboratory
United States of America
Shashi Kuppa
National Highway Traffic Safety Administration
United States of America
Paper Number 07-0041

ABSTRACT

Seats with active head restraints may perform better dynamically than their static geometric characteristics would indicate. Farmer *et al.* found that active head restraints which moved higher and closer to the occupant's head during rear-end collisions reduced injury claim rates by 14-26 percent. The National Highway Traffic Safety Administration (NHTSA) recently upgraded their FMVSS No. 202 standard on head restraints in December 2004 to help reduce whiplash injury risk in rear impact collisions. This upgraded standard provides an optional dynamic test to encourage continued development of innovative technologies to mitigate whiplash injuries, including those that incorporate dynamic occupant-seat interactions. This study evaluates four original equipment manufacturer (OEM) seats with active head restraints in the FMVSS 202a dynamic test environment. The rear impact tests were conducted using a deceleration sled system with an instrumented 50^{th} percentile Hybrid III male dummy. Seat performance was evaluated based on the FMVSS 202a neck injury criterion in addition to other biomechanical measures, and compared to the respective ratings by the Insurance Institute for Highway Safety (IIHS). Three of the four OEM seats tested were easily within the allowable FMVSS 202a optional dynamic test limits. The seat that was outside one of the allowable limits also received only an "acceptable" rating by IIHS while the other three seats were rated as "good." Results also suggest that the stiffness properties of the seat back and recliner influence the dynamic performance of the head restraint.

INTRODUCTION

Serious injuries and fatalities in low speed rear impacts are relatively few. However, the societal cost of whiplash injuries as a result of these collisions is quite high: the National Highway Traffic Safety Administration (NHTSA) estimates that the annual cost of these whiplash injuries is approximately $8.0 billion (NHTSA, 2004). Numerous scientific studies reported connection between the neck injury risk and seat design parameters during a rear impact (Olsson 1990, Svensson 1993, Eichberger 1996, Tencer 2002 and Kleinberger 2003). When sufficient height was achieved, the head restraint backset had the largest influence on the neck injury risk. In addition to its static position relative to the occupant head, the structural rigidity of the head restraint and its attachment to the seat back can have a significant impact on the neck injury risk in a rear impact (Voo 2004). Farmer et al. (2003) and IIHS (2005) examined automobile insurance claims and personal injury protection claims for passenger cars struck in the rear to determine the effects of changes in head restraint geometry and some new head restraint designs. Results from these studies indicated that cars with improved head restraint geometry reduced injury claims by 11-22 percent, while active head restraints that are designed to move higher and closer to occupants' heads during rear-end crashes were estimated to reduce claim rates by 14-26 percent.

In response to new evidence from epidemiological data and scientific research, NHTSA published the final rule that upgrades the FMVSS 202 head restraint standard (49 CFR Part 571) in 2004, and is participating in a Global Technical Regulation on head restraints. The new standard (FMVSS No. 202a) provides requirements that would make head restraints higher and closer to the head so as to engage the head early in the event of a rear impact. The rule also has provisions for a dynamic option to evaluate vehicle seats with a Hybrid III dummy in rear impact sled test that is intended in particular for active head restraints that may not meet the static head restraint position requirements such as height and backset. However, the dynamic option is not limited to active head restraints. By active head restraints we mean head restraints that move or

deploy with respect to the seat back. These active head restraints might perform better in rear impact collisions than their static geometric measures may indicate. The neck injury criterion in this dynamic option uses the limit value of 12 degrees in the posterior head rotation relative to the torso of the dummy within the first 200 milliseconds of the rear impact event.

The Insurance Institute for Highway Safety (IIHS) has been publishing ratings of head restraint geometry since 1995 (IIHS, 2001). IIHS along with the International Insurance Whiplash Prevention Group (IIWPG) developed a dynamic test procedure (IIHS, 2006) to evaluate head restraints and have been rating head restraint systems since 2004 using a combination of their static measurement procedure and the newly developed dynamic test procedure. In this combined procedure, seat systems that obtain a "good" or "acceptable" rating according to the IIHS static head restraint measurement procedure, are put through a dynamic rear impact sled test with the BioRID II dummy, simulating a rear crash with a velocity change of 16 km/h. The dynamic evaluation is based on the time to head restraint contact, maximum forward T1 acceleration, and a vector sum of maximum upper neck tension and upper neck rearward shear force. This evaluation results in a dynamic rating of the seat ranging from "good" to "poor". As a consequence of this evaluation procedure by IIHS, head restraints that obtained a good or acceptable rating from the static head restraint measurements may obtain an overall poor rating from the dynamic test procedure. In addition, some active head restraint systems that obtain a marginal or poor static measurement rating are not even tested dynamically although their dynamic performance may actually be good.

This study evaluates the performance of a select group of automotive seats with active head restraints from original equipment manufacturers (OEM) under the environment of the optional FMVSS 202a dynamic test.

MATERIALS AND METHODS

Driver seats from four different passenger cars were evaluated: Saab 9-3, Honda Civic, Nissan Altima and Subaru Outback. The OEM driver seats were 2006 model year production stock, ordered directly from either the vehicle manufacturers or their suppliers, and included the seatbelt restraints. The seats were not modified in any way. Custom-designed rigid base brackets for each seat were used to anchor the seats to the impact sled such that the height and relative position of the seat to the B-pillar and floor pan would be similar to its position in the car. For each seat model, the corresponding OEM seatbelt was used as the restraining device during each test.

The seats were positioned nominally in accordance with sections S5.1 and S5.3 of FMVSS 202a. However, some aspects of the IIHS procedure (IIHS 2001) were implemented regarding the set up of the SAE J826 manikin and the seat back position. The procedure is briefly described below. Once fixed to the sled with its back toward the impact direction, the seat was positioned at the mid-track setting between the most forward and most rearward positions. Then the seat pan angle was set such that its front edge was at the lowest position relative to its rear edge. The vertical position of the seat was placed at the lowest position if a dedicated height adjustment mechanism existed independent of the seat pan incline adjustment. Once the seat pan angle and height were fixed, the seat back was reclined to a position such that the torso line of SAE J826 manikin (H-point machine) was at 25 degrees from the vertical, following a procedure similar to that used by IIHS (IIHS 2001). The head restraint height was measured at the highest and lowest adjustment settings using the head room probe of the H-point machine, and was then positioned midway between those two points or the next lower lockable setting. The head restraint backset and head-to-head-restraint height were measured using the Head Restraint Measurement Device (HRMD) in combination with the SAE J826 manikin with a procedure adopted by IIHS (IIHS 2001). The H-point of the seat as positioned was then recorded and marked to be used later in positioning the dummy.

A 50^{th} percentile male Hybrid III dummy was used as the seat occupant for this study. The dummy was instrumented with triaxial accelerometers at the head CG and thorax CG, and a single accelerometer at T1. Angular rate sensors (IES 3100 series rate gyro) were mounted in the head and upper spine. The IES triaxial angular rate gyro was designed to meet the SAE J211/1 (rev. March 1995) CFC 600 frequency response requirement specified in FMVSS 202a and is capable of recording angular rates up to 4800 degree/second. The sensor weighs 22 grams and fits at the center of gravity of the Hybrid III dummy head on a custom mount. The Hybrid III head with the IES sensors was balanced so as to meet the mass specifications in Part 572. The upper neck and lower neck were instrumented with six-axis load cells, and the lumbar spine with a three-axis load cell.

The dummy was positioned in the test seat following the procedures outlined in S5.3.7 of FMVSS 202a (Figure 1) with the exception of the right foot and hands. The dummy was seated symmetric with respect to the seat centerline. Adjustments were made to align the hip joint with the seat H-point while keeping the head instrumentation platform level (± 0.5 degree). Both feet were positioned flat on the floor and the lower arms were positioned horizontally and parallel to each other with palms of the hands facing inward. The dummy was restrained using the OEM 3-point seatbelt harness for the corresponding seat during all tests. The position of the dummy head relative to the head restraint was measured in two ways: (1) the vertical distance from the top of the head to the top of the head restraint; and (2) the shortest horizontal distance between the head and the head restraint.

Video images were captured for these tests using two Phantom high-speed digital video cameras operating at 1000 frames per second. One camera was mounted on-board to provide a right lateral view of the dummy kinematics while the second camera was mounted overhead to provide a top view. Video collection was synchronized with the data acquisition system using a sled impact trigger with an optical flash that was visible within the field of view of both cameras to signal the time of initial sled impact.

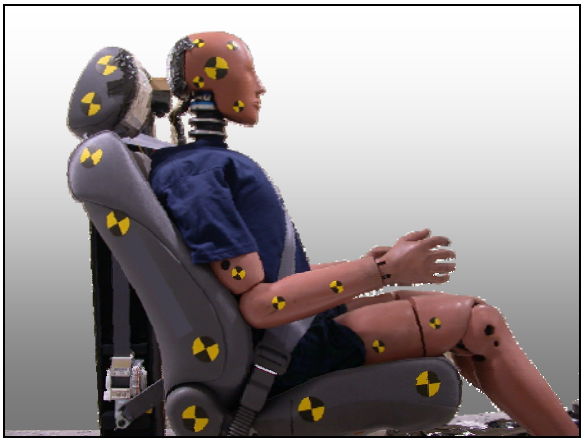

Figure 1. Pre-impact setup of the dummy and seat for the FMVSS 202a rear impact sled tests.

The sled was accelerated to an impact velocity of approximately 17.3 km/h. Upon impact, the sled experienced a deceleration-time curve that conformed to the corridor described in the FMVSS 202a standard when filtered to channel class 60, as specified in the SAE Recommended Practice J211/1 (rev. Mar 95) (Figure 2). Upon sled impact, the sensor and video data were collected synchronously, including a head-to-head restraint contact sensor and the sled linear accelerometer. All data were collected and processed in accordance with the procedures specified in SAE Recommended Practice J211/1 (rev. March 1995). Each seat was tested under FMVSS 202a dynamic conditions only once.

Angular displacements of the dummy head and torso were calculated through numerical integration of the angular velocity data obtained from the rate gyro sensors in the head and upper spine. The relative head-torso relative angular displacement values were calculated at each time step by subtracting the torso angular displacement value from the corresponding head angular displacement value. The maximum head-torso relative rotation value in the posterior direction was used to evaluate the relative whiplash injury risk associated with the different seats tested according to the FMVSS 202a dynamic option. Data from the load cells in the upper and lower neck were used to calculate the Nkm index (Schmitt, 2001). The positive shear (head moves posterior relative to the neck) was used in calculating Nkm and in comparing the upper neck and lower neck shear forces between tests. The moment measured at the lower neck load cell was corrected to represent the lower neck moment.

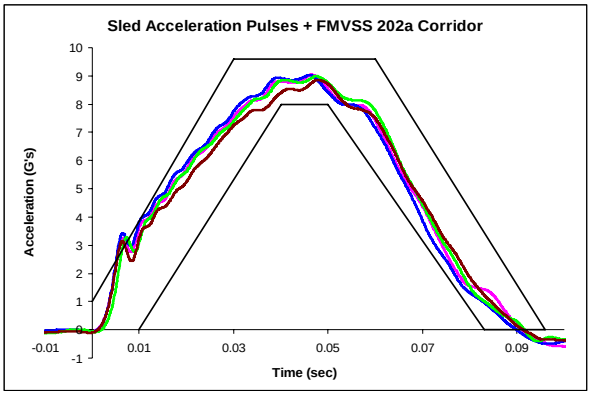

Figure 2. Sled impact deceleration pulses of rear impact testing of the four seats along with the FMVSS 202a corridor.

RESULTS

The head restraint height (vertical distance from the top of the head to the top of the head restraint) and backset (horizontal distance from the head restraint to the back of the head), as measured using the HRMD, ranged 15-45 mm and 25-70 mm respectively, as the OEM head restraint was in its mid-position (Table 1). The similar measurements representing the horizontal and vertical position of the head restraint relative to the Hybrid III dummy head are also presented in

Table 1 for comparison. In general, the head of the seated dummy was lower, but further away from the head restraint than the HRMD (Table 1). Note that among the four seats tested only the Nissan Altima had an independent seat height adjustment where the seat was set at the lowest position while the front edge of the seat pan was at the lowest position relative to its rear edge. For the other seats, the requirement of having the seat pan front edge to be at the lowest position relative to its rear edge forced the overall seat to be at the highest position.

Table 1: Head Restraint Geometric Measurements (Mid-Height Position)

	2006 OEM Seat	Honda	Nissan	Saab	Subaru
HRMD	Backset (mm)*	40	25	70	48
HRMD	Head to HR Height (mm)*	45	39	29	15
Dummy	Horizontal Head to HR Distance(mm)	59	48	78	76
Dummy	Vertical Head to HR Distance(mm)	45	32	19	12

* IIHS procedure (IIHS 2001) was used to set up the SAE J826 manikin and the seat back position

Table 2 presents the results of the dummy responses in the FMVSSS 202a optional dynamic test environment. The time that the dummy head made initial contact with the head restraint ranged from 56 to 74 milliseconds between the four seat tests, somewhat consistent with the horizontal head-to-head restraint distance values of the four seats (Table 1). The maximum posterior head-torso relative rotation of the Hybrid III dummy was less than 8 degrees for the Saab 9-3, Honda Civic, and the Subaru Outback, but exceeded the 12 degrees specified limit in FMVSS No. 202a for the Nissan Altima.

The performance of the seats, as measured by the peak posterior head-torso relative rotation (Figure 3), did not correlate with the initial relative position between the dummy head and head restraint. The greatest rotation occurred in the seat having the smallest horizontal dummy head to head restraint distance as well as the smallest backset and one of the seats with the smallest head-torso relative rotations occurred in a seat having the largest of these static dimensions (Table 1 and Figure 3). The head restraint height did not appear to be a strong factor in seat performance as the head restraint at mid-position for all four seats were significantly higher than the head CG and were in the "Good" range for head restraint height as per the rating system by IIHS (IIHS 2001).

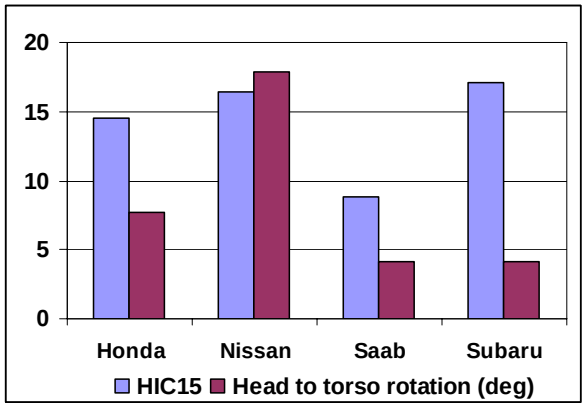

Figure 3. FMVSS 202a injury measures (Head-torso relative rotation in degrees and HIC15) for the four OEM seats in rear impact tests.

Table 2: Dynamic Test Results

2006 OEM Seat	Honda	Nissan	Saab	Subaru
Head Contact Time (ms)	69	56	69	74
Peak Head-Torso Rotation (deg)	7.7	17.9	4.1	4.1
Upper Neck Tension (N)	81	97	101	36
Upper Neck Shear (N)	110	160	87	98
Lower Neck Moment (Nm)	9	26	2	10
HIC 15msec	14.5	16.4	8.8	17.1
Nkm	0.07	0.24	0.13	0.06
Within FMVSS 202a Limits	Yes	No	Yes	Yes

The HIC15 injury measure for all seats was less than 20 (Table 2, Figure 3), which is significantly lower than the specified limit of 500 in FMVSS No. 202a. The relative performance of the seats measured by the head-torso relative posterior rotation was consistent with several other biomechanical measures such as the upper neck shear force (Figure 4), lower neck extension moment (Figure 5), and upper neck

Nkm index (Figure 6). Those measures all showed that the Altima seat, which had the smallest horizontal dummy head-to-head restraint distance and backset at mid-height position, sustained the highest relative motion and neck loads. The Saab had the lowest relative motion and neck loads, except for Nkm, and had the largest horizontal dummy head-to-head restraint distance and backset.

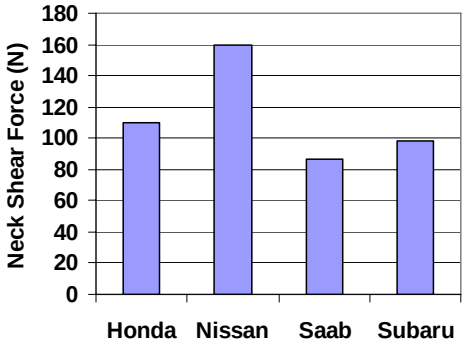

Figure 4. Upper neck positive shear forces for the four OEM seats in the FMVSS 202a dynamic test.

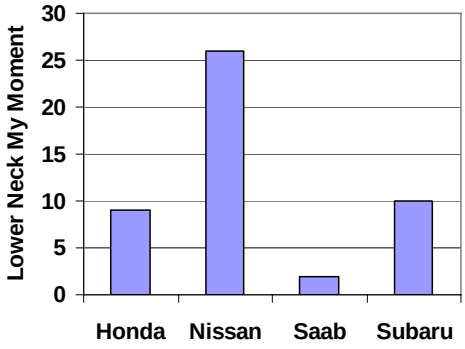

Figure 5. Lower neck extension moments for the four OEM seats in FMVSS 202a dynamic test.

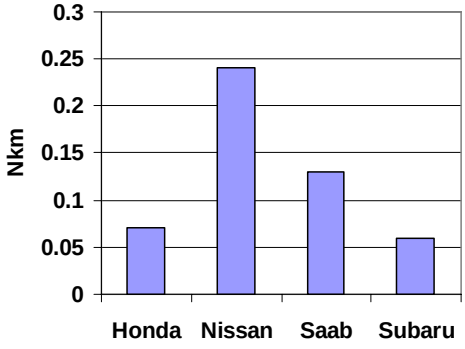

Figure 6. Shear-bending load index (Nkm) for the four OEM seats in FMVSS 202a dynamic test.

The time histories of the head, torso and head-torso relative rotation for the four OEM seats in the FMVSSS 202a dynamic tests are presented in Figures 7-10. The maximum posterior head-torso relative rotation occurred before the maximum head or torso rearward rotation in all the seats. The maximum lower neck extension moment occurred approximately at the time of maximum head-torso rotation in all the seats except for the Saab seat where it had occurred somewhat earlier (Figure 9). The maximum shear force occurred after the maximum lower neck extension moment with all the seats.

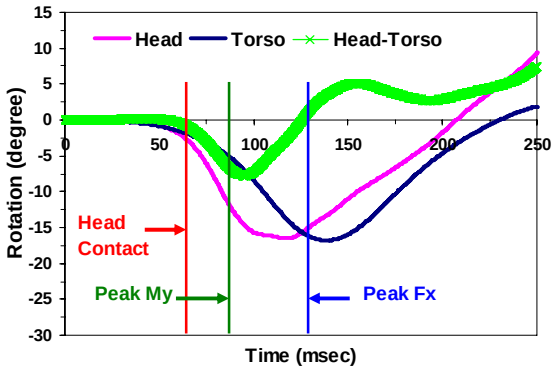

Figure 7. Time histories of the head, torso, and head-torso relative rotation in the Honda Civic seat in FMVSS 202a dynamic test.

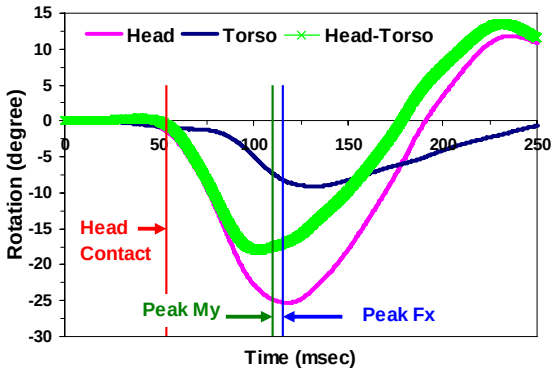

Figure 8. Time histories of the head, torso, and head-torso relative rotation in the Nissan Altima seat in FMVSS 202a dynamic test.

A detailed analysis of the dummy kinematics provided an understanding for the reasons why the Nissan Altima seat did not achieve the FMVSS 202a dynamic test requirements while the other three seats easily met the requirements. At the time of initial head contact with the head restraint, the head-torso rotation in the Altima seat was 0.9 degree (Figure 8) which was similar to that of the other three seats that ranged between 0.5 to 1.7 degrees (Figures 7, 9 and

10). However, after contact with the head restraint, the head continued to rotate up to a peak of 25 degrees in the Nissan Altima seat while the total torso rotation was only 9.1 degrees (Figure 8). The low torso rotation (lowest among all the seats tested) with respect to the head rotation (highest among all the four seats) resulted in high head-torso relative rotation with a peak of 17.9 degrees (Figure 8). On the other hand, the head restraints and the seat backs of the other three seats allowed the torso to undergo a similar total rotation as the head (Figures 7, 9, and 10). The seat-back stiffness, recliner stiffness, and the head restraint stiffness may have contributed to the different performances of the OEM seats.

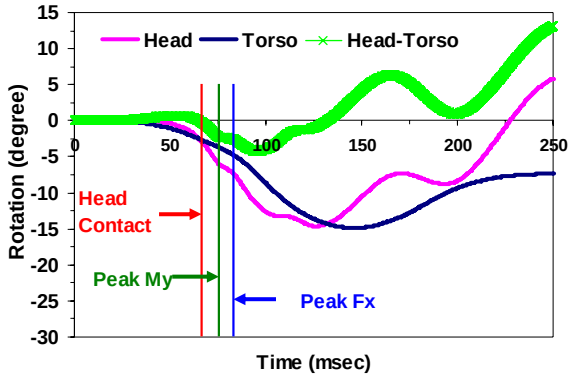

Figure 9. Time histories of the head, torso, and head-torso relative rotation in the Saab 9-3 seat in FMVSS 202a dynamic test.

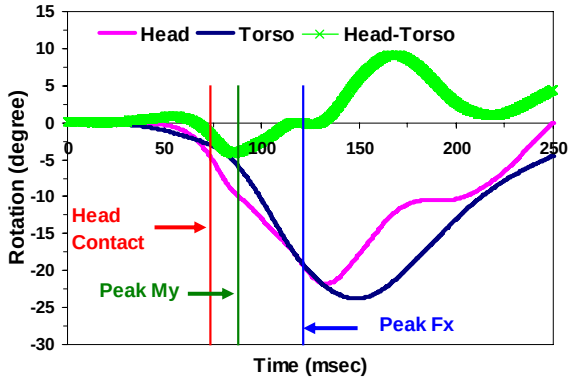

Figure 10. Time histories of the head, torso, and head-torso relative rotation in the Subaru Outback seat in FMVSS 202a dynamic test.

DISCUSSION

IIHS evaluated the 2006 Honda Civic, Nissan Altima, Saab 9-3, and the Subaru Outback using both their head restraint static measurement procedure as well as their dynamic test procedure (Table 3). The Honda Civic, Saab 9-3 and the Subaru Outback received "good" geometric and dynamic ratings, resulting in an overall "good" rating. The Nissan Altima received an "acceptable" geometric and dynamic rating, resulting in an overall "acceptable" rating. Note that the head restraint geometric rating by IIHS is based on height and backset measured in the lowest position or in the most favorably adjusted and locked position of the head restraint. The final static geometric rating is the better of the two, except that if the rating at an adjusted position is used, it is downgraded one category. The head restraint geometric measurements in this study were obtained with the head restraint at a locked position which is approximately mid-point of the highest and lowest position, since that is the position of the head restraint for the dynamic test.

Table 3: IIHS Seat Ratings and Dynamic Test Data using the BioRID Dummy

2006 OEM Seat	Honda	Nissan	Saab	Subaru
Geometric Rating	G	A	G	G
Peak T1 Accel.	13.7	9.7	16.2	11.2
Head Contact Time (ms)	62	64	64	67
Peak Neck Shear (N)	52	221	11	37
Peak Neck Tension (N)	677	660	287	308
Dynamic Rating	G	A	G	G
Overall Rating	G	A	G	G

The FMVSS 202a requirement of the 55 mm limit on the head restraint backset is more stringent than the IIHS backset limit of 75 mm for a "good" rating. This suggests that the seats that meet the FMVSS 202a static measurement requirement would likely receive a "good" geometric rating from IIHS unless the height dimension was insufficient. Comparison of the performance of the four OEM seats tested in the FMVSS 202a optional dynamic test procedure and the IIHS dynamic test procedure suggests that seats with active head restraints that are within the FMVSS No. 202a dynamic test limits are likely to obtain a "good" dynamic rating by IIHS. However, according

to the IIHS procedure, if the seats with active head restraints do not obtain a "good" or "acceptable" geometric rating, they are not tested dynamically.

This study demonstrated that initial head restraint position relative to the head may not be a reliable indicator for the dynamic performance of seats with active head restraints. Real-world data and experimental studies have shown that a head restraint positioned closer to the head would provide more effective whiplash mitigation. Though the head restraints of all four OEM seats moved forward and closer to the head in a similar manner during the rear impact tests, their performance after the initial head contact differed (Figures 7-10). The Nissan Altima seat did not meet the optional dynamic test requirement of 12 degrees head-torso rotation, as a result of the large differential between the head and torso rotation after the initial head contact. This is evidenced in Figure 8, where the torso rotation is significantly smaller than that of the head.

Kinematic evaluation of the video data indicated that the seat back of the Altima was too stiff to allow sufficient torso movement into the seat back such that the torso and the head move together to minimize their relative motion. In contrast, the seat back stiffness, recliner stiffness, and the head restraint stiffness of the Honda Civic, Saab 9-3, and the Subaru Outback seats appeared to be optimized so that the head and torso rotated together and thereby minimized the relative rotation between the head and the torso at this test speed (Figures 7, 9, and 10). In addition, the head restraint of the Altima seat appeared to be too compliant, thus allowing too much posterior head rotation after the head made the initial contact with the head restraint. Previous research has found that a less rigid head restraint can increase the neck injury risk in rear impact (Voo 2004).

There are some seat positioning differences between the FMVSS 202a procedure and that of IIHS (NHTSA 2004, IIHS 2001):

- The FMVSS 202a seat positioning procedure, which this study attempted to follow, resulted in the seats of the Honda Civic, Saab 9-3 and Subaru Outback being at their highest position in order to obtain as shallow angle for the seat pan, which results in the highest H-point position relative to the seat back. The IIHS procedure would place those same seats at their lowest position regardless of the resulting seat pan angle (as per section 5.1.5 and 5.1.7 of IIHS 2001). This resulted in those same seat pans being adjusted to the most rearward tilted position (as per section 5.1.5 and 5.1.7 of IIHS 2001). On the other hand, both procedures would set the Nissan Altima seat at its lowest position. The IIHS procedure would then place the seat pan at the mid-range of inclination.
- All the seats in this study were set at the mid-point between the most forward and most rearward positions of the seat track. The IIHS procedure would have set them at the most rearward position (as per section 5.1.6 of IIHS 2001).

Those seat positioning differences might have resulted in differences in head-restraint position measurement and/or dummy position relative to the head restraint. However, we do not believe that those differences have significantly altered the relative dynamic performance of the seats tested in this study and the similar ones by IIHS, even though different dummies (Hybrid III and BioRID) were used.

This study has demonstrated the complexity of designing a seat to mitigate whiplash injuries during a rear impact collision. Seats with active head restraints that have superior static (undeployed) geometry may not necessarily perform relatively well under dynamic conditions, whereas seats that do not have superior static (undeployed) geometry may still perform relatively well dynamically. The Saab 9-3 seat, for example, had an initial backset measurement of 70 mm (using the HRMD) but was still able to limit the head-torso relative rotation to approximately four degrees.

Results from this study demonstrated the importance of considering both the seat back and head restraint designs as a complete seating system to provide optimal protection to the occupants. Head restraint designs that are too compliant or seat-back designs that are too stiff may both result in excessive motion of the head relative to the torso.

ACKNOWLEDGEMENT

The authors would like to thank the National Highway Traffic Safety Administration for their support of this project under Cooperative Agreement No. DTNH22-05-H-01021.

REFERENCES

Eichberger A, Geigl BC, Moser A, Fachbach B, Steffan H, Hell W, Langwieder K. "Comparison of Different Car Seats Regarding Head-Neck Kinematics of Volunteers during Rear End Impact," International IRCOBI Conference on the Biomechanics of Impact, September, 1996, Dublin.

Farmer, C., Wells, J., Lund, A., "Effects of Head Restraint and Seat Redesign on Neck Injury Risk in Rear-End Crashes," Report of Insurance Institute for Highway Safety, October, 2002.

IIHS, (2005) "Insurance Special Report, Head Restraints and Personal Injury Protection Losses, "Highway Loss Data Institute, April 2005.

IIHS (2001) "A Procedure for Evaluating Motor Vehicle Head Restraints," http://www.iihs.org/ratings/protocols/pdf/head_restraint_procedure.pdf

IIHS (2006) RCAR-IIWPG Seat/Head Restraint, Evaluation Protocol, http://www.iihs.org/ratings/protocols/pdf/rcar_iiwpg_protocol.pdf

Kleinberger M, Voo LM, Merkle A, Bevan M, Chang S, "The Role of Seatback and Head Restraint Design Parameters on Rear Impact Occupant Dynamics," Proc 18th International Technical Conference on the Enhanced Safety of Vehicles, Paper #18ESV-000229, Nagoya, Japan, May 19-22, 2003.

NHTSA, "Federal Motor Vehicle Safety Standards; Head Restraints," (FMVSS 202a), Federal Register 49 CFR Part 571, Docket no. NHTSA-2004-19807, December 14, 2004.

Olsson, I., Bunketorp, O., Carlsson G.,Gustafsson, C., Planath, I., Norin, H., Ysander, L. "An In-Depth Study of Neck Injuries in Rear End Collisions", 1990 International Conference on the Biomechanics of Impacts, September, 1990, Lyon, France.

Schmitt, K., Muser, M., Niederer, P., "A New Neck Injury Criterion Candidate for Rear-End Collisions Taking into Account Shear Forces and Bending Moments," 17th ESV Conference, Paper No. 124, 2001.

Svensson, M., Lovsund, P., Haland, Y., Larsson, S. The Influence of Seat-Back and Head-Restraint Properties on the Head-Neck Motion during Rear-Impact, 1993 International Conference on the Biomechanics of Impacts, September, 1993, Eindhoven, Netherlands.

Tencer, A., Mirza, S., Bensel, K. Internal Loads in the Cervical Spine During Motor Vehicle Rear-End Impacts, SPINE, Vol. 27, No. 1 pp 34–42, 2002.

Voo LM, Merkle A, Wright J, and Kleinberger M: "Effect of Head-Restraint Rigidity on Whiplash Injury Risk," Proc Rollover, Side and Rear Impact (SP-1880), Paper #2004-01-0332, 2004_SAE World Congress, Detroit, MI, March 8 - 11, 2004.

CONSIDERATION OF POSSIBLE INDICATORS FOR WHIPLASH INJURY ASSESSMENT AND EXAMINATION OF SEAT DESIGN PARAMETERS USING HUMAN FE MODEL

Yuichi Kitagawa
Tsuyoshi Yasuki
Junji Hasegawa
Toyota Motor Corporation
Japan
Paper Number 07-0093

ABSTRACT

Rear impact simulations were conducted using a validated human body FE model representing an average-sized male occupant. Prototype seat models were also prepared to simulate actual rear impact conditions. The features of occupant responses including head and neck kinematics were investigated considering the interaction between the occupant and the seat (and the head restraint). NIC and joint capsule strain (JCS) were taken as injury indicators. NIC is a widely used indicator in laboratory tests, while the joint capsules have recently been focused on as a potential site of neck pain. Precise modeling of the neck soft tissues enabled the estimation of tissue level injury. The results suggested that NIC corresponds to the difference in motion between the head and the torso, while JCS indicates the difference in their position. Two studies on seat design changes were conducted to examine the contribution from the seat design parameters and to understand the meaning of injury indicators. A parametric study was conducted on thirteen cases where major seat design factors were changed on a single seat configuration, while the second study focused on three different seat configurations with greater differences in dimensions, structure, and mechanical and material properties. The parametric study revealed that the stiffness of the reclining joint greatly affects the resultant NIC values, while JCS was more influenced by the thickness of the upper-end of the seat-back frame. The other finding showed strong correlations between NIC and the head restraint contact timing (HRCT), and JCS and the neck leaning angle (NLA). Introducing the results of the three different seat configurations, the second study suggests that NLA could be used as an injury indicator instead of JCS in dummy tests, while HRCT would not be a good indicator in terms of injury assessment.

INTRODUCTION

It is generally understood that rear-end collisions and associated neck injuries are relatively common in traffic accidents in many countries. In Japan, the number of rear-end collisions has increased during this decade even while the number of fatalities has decreased, based on a report from the Japanese National Police Agency [1]. A typical neck injury form is known as ‘whiplash’ which is not life-threatening but is accompanied by dull pain that is sometimes long lasting. Despite the frequency of rear-end collisions and whiplash injuries, its injury mechanism is not completely understood. Because whiplash injuries are relatively minor and are not necessarily accompanied by obvious clinically detectable tissue damage, it is not easy to identify the relationship between loading to the neck and injury outcome. A common understanding is that relative motion between the head and the torso may load the neck in a way not generated in natural (physiological) motions. Hyperextension of the neck was thought to be a cause of injury based on this aspect. However, it was recognized as not being a significant factor considering the fact that whiplash injuries were still reported even after most vehicles were equipped with head restraints. In order to understand a possible injury mechanism without causing large neck extension, cervical kinematics have been studied with human subjects (Deng et al. [2], Ono et al. [3]). Svensson et al. [4] aimed at a form of neck retraction where the head stays at the same place but the torso is pushed forward, resulting in the cervical spine causing an s-shape. Böstrom et al. [5] proposed an injury indicator called NIC assuming that the pressure gradient in the spinal fluid generated in the s-shape motion could be a cause of injury. Regardless of the controversy related to injury mechanisms, NIC has become a popular indicator because it actually includes relative acceleration and velocity terms between the head and the torso in its formulation. Recent studies focus more on facet joint motions, as the whole of cervical kinematics is related to a series of vertebral motions and motion is generated along or around the facet joints. Based on a hypothesis that the facet joint capsules could be a potential site of neck pain, deformation of the capsule tissue has been analyzed sometimes in a functional spine unit (Winkelstein et al. [6]) and sometimes in a whole body (Sundararajan et al. [7]). Lu et al. [8] studied the neural response of the facet joint capsules under stretch applying artificial stimulation to animal subjects. These results suggested a possible

mechanism of neck pain that supports the hypothesized role of joint capsule strain in whiplash injury. The objective of this study is to analyze cervical kinematics based on finite element analysis simulating rear impacts, taking into account the hypothesis mentioned above, and then to discuss the validity of possible indicators for whiplash injury assessment. The study also examines the influence of seat design parameters on the injury indicators.

METHODS

Human Body Modeling

A finite element human body model named the Total Human Model for Safety (THUMS) is used in this study. The model was developed in collaboration between Toyota Motor Corporation and Toyota Central Research and Development Laboratory. The skeletal system of the human body including joints was precisely modeled to simulate occupant/pedestrian behavior in car crashes. The cortical part of bones was modeled with shell elements while the trabecular part was modeled with solid elements. The geometry (feature lines) of each bony part was based on a commercial human body database ViewPoint^{TM}, but the finite element mesh was newly generated. The ligaments connecting bony parts were also included in the model. The length, thickness and insertion points of the ligaments were carefully defined referring to anatomy textbooks. Soft tissues surrounding the bones such as skin, fat and muscles were represented by a single solid layer. The muscles along the cervical spine were separately modeled with 1D elements to simulate passive muscular responses under stretch by external forces. The brain and internal organs were also included but simplified as solid blocks. Material properties for these parts were defined referring to the literature [9], [10]. The entire model has 60,000 nodes and 80,000 elements with a time-step of approximately one microsecond in an explicit time integration scheme. The body size represents a 50th percentile adult male (AM50) with a height of 175 cm and weighing 77 kg. The model runs on a commercial finite element software LS-DYNATM. Basically, the model (Version 1.61) has been validated against literature data where Post Mortem Human Subject (PMHS) were impacted at different body parts at various loading conditions [11], [12]. In this study, the neck part of the model was revised to further examine cervical kinematics in rear impacts. Figure 1 shows the anatomy of the cervical vertebrae and models. As described above, the ligaments in the joints were modeled so as to connect adjacent vertebrae. The major ligaments are the anterior longitudinal ligament (ALL), the posterior longitudinal ligament (PLL), the ligamentum flavum (LF), the interspinous ligament (ITL), the supraspinous ligaments (SSL), and the intertransverse ligament (ISL). Relative motion between adjacent vertebrae generally occurs around the facet joints located on the right and left sides of the neural arch. The joints are covered with the joint capsules. The capsule tissues were modeled with membrane elements. The joints can move along or around the facet joint surfaces with some resistance and under some restriction from the ligaments.

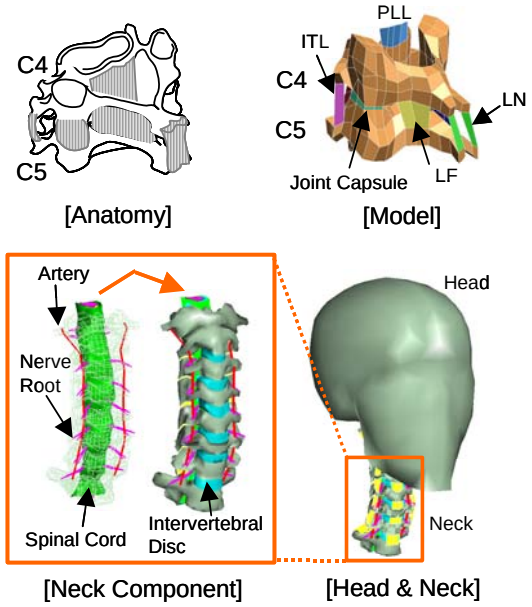

Figure 1. Anatomy of Cervical Vertebrae and Models.

Model Validation

The model has been previously validated against literature data by the authors [13]. The validation was conducted at three levels: component level, subsystem level and whole body level. Only the validation at component level was described in this paper. Siegmund et al. [14] conducted a series of PMHS tests where the unit of C3-C4 was subjected to shear loading with compressive force as shown in Figure 2. Anterior-posterior (A-P) displacement and sagittal rotation of C3 with respect to C4 were measured in the tests. Additionally, the maximum principal strain in the joint capsule was estimated by measuring distance change among markers posted to the tissue. The corresponding part of the C3-C4 unit was extracted from the THUMS neck model, and then equivalent boundary conditions were applied to the model. The A-P displacement of C3 was obtained directly from nodal output while the sagittal rotation was calculated from nodal displacement data of two vertebrae. The maximum principal strain in the joint capsule was directly output from the elements forming that part. Figure 3 compares the measured and calculated data. A-P displacement, sagittal rotation and joint capsule strain were plotted with respect to the applied shear force. Corridors were created connecting upper points and lower points in

the measured data while the calculated results were plotted as curves. The calculated curve for the A-P displacement and that for the sagittal rotation are within the range of the corridors. It was found that the calculated A-P displacement and sagittal rotation were within the test corridors. On the other hand, the calculated joint capsule strain did not have a good match with the test data. The strain rose rapidly at the beginning then showed a flat corridor in the test data while it increased linearly in the model. The cause of the initial rise in the test corridor is not clear while the reason for the latter difference may be an assumption in modeling. In the THUMS neck model, the joint capsule elements simply connect the nodes at the edges of joint surfaces while the actual joint capsules cover a wider area surrounding the joint surfaces. The length of the capsule elements is around 1.2 mm which is around 20% of the actual tissue. This difference may lead overestimating the strain level in the model. Due to the imprecision in modeling the capsule tissue and in predicting absolute strain values, only relative evaluations comparing cases were conducted in this study.

Seat models are necessary to conduct rear impact simulations. Three prototype seats with different configurations (dimensions, structures and materials) were modeled for the study. In each model, the geometrical features, construction of components, and mechanical and material properties of the components were carefully incorporated. Figure 4 shows overall views of the seat models. The models were then validated against test data as assembled seat systems. Considering a typical loading case in rear impacts where the occupant loads on the seat-back, the mechanical responses of the actual prototype seats were examined applying quasi-static loading to the upper end of the seat-back frames. Simulations were conducted on the models to duplicate the loading tests. The moment around the reclining joint and the rotational angle of the seat-back were compared between the test data and the simulation results to confirm the validity of the model. Figure 5 shows an example of validation on Seat A. A linear increasing trend in the calculated data showed a good match with the test data.

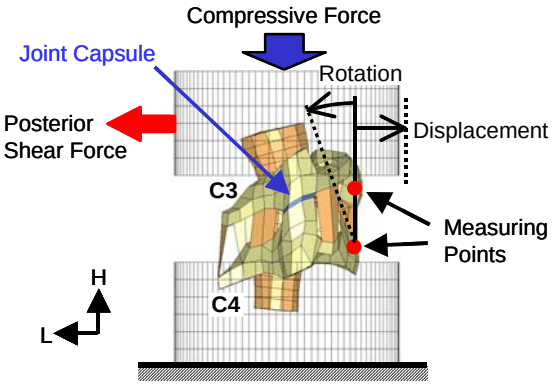

Figure 2. C3-C4 Joint Model for Validation.

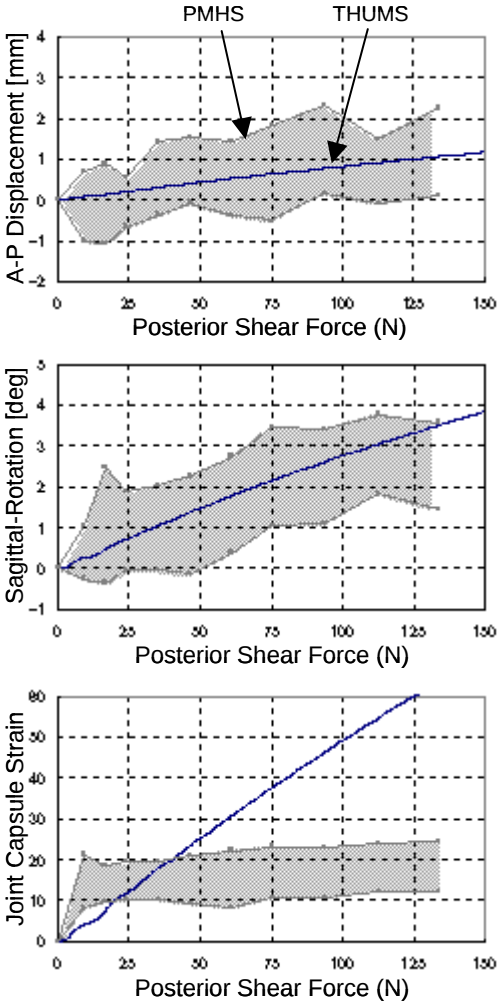

Figure 3. Comparison of A-P Displacement, Sagittal Rotation and Joint Capsule Strain between PMHS and THUMS.

Rear Impact Simulation

A rear impact simulation was conducted using the Seat A model with THUMS in a seated position. The posture of THUMS was adjusted to a standard seating position supposing an AM50 size front-seat occupant. The hip point (including the torso angle) was adjusted first. Then the femur angle was given considering the height difference from the floor-pan. During the adjusting process, deformation of the seat cushion was considered for the initial geometry. The seat was mounted on a rigid plate representing a floor-pan. Contacts were defined between the torso back and the seat-back, the head (occiput) and the head restraint, the buttocks and the seat pan to handle interaction among them. The impact condition was defined so as to simulate an actual rear impact case. Kraft et al. [15] analyzed acceleration pulses of actual rear collisions obtained from vehicles fitted with data recorders, and have

[Seat A] [Seat B] [Seat C]

Figure 4. Prototype Seat Models.

proposed representative pulse curves to be used as acceleration input in sled tests. Research organizations like Folksam, IIWPG and ADAC have adopted these proposed acceleration pulses to help evaluate the performance of production vehicle seats. A triangular pulse with a delta-V of 16 km/h is the most popular impact condition adopted in laboratory tests. A delta-V of 16 represents a rear-end collision where one vehicle strikes another vehicle with the same weight at 32 km/h. According to a study conducted by the Ministry of Land, Infrastructure and Transport of Japan [16], this impact condition is more severe than 60 percent of all rear collisions on the roads in Japan. By elevating the delta-V to 25 km/h, which corresponds to a vehicle to vehicle collision at 50 km/h, approximately 90 percent of all rear collisions are less severe. This study adopted the higher delta-V to understand the cervical kinematics in relatively severe conditions, and to magnify the influence of the seat design parameters. Figure 6 shows a triangular acceleration pulse that is used as an input to accelerate the sled in the forward direction (X-direction). The simulation was terminated 200 ms after impact. Time history data for displacement, velocity and acceleration were output at selected nodes as well as the entire motion in the model. NIC and joint capsule strain (JCS) were then examined. NIC was calculated from the acceleration and velocity data. JCS was represented by the maximum principal strain in the capsule tissue. The strain value was output directly from the elements composing the capsule part. Only the maximum value in the capsule elements among the cervical joints was taken for evaluation.

Seat Design Study

Two studies were conducted to examine the influence of seat design. The first one was a parametric study conducted on a single seat configuration but changing parameters that would potentially affects the head-neck motion of the occupant in a rear impact. The Seat B model was chosen for the study. The selected parameters were; the fore-aft and vertical locations of the head restraint, the stiffness of the head restraint foam material, the thickness of the seat-back upper-end frame, the stiffness of the reclining joint, and the stiffness of the bracket plate inserted between the seat-pan and the seat adjusting rails. Table 1 summarizes the parameters and the range of design change assumed for each parameter. A total of thirteen cases was prepared based on the Seat B configuration with different specifications. The ranges of design parameters were determined considering possible high and low values that could be seen in actual prototype seats. Rear impact simulations were conducted for the thirteen cases using the same acceleration pulse (Figure 6) for the

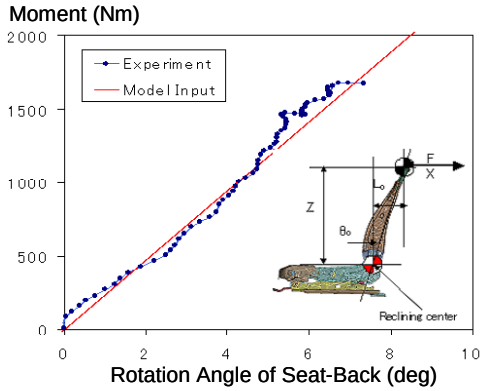

Figure 5. Validation of Mechanical Response of Reclining Joint in Seat A.

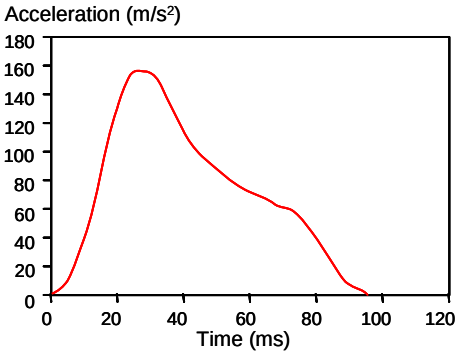

Figure 6. Triangle Acceleration Pulse for Input.

input. Instead of analyzing time history responses of the occupant head and neck, the results were evaluated with NIC and joint capsule strain to identify a dominant parameter for the indicators.
The second study was conducted considering differences in seat configuration. The purpose of this study was to investigate the correlation among the whiplash injury indicators proposed by researchers and adopted in some assessment tests. The examined indicators were NIC and JCS as already used in the previous study, head restraint contact timing (HRCT) and neck leaning angle (NLA). HRCT is the timing when the head contacts the head restraint. This indicator is actually adopted in some assessment tests as a seat design factor but not as an injury indicator. There is discussion if the indicator really reflects the whiplash injury risk in terms of assessment [13]. In rear impact simulations, HRCT can be detected by monitoring the contact force between two parts. NLA is the rotation angle of the head with respect to T1 as shown in Figure 7. The reason for using this indicator is that JCS is only available in FE simulations with a human body model that has cervical joint capsule tissues. It is practical to have an alternative indicator that is measurable on the crash test dummy. All three seat models shown in Figure 4 were used in this study. The geometry and dimensions, composition of mechanical parts, and mechanical and material properties of the components are completely different among the seats. Using the Seat B model as the reference base, the Seat A model has relatively lower stiffness in its reclining joint, less rigidity in its head restraint support and a head restraint located more to the rear with respect to the upper-end frame. The Seat C model has higher stiffness in the reclining joint, more rigidity in the head restraint support, and a head restraint located in the forward direction.
Rear impact simulations were conducted using these seat models in the same manner as described above. The sitting postures of the occupant on these three seat models were the basically the same but were adjusted to those used in seat design. The indicators, NIC, JCS, HRCT, and NLA, were calculated from the results. The correlations among the indicators were investigated in detail.

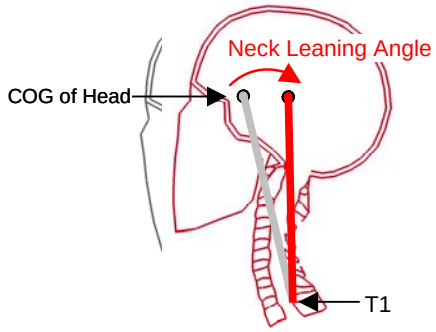

Figure 7. Definition of Neck Leaning Angle.

RESULTS

Results of Rear Impact Simulation

Figure 8 shows the entire motion of THUMS on Seat A observed from a lateral view. The frames were selected considering interaction events between the occupant body and the seat. In the initial seating posture, there is a small gap between the occiput and the head restraint, while the lower torso contacts the seat-back. The torso is pushed forward immediately after the rear impact begins, while the head does not move until the gap becomes zero. In this case, the head contacts the head restraint around 50 ms. The seat-back frame deforms rearward as the occupant body loads on it. The deformation of the seat-back frame reaches its maximum peak around 100 ms. The torso starts moving back forward after this, which is called a ‘rebound’ motion. The head still moves back for a while but the head restraint deformation reaches its maximum peak before long. It was around 130 ms in this case. Then the head starts moving forward again. Figure 9 shows the acceleration responses at the head, T1, and pelvis. As the buttocks remain in the seat, the pelvis acceleration rises immediately after impact. Although the lower torso also remains against the seat-back, there is some delay in acceleration rise at T1 because of the small gap between the upper torso and the seat-back. The head acceleration does not start until the occiput contacts the head restraint. The

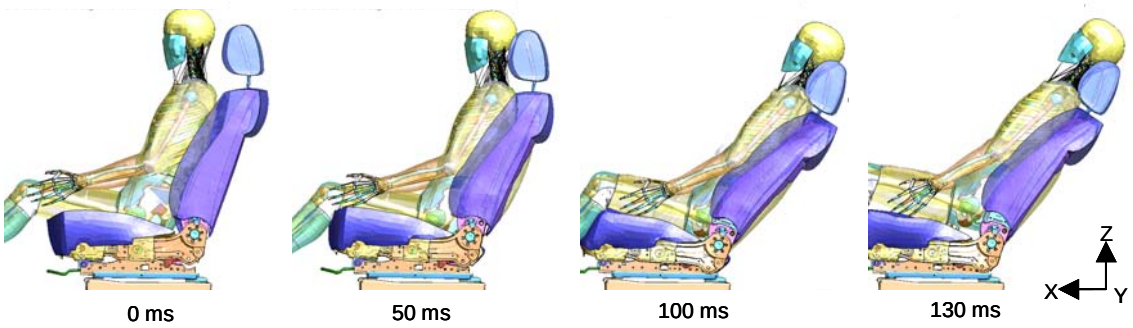

Figure 8. Gross Motion of THUMS Occupant in Rear Impact (Seat A, Delta-V=25km/h).

pelvis and the head show triangular acceleration pulses, while that of T1 has two peaks. The maximum peak in the T1 acceleration is lower than that in the pelvis, while the head acceleration has a higher peak than the pelvis. The convergence of the acceleration pulses occurs in the same order as seen in the rising timings. Contact forces between the occupant body and the seat are plotted in Figure 10. The contact force at the pelvis indicates the force between the buttocks and the seat-back, while the contact force at the torso indicates that between the torso-back and the seat-back, where the boundary between the buttocks and the torso-back is assumed

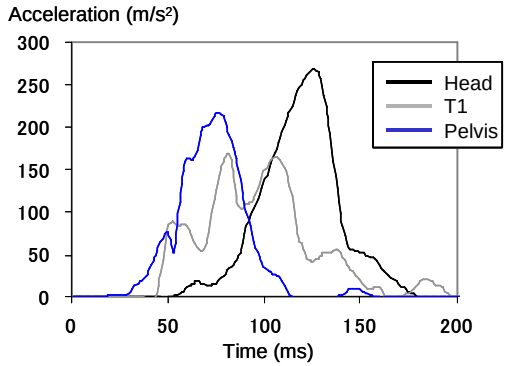

Figure 9. X-accelerations at Head, T1 and Pelvis.

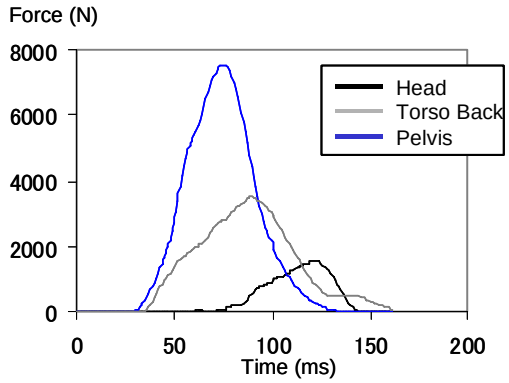

Figure 10. Contact Forces between Head, Tor Back, Pelvis and Seat.

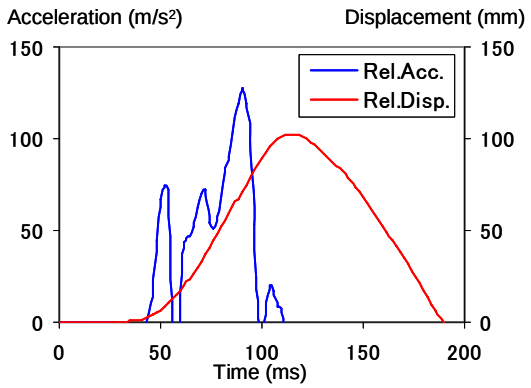

Figure 11. Relative Acceleration and Relative Displacement between Head and T1.

around the waist. The contact force at the head is the force between the occiput and the head restraint. The order of rising timings is exactly the same; the pelvis is first, followed by the thorax and the head is the last. The rising timings are around 30, 40 and 70 ms respectively. The maximum force peak is largest at the pelvis, followed by the thorax and the head. Figure 11 shows the relative acceleration and the relative displacement between the head and T1. Only the positive part of the relative acceleration is shown in this figure, in which the head acceleration is higher than that of the pelvis. The maximum peak around 50 ms indicates the initial peak in relative motion between the head and the torso. This is called 'retraction.' There is another peak around 80 ms with higher amplitude. The relative acceleration finally converges to zero around 100 ms after impact. The displacement data was output from the same nodes where the acceleration values were obtained. There is mostly the positive part up to 200 ms, in which the head is in the posterior side of the torso. There is only one peak in the relative displacement curve and its timing is around 110 ms after impact, later than that of the relative acceleration. Figure 12 plots time history curves of NIC and JCS. NIC was calculated from the relative acceleration and velocity between the upper and lower ends of the cervical spine as described above. The JCS values were obtained from all the capsule elements in the cervical joints. The highest value was regarded as the representative JCS for evaluation. A comparison of Figure 11 and 12 finds that the time history curve of NIC is quite similar to that of the relative acceleration curve, and that JCS has its maximum peak at the same timing of the relative displacement peak.

Results of Seat Design Study

In both studies on seat design, the nodal output data and element output data were obtained first as in the rear impact simulation conducted previously. NIC, JCS, HRCT and NLA were obtained in each case. Table 2 summarizes the calculated indicator values for the thirteen cases conducted in the first study.

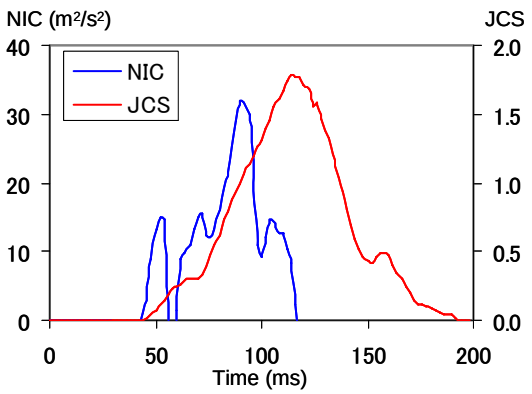

Figure 12. Time History Curves of NIC and JCS.

The calculated NIC values ranged from 10.91 to 42.38, JCS ranged from 0.492 to 1.140, HRCT was found between 49.7 and 79.4, and NLA was obtained from 5.48 to 13.61. The lowest NIC value of 10.91 was obtained in the case where the head restraint was located at the front-most and highest position. The same case showed the smallest number for HRCT. The smallest JCS value of 0.492 was found in the case where the thickness of the upper-end seat-back frame was increased. The same case showed the smallest NLA among the cases.

Figure 13 plots the trends of NIC and JCS changes for each design parameter. When the stiffness of the head restraint was changed, neither NIC nor JCS showed big changes. Both values decreased when the head restraint was moved forward. The magnitude of changes was relatively smaller when the vertical position of the head restraint was 35 mm. The stiffness of the reclining joint in rotation and in the vertical direction only affected NIC, while the thickness of the upper-end seat-back frame had a great influence on JCS but not on NIC.

Figure 14 shows the relationship among the indicators The correlations between NIC and HRCT, NIC and NLA, JCS and HRCT, JCS and NLA were plotted. The values were obtained from the thirteen cases. The first plot suggests that NIC strongly correlates with HRCT, although its correlation is not linear. No prominent correlations were found in the next two plots, between NIC and NLA, and between JCS and HRCT. There is a strong correlation between JCS and NLA as shown in the last plot. The R^2 value was 0.917 for this case.

Table 3 shows the result of the other seat design study on the different seat configurations. The data for Seat B is the same as that of Case 1 in Table 1. Compared to this case, Seat A showed relatively higher NIC (35.80 > 18.25), larger JCS (1.790 > 1.010), longer HRCT (70.6 > 65.8), and greater NLA (26.80 > 12.36), while Seat C gave relatively higher NIC (21.79 > 18.25), but smaller JCS (0.616 < 1.010), shorter HRCT (58.6 < 65.8), and less NLA (6.49 < 12.36).

DISCUSSION

Comparing the time history curves of acceleration and the contact forces plotted in Figure 9 and 10, it was noted that the timings of acceleration rises and their maximum peaks basically correlate with those in the contact forces. For example, both the pelvis acceleration and contact force start around 30 ms and their maximum peaks appear around 75 ms. It is considered that this acceleration is a result of motion change induced by the external force. Assuming that the motion can be simply described using Newton's laws, the amplitude of acceleration depends on the magnitude of the applied force and the mass of the part. The relatively high pelvis acceleration is mostly generated by the large contact force. The deformation of the seat-back frame generally occurs around the reclining joint. When loading the seat-back frame, the moment arm becomes shorter as the loading point is closer to the joint center. The seat-back frame generally has relatively wider sectional geometry in its lower-end part. Even if the seat-back pushes the occupant body in a horizontal direction, the contact force tends to be larger in the

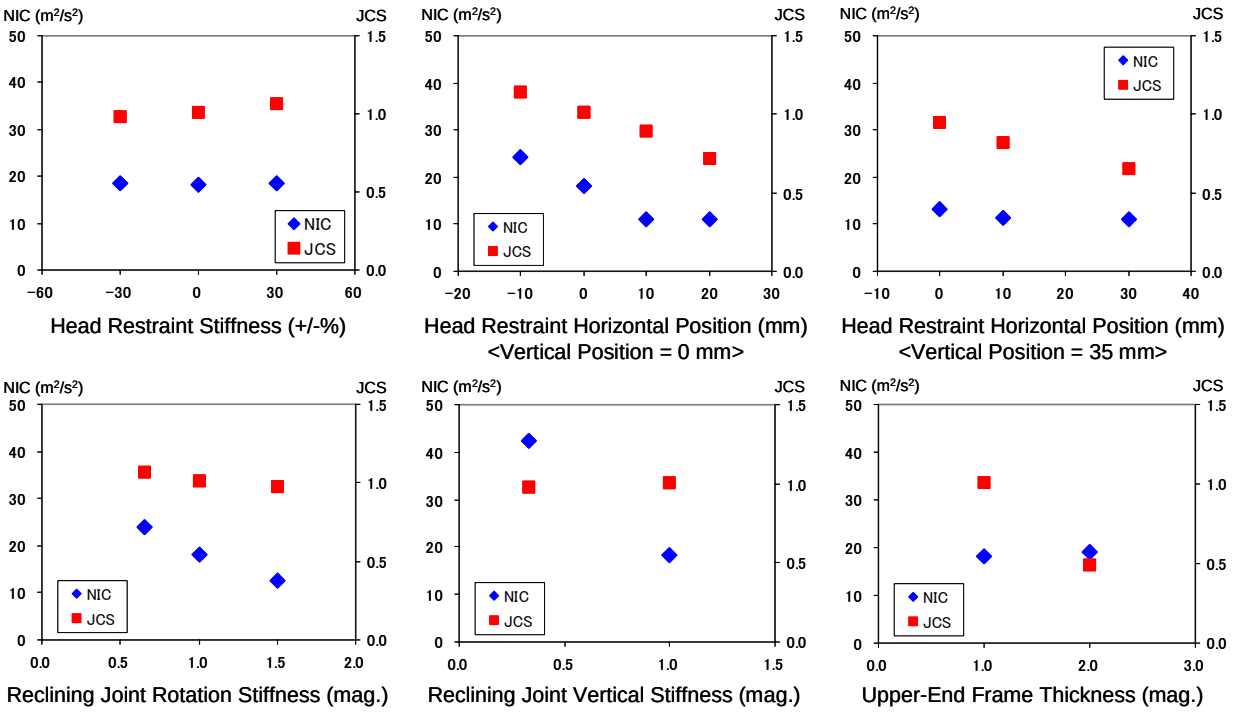

Figure 13. Correlation among Indicators.

pelvis area compared to that in the upper area. The effective mass of the pelvis is higher than the thorax or the head. Despite the relatively heavier weight, however, the pelvis can be accelerated strongly because of the greater magnitude of the contact force. Conversely, the higher acceleration of the head comes from its light mass. However, the contact force between the head and the head restraint is very small. Less stiffness in the upper part of the seat-back frame may be a reason for the small magnitude of contact force. The other possible reason is that the head restraint moves away from the occiput as the seat-back deforms backward. Although the magnitude of contact force is smaller, the head was accelerated greatly because of its smaller mass, which is around 4 kg. Unlike the pelvis and the head, the thorax acceleration has two peaks. A more complicated mechanism is assumed to explain this. Actually, the timings of the acceleration peaks do not necessarily correspond to those of the contact forces. It should be noted that T1 does not directly contact the seat-back, but there is some gap between them. The T1 acceleration is generated both by the force to the torso and by that to the head. The peaks in T1 acceleration may come from such a combination of forces. The first acceleration peak appears between the peaks of the pelvis force and the thorax force, while the second peak is in between the peaks of the thorax force and the head force. The results suggest that the acceleration pulse is greatly affected by interaction between the occupant's body and the seat. The rising timings correspond to the beginning of motion while backward motion rebounds at the timing of the maximum peak.

The initial peak in relative acceleration shown in Figure 11 indicates the difference between the timing of the starting motions of the head and the torso. The head stays at the initial position for a while due to inertia while the torso is pushed forward by the seat-back. After the occiput contacts the head restraint, the contact force pushes the head forward, in the same direction as the torso. The relative motion becomes smaller after the head restraint contact. In this case, however, the head restraint moves away from the occiput due to the seat-back deformation. The relative acceleration rises again until the head is supported firmly. Anyway, the relative acceleration indicates the relative motion between the head and the torso in terms of the timing of motion change. The maximum peak was observed around 90 ms after impact in this case. On the other hand, the relative displacement has its peak around 110 ms, which is later than that of the relative acceleration peak. It is considered that the relative displacement correlates more with the seat deformation. As observed in Figure 10, the timing of the maximum contact force at the seat-back is around 95 ms, while the contact force at the head restraint reaches its peak around 125 ms. Considering the fact that the seat deformation is caused by the contact force from the occupant, the head restraint starts deforming later than the seat-back and the maximum deformation also appears later. This is rational based on the nature of seat deformation mentioned above. The maximum relative displacement between the head and T1 is actually the difference between their positions, while the relative acceleration indicates only the difference in the timings of the starting motions. In other words, the relative displacement is the resultant difference in position induced by the contact force, but is more affected by the seat deformation. It appears that the surface geometry of the deformed seat determines the position of the occiput and the torso back. The difference in position between the head and T1 represents a neck extension when the head is relatively on the posterior side compared to T1.

The timing of the NIC peak observed in Figure 12 is almost the same as that of the relative acceleration peak between the head and T1. Based on the NIC formulation [(1)], it is obvious that the NIC value is highly affected by the acceleration term.

$$NIC=0.2*(AT1-AHead)+(VT1-VHead)^2 \quad (1).$$

where *AHead* and *AT1* are the accelerations measured at the head and T1 respectively, and *VHead* and *VT1* are the velocities at the head and T1. The timing of JCS is, on the other hand, close to that of the maximum relative displacement. This is again rational considering the fact that the relative displacement between the head and T1 indicates a neck extension. Any neck motions accompany deformation in the cervical joints. The deformation can stretch or shear the joints, causing strain in the joint capsules. Therefore, JCS is an inevitable result of cervical joint motion. This is why the timing of peak JCS is close to that of the maximum relative displacement. The timings are not exactly the same because the difference in position between the head and T1 is a summation of the joint motions from OC-C1 to C7-T1.

These findings explain possible reasons for the correlation among the indicators, obtained from the parametric study shown in Figure 14. It has already been described that the relative acceleration between the head and T1 has its peak at the timing of head restraint contact, and that NIC is mostly given by the relative acceleration. It was also explained that JCS originates from the joint deformation attributed to neck extension, and NLA actually means the magnitude of neck extension. Therefore, the correlation between NIC and HRCT, and that among JCS and NLA are reasonable considering the findings from the results obtained from the study. It should be noted, however, that HRCT is a major factor affecting NIC but not the sole element. The contact timing determines the duration in which the relative acceleration is taken into account. The

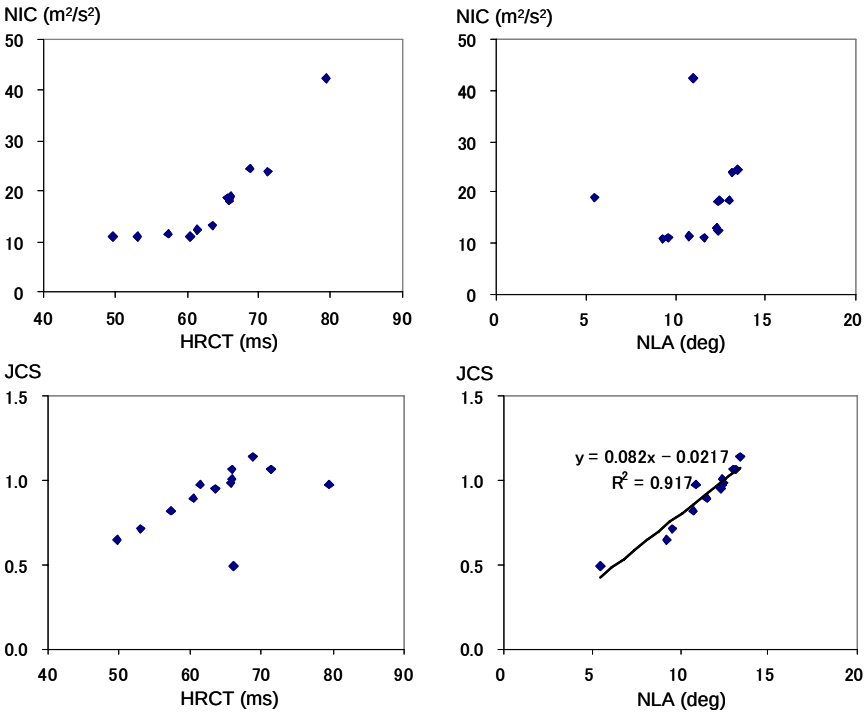

Figure 14. Correlation among Indicators.

maximum amplitude of relative acceleration in that duration actually gives the NIC value. Because the head acceleration is quite small before contacting the head restraint, the amplitude mostly comes from the T1 acceleration level. It should be remembered that the first study was conducted on a single seat configuration, which means that the resultant T1 acceleration curves are similar to one another among the cases. It is a natural result that the difference in NIC is mostly given by HRCT. Figure 15 explains the mechanism. The time history curves of the T1 acceleration, the head acceleration and NIC are plotted for Cases 1, 8 and 9. The difference in seat configuration among the cases is the location of the head restraint. The head restraint was located at the original position in Case 1. It was 10 mm ahead of the original position in Case 9 and 10 mm rearward in Case 8. The T1 acceleration pulses are close to one another while the timings of the rises in head acceleration are different between the cases. The timings of the head acceleration rises correspond to HRCT in each case. It is clear that NIC is mostly given by the T1 acceleration level at the contact time. It should be also noted that the T1 acceleration pulse in this seat has a flat level from 45 to 60 ms. This is the reason why NIC does not decrease any more when HRCT becomes shorter than 60 ms. The nonlinear correlation between NIC and HRCT shown in Figure 14 comes from the plateau in the T1 acceleration curve. If the seat configurations are different among the cases to be compared, however, the T1 accelerations may be different. This may show that HRCT does not directly indicate which seat gives a lower or higher NIC value.

Looking at the results of the other study on the different seat configurations as summarized in Table 2, it is noted that Seat C shows a higher NIC value than Seat B despite a shorter HRCT. This is possibly because the T1 accelerations are different between the two cases. Figure 16 shows the time history curves of T1 acceleration for the three cases. A comparison shows a relatively lower T1 acceleration

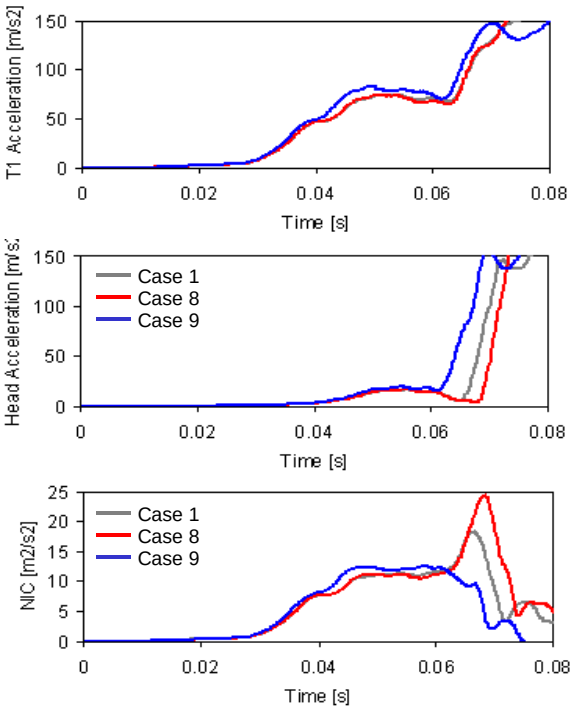

Figure 15. Time History Curves of NIC and JCS.

in Seat A. The low acceleration comes from the lower stiffness in the reclining joint. A larger deformation of the seat-back frame reduces the amplitude of T1 acceleration. The amplitude of T1 acceleration in Seat C is slightly higher but close to that in Seat B, but the profile of the acceleration pulse is different. Figure 17 inserts the NIC and JCS values into the plots showing the correlation among the indicators. Only the plots of NIC-HRCT and JCS-NLA were examined as these combinations showed strong correlations. It is found that the inserted NIC value does not follow the correlation with HRCT that was derived from the first study on a single seat configuration. This is because the three seats had different T1 acceleration pulses as shown in Figure 16. The result suggests that the validity of HRCT in terms of whiplash injury assessment is limited to a comparison among design changes on a single seat configuration. On the other hand, the inserted JCS values were found to be almost on the correlation line between JCS and NLA. This suggests that NLA can predict increase or decrease of JCS when the seat design is changed or even among different seat configurations. JCS can be calculated in the THUMS occupant model used in this study but not measured on a crash dummy. NLA can be obtained even from a dummy if the kinematics of the head and the torso are monitored. Assuming that JCS is a valid indicator to assess whiplash injury risk, NLA can be an alternative indicator for injury assessment with a dummy. A possible technical issue is that the accuracy in measuring rotational angle is less reliable compared to that when measuring acceleration or force. An alternative measurement could be neck moment assuming a linear relationship between the moment and the rotational angle.
It should be re-stated that the joint capsule model used in this study tends to overestimate the strain level. A future study will focus on improving the joint capsule model to predict the strain level more accurately.

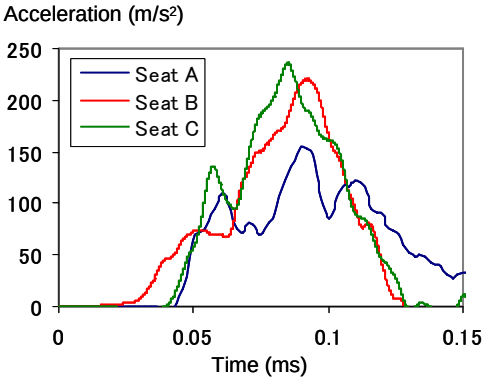

Figure 16. Comparison of T1 Accelerations.

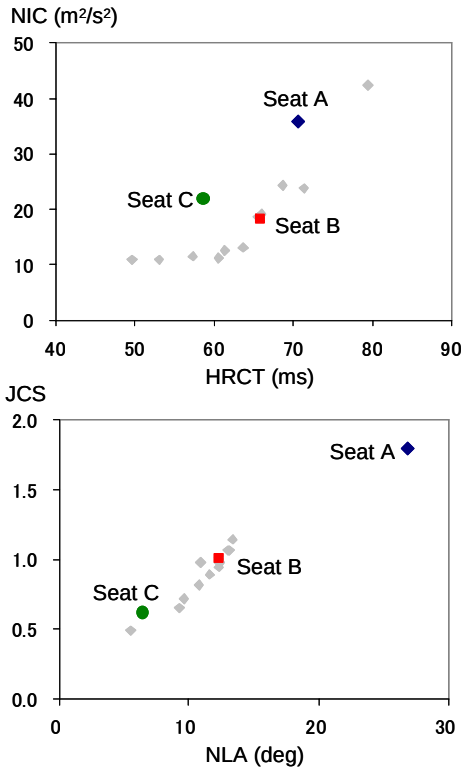

Figure 17. Correlations among Indicators in Different Seat Configurations.

CONCLUSIONS

Rear impact simulations were conducted using a human body FE model, THUMS Version 1.61, representing a male occupant with an average body size. The model included the cervical joint capsules, which are considered as a potential site of neck pain, to calculate the strain level due to neck deformation. The model was then validated against PMHS test data obtained from the literature. Although the calculated displacement and rotation data were found almost within the test corridors, the model tended to overestimate the strain level. Only relative comparisons were therefore adopted in the following studies.
Prototype seat models were also prepared to simulate actual rear impact conditions. Their mechanical responses were validated against loading test data. A rear impact simulation was conducted at a delta-V of 25 km/h. The head and neck motions and responses were analyzed in correlation with timings of rises and peaks in acceleration and force. NIC was calculated from the nodal acceleration and velocity output from the model, and JCS was obtained directly from the elements representing the capsule tissues. The results suggested that NIC indicates the difference in motion between the head and the torso while JCS indicates the difference in their positions. A parametric study was conducted on thirteen cases where major seat design factors were changed on a single seat configuration. It was shown from the results that the stiffness of the reclining joint affects the resultant NIC values while JCS is more

influenced by the thickness of the upper-end of the seat-back frame. The forward position of the head restraint was effective for both indicators. As for the relationship among the indicators, relatively strong correlations were found between NIC and HRCT, and JCS and NLA. It was explained that NIC was mostly given by the T1 acceleration level at the timing of head to head restraint contact. HRCT is, therefore, thought to be useful for comparison.
The second study focused on the difference in overall seat design, that is relatively larger design changes compared to minor changes in characteristics. Three prototype seat models with different configurations were used for the study. The results showed a case showing higher NIC with shorter HRCT. The results suggested that HRCT could be useful to compare seats with design changes and the same configuration, but not necessarily for injury assessment among different seat configurations. Introducing the results of the second study into that of the first one, NLA is thought to be an alternative indicator to help assess whiplash injury risk instead of JCS in dummy tests.

ACKNOWLEDGMENTS

THUMS has been developed in collaboration with the Toyota Central Research and Development Laboratory. The authors would like to thank Toyota Technical Development Corporation for its assistance with the modeling and simulation work.

REFERENCES

[1] Japanese National Police Agency. 2004. “Traffic Green Paper 2003” (in Japanese). 1-23.

[2] Deng, B., P. Begeman, K. Yang, S. Tashman and A. King. 2000. “Kinematics of Human Cadaver Cervical Spine During Low Speed Rear-End Impacts.” Stapp Car Crash Journal 44: 171-188.

[3] Ono, K. and K. Kaneoka. 1997. “Motion Analysis of Human Cervical Vertebrae During Low Speed Rear Impacts by the Simulated Sled.” Proc. International Conference on the Biomechanics of Impacts. 223-237.

[4] Svensson, Y., B. Aldman, P. Lövsund et al. 1993. “Pressure Effects in the Spinal Canal During Whiplash Extension Motion: A Possible Cause of Injury to the Cervical Spinal Ganglia.” Proc. International Conference on the Biomechanics of Impacts. 189-200.

[5] Böstrom, O., M. Svensson, B. Aldman, H. Hansson, Y. Haland, P. Lovsund, T. Seeman, A. Suneson, A. Saljo and T. Ortengen. 1996. “A New Neck Injury Criterion Candidate Based on Injury Findings in the Cervical Spinala Ganglia after Experimental Neck Extension Trauma.” Proc. International Conference on the Biomechanics of Impacts. 123-136.

[6] Winkelstein, B., R. Nightingale, W. Richardson and B. Myers. 1999. “Cervical Facet Joint Mechanics: Its Application to Whiplash Injury.” Proc. 43rd Stapp Car Crash Conference. 243-265.

[7] Sundararajan, S., P. Prasad, C. Demetropoulos, S. Tashman, P. Begeman, K. Yang and A. King. 2004. “Effect of Head-Neck Position on Cervical Facet Stretch of Post Mortem Human Subjects during Low Speed Rear End Impacts.” Stapp Car Crash Journal 48: 1-42.

[8] Lu, Y., C. Chen, S. Kallakuri, A. Patwardhan and J. Cavanaugh. 2005. “Neural Response of Cervical Facet Joint Capsule to Stretch: A Study of Whiplash Pain Mechanism.” Stapp Car Crash Journal 49: 49-66.

[9] Yamada, H. 1970. “Strength of Biological Materials.” Evans, F. G. (Ed). Williams & Wilkins Company, Baltimore.

[10] Yoganandan, N., A. Pinter, S. Kumaresan and A. Elhagediab. 1998. “Biomechanical Assessment of Human Cervical Spine Ligaments.” 42nd Stapp Car Crash Conference.

[11] Hasegawa, J. 2004. “A Study of Neck Soft Tissue Injury Mechanisms During Whiplash Using Human FE Model.” Proc. International Conference on the Biomechanics of Impacts. 321-322.

[12] Iwamoto, M., Y. Kisanuki, I. Watanabe, K. Furusu, K. Miki and J. Hasegawa. 2002. “Development of a Finite Element Model of the Total Human Model for Safety (THUMS) and Application to Injury Reconstruction.” Proc. International Conference on the Biomechanics of Impacts. 31-42.

[13] Kitagawa, Y., T. Yasuki and J. Hasegawa. 2006. “A Study of Cervical Spine Kinematics and Joint Capsule Strain in Rear Impacts Using a Human FE Model.” Stapp Car Crash Journal 50: 545-566.

[14] Siegmund, G. P., B. S. Myers, M. B. Davis, H. F. Bohnet and B. A. Winkelstein. 2000. “Human Cervical Motion Segment Flexibility and Facet Capsular Ligament Strain under Combined Posterior Shear, Extension and Axial Compression.” Stapp Car Crash Journal 44: 159-170.

[15] Kraft, R., A. Kullugren, A. Ydenius, O. Bostrom, Y. Haland and C. Tingvall. “Rear Impact Neck Protection by Reducing Occupant Forward Acceleration – A Study of Cars on Swedish Roads Equipped with Crash Recorders and a New Anti-Whiplash Device.” Proc. International Conference on the Biomechanics of Impacts. 221-231.

[16] Ministry of Land, Infrastructure and Transport. 2002. The 3rd Car Safety Symposium.

Table 1.
Simulation Matrix for Parametric Study

Case#	Head Restraint Stiffness	Head Restraint Fore-aft Position	Head Restraint Vertical Position	Reclining Joint Rotation Stiffness	Reclining Joint Vertical Stiffness	Upper-End Frame Thickness
1	±0	±0	±0	±0	±0	±0
2	-30%					
3	+30%					
4				x1.5		
5				x0.65		
6						x2.0
7					x0.33	
8		-10				
9		+10				
10		+20				
11			+35			
12		+10	+35			
13		+30	+35			

Table 2.
Summary of Results from Parametric Study

Case#	NIC (m2/s2)	JCS	HRCT	NLA (deg)
1	18.25	1.010	65.8	12.36
2	18.56	0.981	65.6	12.47
3	18.47	1.067	65.8	12.99
4	12.48	0.978	61.4	12.36
5	23.78	1.066	71.3	13.14
6	19.00	0.492	66	5.48
7	42.38	0.978	79.4	10.93
8	24.36	1.140	68.7	13.41
9	11.08	0.892	60.5	11.55
10	11.04	0.717	53.1	9.61
11	13.08	0.949	63.6	12.28
12	11.42	0.816	57.3	10.77
13	10.91	0.649	49.7	9.23

Table 3.
Comparison among Different Seat Configurations

Seat Model	NIC (m2/s2)	JCS	HRCT	NLA (deg)
Seat A	35.80	1.790	70.6	26.80
Seat B	18.25	1.010	65.8	12.36
Seat C	21.79	0.616	58.6	6.49

Development of Rear Pre-Crash Safety System For Rear-End Collisions

Kiyoka Matsubayashi
Yukinori Yamada (co-author)
Motomi Iyoda (co-author)
Shin Koike (co-author)
Tomoya Kawasaki (co-author)
Masanori Tokuda (co-author)
Toyota Motor Corporation
Japan
Paper Number 07-0146

ABSTRACT

Pre-crash safety systems using radar detecting technology have been commercialized in the market. While the primary focus of these systems have been for frontal collisions, rear-end collisions actually have a higher proportion of the traffic accident injuries in Japan.
In this paper, a new pre-crash safety system for rear-end collisions is explained. It was developed to help alert drivers of vehicles approaching from behind, and also to reduce whiplash injury. This new system uses a millimeter-wave radar installed in the rear bumper to detect a vehicle approaching closely from behind. If it judged that there is high risk of collision, the hazard lights would flash to warn the driver of the approaching vehicle and the headrests are automatically moved forward. Sensors in the headrests detect the location of the occupants' head and shifts the headrests to a closer position to the head before the collision occurs, thereby reducing the risk of whiplash injury. This paper shows the effectiveness of the pre-crash hazard light and pre-crash headrest technology.

INTRODUCTION

According to accident analysis of crashes in Japan, rear-end collisions account for only 4% of fatalities, but approximately 50% of injuries (Fig. 1).

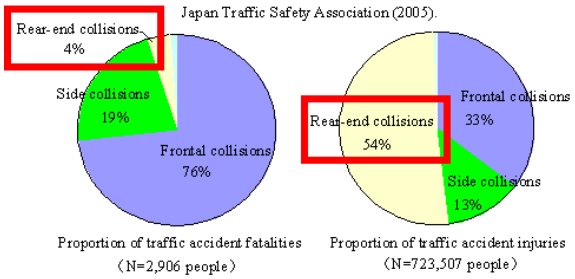

Figure 1. Proportion of Fatalities and Injuries per Location of Vehicle Damage.

In addition, a high proportion (77%) of rear-end collisions result in neck injury, most of which can be categorized as whiplash injury (Fig. 2).

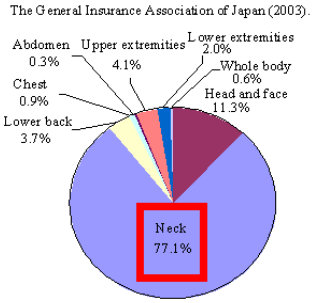

Figure 2. Proportion of Locations of Injury in Rear-End Collisions.

The primary cause of rear-end collisions is driver's poor attention to which caused by distraction ahead when driving, approximately 14% of accidents occur when the driver is looking forward but make's misjudgment by carelessness (Fig. 3).

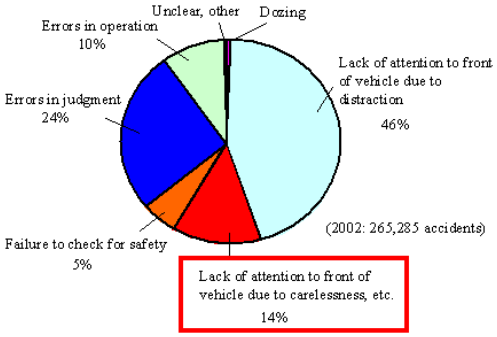

Figure 3. Causes of Rear-End Collisions Resulting in Fatality or Injury.

This figure suggests that providing some kind of warning to the driver of approaching vehicle from the rear would be an effective.
These facts provided the impetus for the development of the rear pre-crash safety system for rear-end collisions to lessen whiplash injury and reduce rear-end collisions itself.

Rear Pre-Crash Safety System

The pre-crash safety system for rear-end collisions consists of an obstacle detecting sensor, a control computer which judges a collision is impending or not, and actuators such as the hazard lights, headrests, and so on. The sensor is installed in the

rear bumper, and is made up of a version of the conventional frontal pre-crash safety system millimeter wave radar unit, which has been enhanced to enable short range monitoring of vehicles approaching from the rear.
The pre-crash computer controls the motion of pre-crash headrest which move forward to help reduce whiplash injury. The structure of the system is shown in Fig.4.

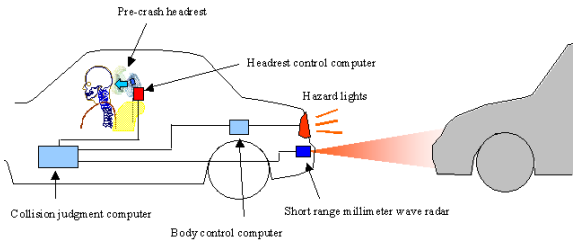

Figure 4. Structure of Pre-Crash Safety System for Rear-End Collisions.

Rear Short Range Millimeter Wave Radar – A compact millimeter wave radar which judge the possibility of rear-end collision has been developed as the sensor for detecting the risk of rear-end collision (Fig. 5).

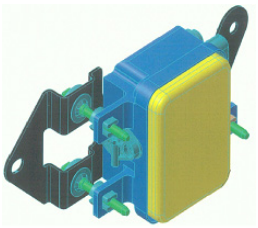

Figure 5. Rear Short Range Millimeter Wave Radar.

In general, the size of radar devices depends on the size of the antenna, and higher frequencies require smaller antennas. Since the size of the radar sensor is critical for installation in various types of vehicles, a high-frequency 76 GHz millimeter wave radar is adapted. This frequency has already been allocated for vehicle-installed radars throughout the world.
The types of objects to be detected are restricted to vehicles approaching from the rearward. Normally, vehicle radars for forward monitoring require sophisticated processing technology to distinguish stationary solid obstacles such as the road or objects on the roadside. However, rear-end collision detection can ignore such stationary solid obstacles, enabling simpler collision judgment than forward monitoring radars. For this reason, a less complex 3-channel electronic angle detection method was used for the circuit configuration, and the FM-CW method was used for the radar to achieve commonality with other radar devices. Table 1 shows the main radar specifications.

Table 1.
Main Radar Specifications

Item		Rear Short Range Millimeter Wave Radar	Frontal Millimeter Wave Radar
Radar system		FM-CW 3-channel electronic angle detection	FM-CW Electronic scanning
Center frequency		76.5 GHz	76.5 GHz
Detection performance	Distance	2~30 m	2~150 m
	Relative velocity	0~100 km/h	-200~+100 km/h
	Angle	+/- 15 deg	+/- 10 deg
Size		W67×H88×D47 mm	W107×H77×D53 mm

The locations where radar devices can be installed are restricted due to the effects of surrounding metallic objects on electrical waves. Installing the sensor inside the rear bumper prevents any part of the sensor from being exposed and has no adverse effects on the exterior vehicle design.
This rear millimeter wave radar detects the distance, relative velocity, and directional angle of vehicles approaching from the rear with an update cycle of approximately 20 msec, and transmits the detection data to the collision judgment computer via CAN communication.

Collision Judgment Computer – The collision judgment computer uses the detection data from the millimeter wave radar to calculate the estimated paths of vehicles approaching from the rear. This is then used as the basis to estimate the lateral time to collision (LTTC) after the estimated time to collision (TTC). TTC is calculated by dividing the distance to the vehicle approaching from the rear by the relative velocity. LTTC is obtained by monitoring time changes in the lateral position of the vehicle approaching from the rear and then calculating the lateral position after TTC by vector estimation.
In addition, because vehicles usually negotiate curves in set lanes, logic is employed to correct lateral position to follow the lane curvature. This curvature is calculated from the yaw rate or steering angle of the driver's vehicle (Fig. 6).

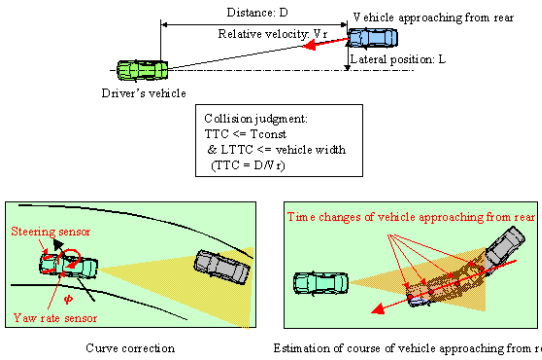

Figure 6. Rear-End Collision Judgment.

When the system judges that LTTC has almost passed through a range equal to the width of the driver's vehicle at a timing when the collision risk is high, it activates flashing of the hazard lights.
Additionally, judgment that LTTC has almost passed

through a range equal to the width of the driver's vehicle at a timing when a collision is unavoidable will also activates the pre-crash headrest.

Pre-Crash Hazard Lights – The hazard lights are flashed automatically as a warning to drivers of vehicles approaching from behind.
Once the collision judgment computer judges that there is a high risk of a rear-end collision, it transmits a signal to the body computer to activate automatic flashing of the hazard lights. The body computer uses this signal to flash the hazard lights for around 2 sec at a frequency of approximately 2 Hz (Fig. 7).

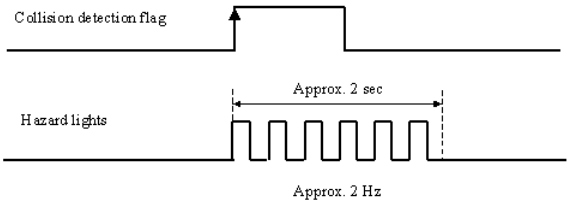

Figure 7. Pre-Crash Hazard Lights.

However, this system also gives priority to driver operation in the same way as other driver assistant systems. This means that automatic hazard light flashing is not activated when manual operation of the hazard lamps or turn signals is detected.
Additionally, in consideration of driver reaction time, warning approaching vehicles as early as possible is a more effective way of reducing rear-end collision speed. However, issuing needless warnings when drivers are already aware of the situation is irritating. Experiments showed that when there is the impending danger of a collision, drivers complete avoidance operations up to the period approximately 2 sec before the collision occurs.

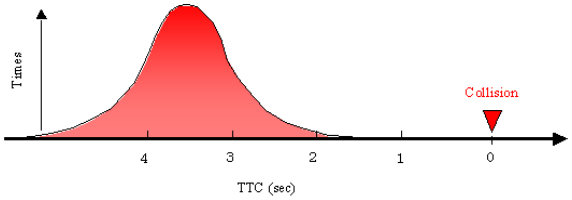

Figure 8. Avoidance Timing Distribution.

It is therefore highly likely that drivers would find warnings issued earlier than a TTC of 2 sec irritating. In response, the timing of hazard light flashing was set to a TTC of 1 to 2 sec.

Pre-Crash Headrest – Simultaneous restraint of the head and chest is regarded as the key to reducing whiplash injury.[1][2] The pre-crash headrest system was developed to achieve this instantaneously when a rear-end collision is judged as unavoidable by moving the headrests forward toward the head of the occupant before the collision occurs.
When the collision judgment computer detects an unavoidable collision, it transmits a pre-crash headrest activation signal to the headrest control computer. Figs. 9 and 10 show the structure and electrical circuit configuration of the pre-crash headrest. Once the activation signal is received via CAN communication, a motor moves the headrest forward closer to the head of the occupant.

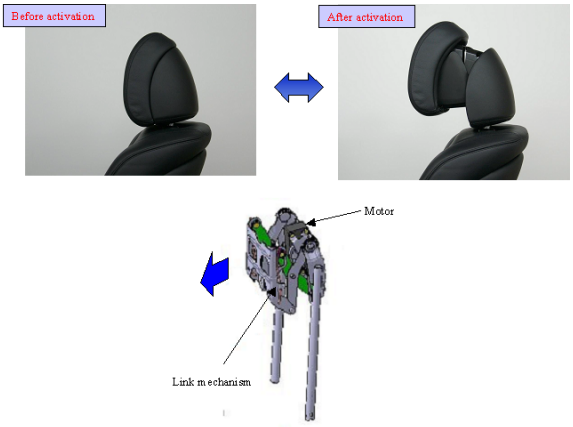

Figure 9. Pre-Crash Headrest.

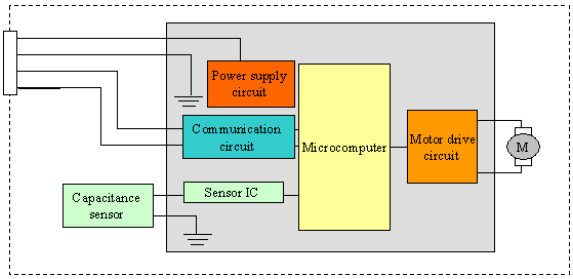

Figure 10. Electrical Circuit Configuration.

However, pushing the head more than necessary is only likely to worsen whiplash injury. The surface layer of the headrest therefore contains a head detection sensor, and utilizes a headrest position control mechanism.
This system uses changes in capacity as detected by the capacitance sensor when the headrest nears the head to stop the headrest immediately before contact. Fig. 11 shows the structure of the sensor. The headrest is programmed to move no more than approximately 60 mm in the forward direction.

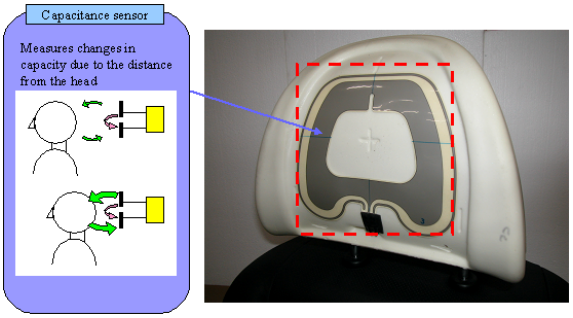

Figure 11. Head Detection Sensor.

In addition, because the motor can return the

pre-crash headrest to the original position after it has been activated, it can be re-used without requiring repair in situations such as when the seat is unoccupied.

System Activation Timing – Fig. 12 shows the activation timing of the pre-crash hazard light and pre-crash headrest functions. The horizontal axis shows the time to rear-end collision.

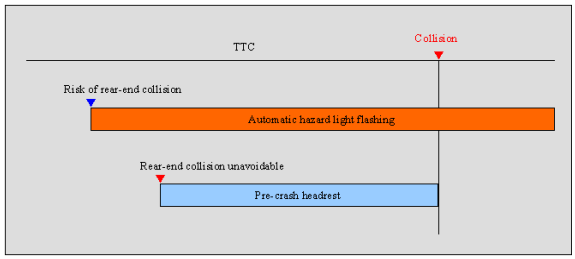

Figure 12. Activation Timing of Rear Pre-Crash Safety System for Rear-End Collisions.

Experimental Results and Effect

Actual Vehicle Test of Rear Radar – Fig. 13 shows detection data for vehicles approaching from the rear as measured during tests of the rear pre-crash safety system for rear-end collisions.

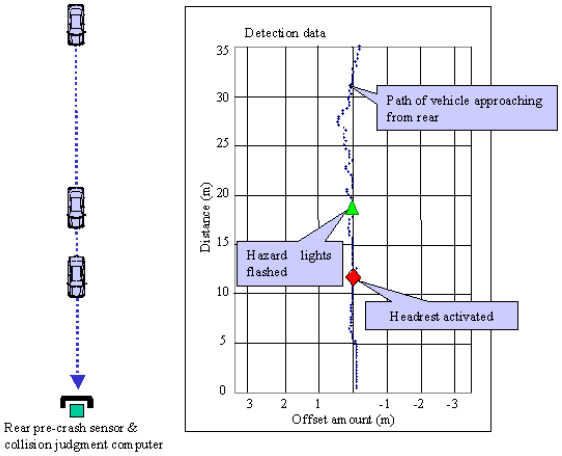

Figure 13. Actual Vehicle Experimental Data.

A vehicle was driven straight toward the pre-crash sensor at a constant speed of approximately 50 km/h. The graph shows the path of the vehicle as detected by the sensor, and the activation judgment timings for the pre-crash hazard light and pre-crash headrest functions. The test verified that the rear pre-crash sensor is capable of definitely detecting vehicles approaching from the rear.

Effect of Pre-Crash Hazard Lights – A test was performed to verify the effect of hazard light operation on the awareness of the driver in a following vehicle. Two vehicles were driven one behind the other at a speed of approximately 45 km/h and a following distance of approximately 18 m. The danger awareness reaction time (i.e., the time to brake pedal operation) of the driver in the following vehicle was then measured from the start of deceleration of the leading vehicle. It was verified that supplementing deceleration of the leading vehicle with automatic flashing of the hazard lights reduced the awareness time by approximately 20% from when the vehicle decelerated without flashing of the hazard lights (Fig. 14).

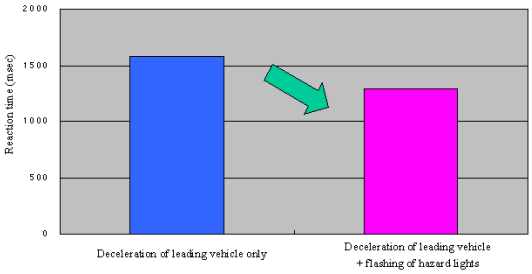

Figure 14. Reaction Time Comparison.

The effect when the vehicle equipped with the pre-crash hazard light function is stopped was obtained by calculation. The first case study in Fig. 15 examines a rear-end collision in which the vehicle approaching from the rear is traveling at approximately 60 km/h. In this case, when the provisional TTC is approximately 1.5 sec, the free running time is approximately 0.8 sec, and the vehicle approaching from the rear performs emergency braking of 6 m/sec^2, the driver is able to reduce vehicle speed to approximately 40 km/h at the point of collision. Under the same conditions, but with an approaching speed of approximately 30 km/h, the second case study in Fig. 15 shows that the driver is able to stop the vehicle before the collision occurs.

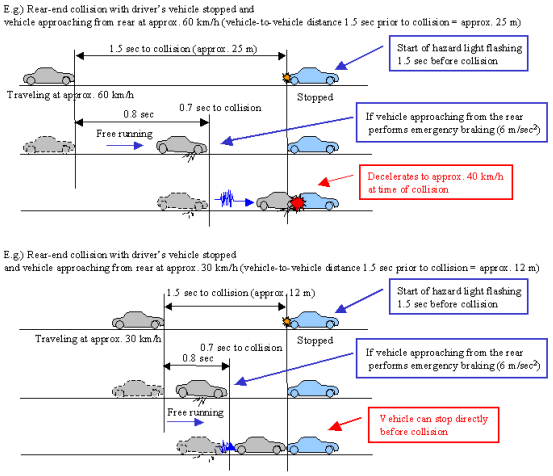

Figure 15. Case Studies.

Effect of Pre-Crash Headrest – A comparative evaluation with and without the pre-crash headrest was performed to verify its whiplash injury reduction effect. The test conditions followed the IIWPG protocol, and used a BioRID II dummy to

measure the neck injury criteria (NIC) in a Δ V16 km/h impact sled test. The test verified that use of the pre-crash intelligent headrest reduced NIC by approximately 50%.

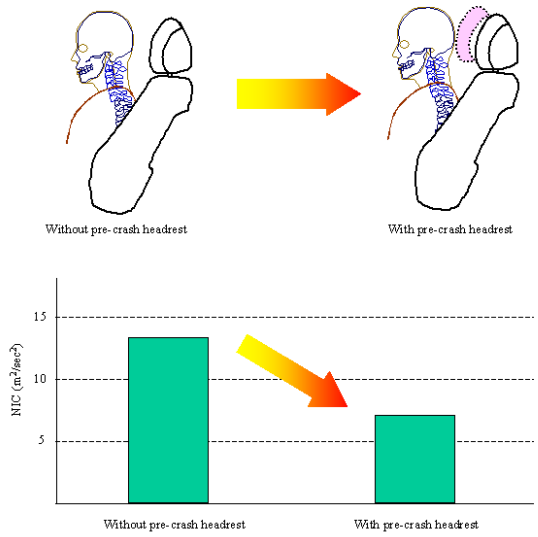

Figure 16. Whiplash Injury Evaluation.

CONCLUSIONS

A rear pre-crash safety system for rear-end collisions has been developed to lessen whiplash injury and reduce the number of rear-end collisions.
The newly developed system is able to lessen whiplash injury and reduce vehicle speed in rear-end collisions.

ACKNOWLEDGMENTS

The authors would like to extend their gratitude to all the suppliers involved in the development of this system for their substantial contribution to the development of the radar sensor, pre-crash headrest, and control computers.

REFERENCES

[1] Sekizuka. M. 1998. “Seat Designs for Whiplash Injury Lessening.” 16th ESV Conference Paper Number 98-S7-O-06.

[2] Sawada M. and Hasegawa. 2005. “Development of New Whiplash Prevention Seat.” 19th ESV Conference Paper Number 05-0288.

Japan Traffic Safety Association. 2005. “Aiming for Safe, Smooth, and Comfortable Road Traffic” (in Japanese).

The General Insurance Association of Japan. 2003. “The State of Traffic Accidents Based on Automobile Accident Insurance Data.” (in Japanese).

INFLUENCE OF VEHICLE PROPERTIES AND HUMAN ATTRIBUTES ON NECK INJURIES IN REAR-END COLLISIONS

Yoichi Watanabe
Satoko Ito
Institute for Traffic Accident Research and Data Analysis (ITARDA)
Japan
Paper Number 07-0160

ABSTRACT

While traffic accident fatalities in Japan have been declining, the number of injuries has continued on an upward trend for many years. One salient aspect of that rising trend is the number of casualties attributed to rear-end collisions. In 2005, such accidents accounted for approximately 35% of all fatalities and injuries. Regarding ordinary passenger cars, many of the drivers of the struck vehicles in rear-end collisions suffer slight neck injuries, while nearly all of the drivers of the striking vehicles are not injured. In this study, the influence of vehicle properties and human attributes on the incidence of neck injuries in rear-end collisions was analyzed using an integrated accident database developed by the Institute for Traffic Accident Research and Data Analysis (ITARDA). The results revealed, among other things, that an active head restraint system, which is one type of anti-whiplash device, is effective in suppressing the occurrence of neck injuries; that females tend to be injured more often than males; that age and generation influence the tendency for men to be injured; and that the trip purpose influences the tendency for neck injuries to occur. This tendency for generation and trip purpose to exert such an influence suggests the possibility that the health consciousness of the parties involved in rear-end collisions might affect the incidence of neck injuries. Among the other issues discussed in this paper is the concern that neck injuries due to rear-end collisions might increase in the future.

INTRODUCTION

In Japan, the number of traffic accident fatalities occurring within 24 hours totaled 11,451 in 1992. It has decreased consistently since then, falling to 7,358 in 2004 and to 6,871 in 2005. The number of fatalities occurring within 30 days has also steadily declined, dropping to 8,492 in 2004 and to 7,931 in 2005 as shown in Figure 1. This decrease is thought to result from various measures, including more extensive traffic safety education, road and vehicle improvements and better emergency medical care [1-3]. In contrast, the number of traffic accident injuries has been increasing for many years, totaling more than 1.1 million annually in recent years as shown in Figure 1, so further measures to reduce injuries are necessary.

This study focused on rear-end collisions which account for many traffic accident injuries. The situation (as of 2005) for rear-end collisions in Japan and resultant neck injuries was analyzed using an integrated accident database developed by the Institute for Traffic Accident Research and Data Analysis (ITARDA). And the influence of vehicle properties and human attributes on the incidence of neck injuries in rear-end collisions was analyzed using an integrated accident database.

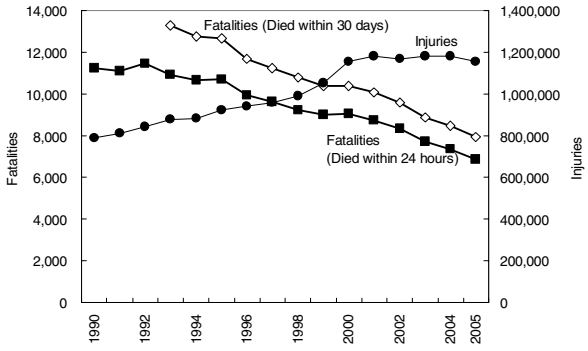

Figure 1. Trends in traffic accident fatalities and injuries.

ACTUAL SITUATION FOR REAR-END COLLISIONS AND INJURIES

Rear-end Collisions

The trends in the number of traffic accidents by type are shown in Figure 2. Rear-end collisions show a marked upward trend and have consistently been the most numerous of all types of traffic accidents since 1996. In 2005, they accounted for approximately 32% of all traffic accidents. Figure 3 shows the trends in the number of casualties by type of accident. The number of casualties occurring in rear-end collisions has also tended to increase and accounted for approximately 35% of the total in 2005.

Limiting rear-end collisions to the combination that the striking vehicle is the primary party (culpable) and the struck vehicle is the secondary party (less culpable), the number of such combinations that year was 263,993. The combinations are broken down by vehicle type in Table 1. According to the table, the number of rear-end collisions in which the striking vehicle was an ordinary passenger car was 156,324, or approximately 59%. Of them, the number of cases in which the struck vehicle was a "passenger car or truck" and "ordinary or light" was 155,502, or approximately 99%. The number of rear-end collisions in which the struck vehicle was an ordinary passenger car was 162,521, or approximately 62%, and, of them, the number of cases in which the striking vehicle was a "passenger car or truck" and "ordinary or light" was 158,129, or approximately 97%. These figures indicate that many of the striking and struck vehicles were ordinary passenger cars and that most of the other parties were passenger cars or trucks and were ordinary or light vehicles. Accordingly, the target vehicles for the subsequent analyses were limited to ordinary passenger cars whose other parties were passenger cars or trucks and were ordinary or light vehicles.

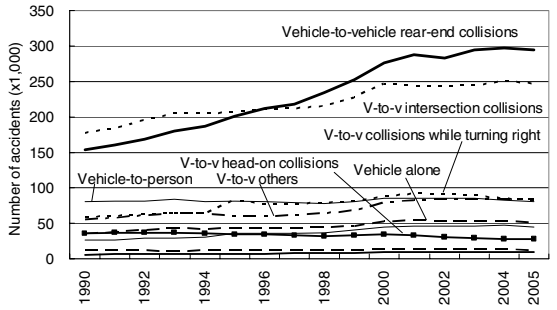

Figure 2. Trends in traffic accidents by type of accident.

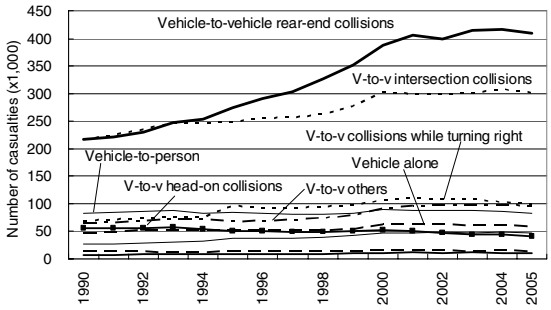

Figure 3. Trends in traffic accident casualties by type of accident.

Table 1.
Number of rear-end collisions between vehicles by vehicle classification (2005)

			Striking vehicle (primary party)								
			Passenger car				Truck				
			Bus, Minibus	Ordinary	Light	Mini-car	Large-sized special, Large-sized	Ordinary	Light	Special vehicle	Total
Struck vehicle (secondary party)	Passenger car	Bus, Minibus	25	224	61	0	30	107	24	1	472
		Ordinary	414	100,049	26,782	2	3,927	20,962	10,336	49	162,521
		Light	108	33,330	12,428	0	1,073	6,003	4,413	24	57,379
		Mini-car	0	1	3	3	0	2	3	0	12
	Truck	Large-sized special, Large-sized	9	482	154	0	733	564	92	0	2,034
		Ordinary	69	10,361	2,489	1	1,296	4,568	1,329	11	20,124
		Light	57	11,762	3,997	0	528	3,070	1,774	10	21,198
	Special vehicle		3	115	48	0	15	36	36	0	253
	Total		685	156,324	45,962	6	7,602	35,312	18,007	95	263,993

Injuries Incurred by Ordinary-passenger-car Occupants in Rear-end Collisions

The injuries incurred by ordinary-passenger-car occupants in rear-end collisions in 2005 were analyzed in the striking and struck vehicles respectively under the following assumptions:

- Target vehicles for analysis: ordinary passenger cars
- Other-party vehicle: passenger car or truck and ordinary or light vehicle
- Striking vehicle: primary party (culpable)
- Struck vehicle: secondary party (less culpable) and struck in the entire rear-end area
- Multiple collision: excluded

The first analysis focused on the drivers. Figure 4 shows that approximately 99% of the 119,678 striking-vehicle drivers were not injured. In contrast, approximately 87% of the 124,172 struck-vehicle

drivers were slightly injured, mainly in the neck, as shown in Figure 5. This suggests that attention should be paid to neck injuries in struck vehicles in rear-end collisions. On the other hand, approximately 73% of the 148,423 struck-vehicle occupants who mainly suffered neck injuries were drivers, approximately 17% of them were front-seat passengers and approximately 10% of them were rear-seat passengers as shown in Figure 6. These figures indicate that neck injuries of struck-vehicle drivers have a high priority.

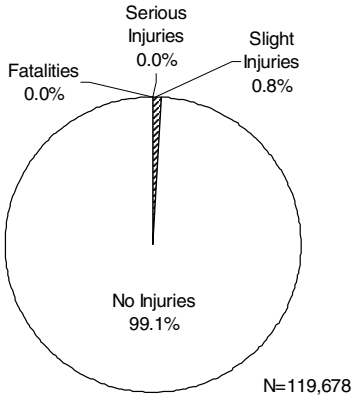

Figure 4. Injury severities of striking-vehicle drivers in rear-end collisions (ordinary passenger cars, primary parties, 2005).

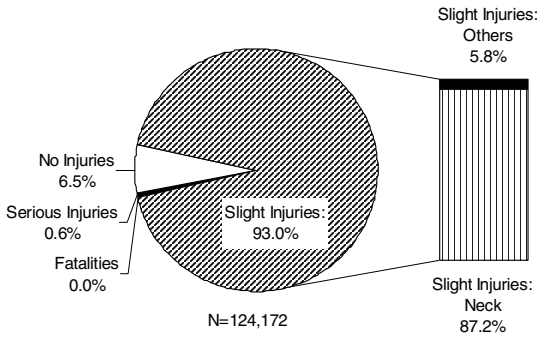

Figure 5. Injury severities of struck-vehicle drivers in rear-end collisions (ordinary passenger cars, secondary parties, 2005).

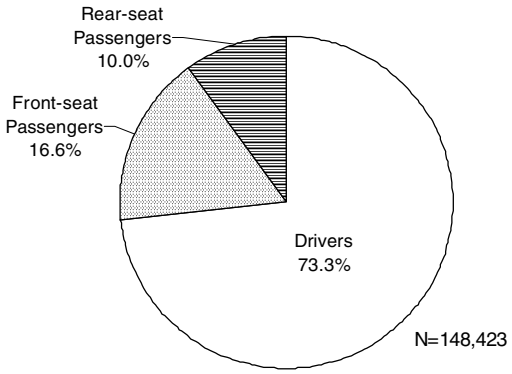

Figure 6. Seating positions of all occupants of struck vehicles in rear-end collisions (ordinary passenger cars, secondary parties, neck injured, 2005).

Neck Injury Incidence in Rear-end Collision

Measures to prevent whiplash neck injuries in struck vehicles are desired. However, the mechanism of whiplash injuries is not fully understood at present, and there are differing opinions about the mechanism causing such injuries [4-8].

DEFINITION OF NO-NECK-INJURY RATE

An analysis was made of the relation of struck-vehicle properties to neck injuries in struck vehicles, which account for the greater portion of rear-end collision casualties. The index used in the analysis was the no-neck-injury rate defined as follows, based on the injury severity of struck-vehicle drivers:

$$\text{No-neck-injury rate (\%)} = \frac{\text{No injuries}}{\text{Fatalities+ Serious/Slight injuries+ No injuries}} \times 100$$

Casualties (fatalities, serious injuries and slight injuries) were restricted to those that mainly involved neck injuries. The types of serious and slight injuries were limited to sprains, dislocations or fractures in order to focus on injuries thought to be whiplash or an extension thereof. It will be noted that this index is used only for drivers because only drivers, as a rule, are counted among the no-injury vehicle occupants in ITARDA's integrated accident database.

INFLUENCE OF STRUCK-VEHICLE PROPERTIES

The struck-vehicle properties analyzed in this study with this index were the initial year of registration and presence/absence of an anti-whiplash device.

Relation to Initial Year of Registration

Method and Data - An investigation was made of whether neck injuries were apt to occur in newer struck vehicles, in view of the upward trend for casualties in rear-end collisions as shown in Figure 3. The relationship between the initial year of registration and the no-neck-injury rate of drivers in struck vehicles was analyzed using the integrated accident database. Each passenger car class was analyzed separately because the differing shapes and weights of different vehicle classes would affect the no-neck-injury rate. The definitions of the passenger car classes used by ITARDA are shown in Table 2. The analysis focused on rear-end collisions in 2004 that met the following conditions:

- Struck vehicle: secondary party and struck in the entire rear-end area
- Striking vehicle: passenger car or truck, ordinary or light , and primary party
- Multiple collision: excluded

Results - The results in Figure 7 show that there was no tendency for the no-neck-injury rate of struck-vehicle drivers to decrease with a later initial year of registration of the struck vehicle. On the contrary, for the Sedan-B class (engine displacement of 1500-2000 cc) and the Sedan-C class (engine displacement of over 2000 cc), the no-neck-injury rate tended to increase with a later initial year of registration of the struck vehicle.

Table 2.
Definitions of passenger car classes

Passenger car class
Family-Light
Sedan-A (engine displacement of under 1500 cc)
Sedan-B (engine displacement of 1500-2000 cc)
Sedan-C (engine displacement of over 2000 cc)
Sports & Speciality
Wagon
1-Box & Minivan
SUV (Sport-utility vehicle)

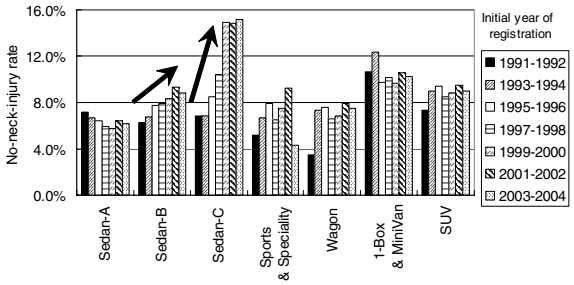

Figure 7. Relationship between no-neck-injury rate and initial year of registration of struck vehicles in rear-end collisions (ordinary passenger cars, secondary parties, 2004).

Effect of an Anti-whiplash Device: Analysis Based on No-neck-injury Rate

Method and Data - To examine the effect of an anti-whiplash device, which has been spreading in recent years, vehicle models meeting the following requirements were selected, and the difference in the no-neck-injury rate between drivers of vehicles with and without such a device was analyzed.

- Ordinary passenger car with and without an anti-whiplash device (To exclude body influences such as the crash characteristics of the rear end)
- The device is not an option. (To eliminate driver consciousness of whiplash)
- Presence of the device can be clearly distinguished according to the model code. (To calculate the no-neck-injury rate in the presence of the device)
- Vehicle models with and without the device were put on the market by 1999. (To secure a sufficient volume of accident data)

Only one vehicle model meeting these requirements was found. This vehicle was Sedan-C put on the market in 1996. The anti-whiplash device fitted on this vehicle was an active head restraint (AHR) system [9]. An AHR system was not provided initially and became standard equipment on all models of this vehicle in the latter half of 1998.

The analysis focused on rear-end collisions occurring over five years from 2000 to 2004 and meeting the following conditions:

- Struck vehicle: the above-mentioned vehicle model, struck in the entire rear-end area, and secondary party
- Striking vehicle: passenger car or truck, ordinary or light, and primary party
- Multiple collision: excluded

Results - Under the conditions above, the numbers of drivers incurring mainly neck injuries or no injuries in this vehicle are shown in Table 3. Of 760 drivers, 105 suffered neck injuries with the AHR and 21 reported no injuries, whereas 587 incurred injuries without the AHR and 47 reported no injuries. The no-neck-injury rate with the AHR (16.7%) was higher than that without the AHR (7.4%) as shown in Table 3 and Figure 8.

A two-sample test for equality of proportions was conducted between these no-neck-injury rates. The test statistic Z is given by:

$$Z = | p_1 - p_2 | / \sqrt{p(1 - p)(1/n_1 + 1/n_2)}$$

where,

$$p = (n_1 p_1 + n_2 p_2) / (n_1 + n_2)$$

According to these formulas, Z was 3.324, which means that the P-value in the two-sided test was 0.0009. These figures show that the no-neck-injury rate with the AHR was higher than that without the AHR at the 1% significance level.

Table 3.
Incidence of casualties and no injuries with/without AHR and results of statistical analysis

	with AHR	w/o AHR
Fatal neck injuries	0	0
Serious neck injuries (sprains, dislocations, fractures)	1	4
Slight neck injuries (sprains, dislocations, fractures)	104	583
No injuries/ Overall	21	47
Total	126	634
No-neck-injury rate	16.7%	7.4%
Z-statistic	3.324	
P-value	0.0009 (<0.01)	

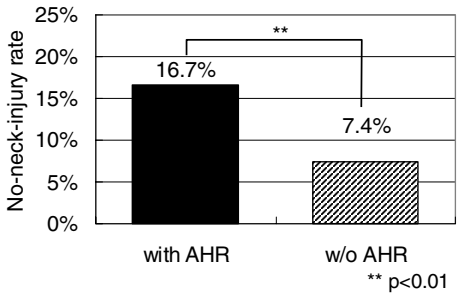

Figure 8. Influence of AHR on no-neck-injury rate.

Results of Additional Analysis Following Classification of Factors - In the preceding discussion, it was statistically confirmed that the presence of an AHR influences the no-neck-injury rate. However, other factors that might influence the incidence of neck injuries in rear-end collisions, such as impact severity, gender and age, were not considered. For that reason, an investigation was made of whether there was a large difference in the composition of the factors in relation to the presence of an AHR. The results are shown in Figures 9 to 11. Pseudo-ΔV [10] is used as an index in Figure 9 to indicate the impact severity in a rear-end collision. Pseudo-ΔV of a struck vehicle can be calculated with the following equation, based on the struck-vehicle impact speed V_1, struck-vehicle weight M_1, striking-vehicle impact speed V_2 and striking-vehicle weight M_2 as shown in Figure 12.

$$\text{Pseudo-}\Delta V = V - V_1$$

$$= (M_1 V_1 + M_2 V_2) / (M_1 + M_2) - V_1$$

$$= (V_2 - V_1) M_2 / (M_1 + M_2)$$

Here, V means the speed of both vehicles after a rear-end collision and is assumed as follows:

- The coefficient of rebound is 0 (e = 0).
- The impact speed is equal to the speed reported by the driver.
- The vehicle weight is equal to the unladen vehicle weight.

The results in Figures 9 to 11 indicate that there was no large difference in the composition of these factors due to the presence of an AHR, so it can be concluded that the factors did not influence the

no-neck-injury rate. Moreover, after classifying the 760 persons in Table 3 separately according to each factor, additional analyses were conducted for the sake of reference.

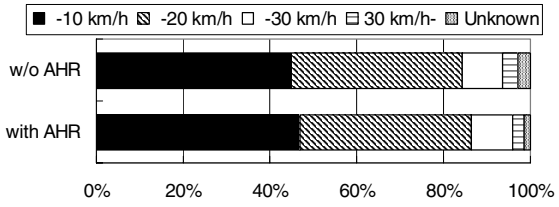

Figure 9. Distribution of pseudo-ΔV with/without AHR.

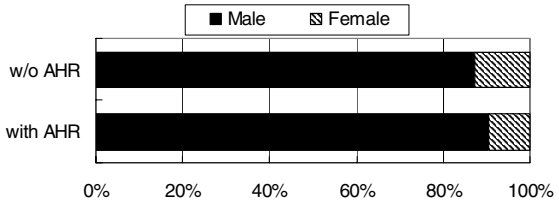

Figure 10. Distribution of gender with/without AHR.

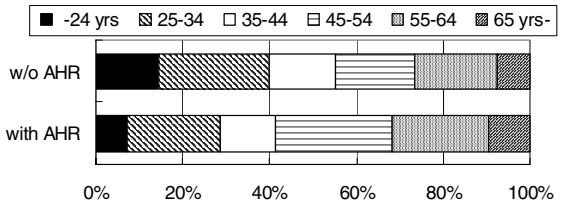

Figure 11. Distribution of age with/without AHR.

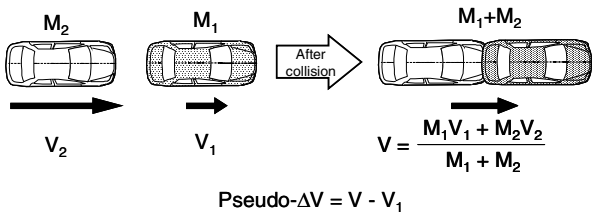

Figure 12. Definition of pseudo-ΔV.

The results of a comparison of the no-neck-injury rate according to the presence of an AHR in each group into which the 760 persons were divided on the basis of pseudo-ΔV are shown in Figure 13. It is seen that the no-neck-injury rate with an AHR was statistically higher than that without an AHR for the 0–10 km/h group and the 11–20 km/h group that accounted for the majority of the 760 persons. It was significantly higher at the 5% significance level for the 0–10 km/h group. For the 11–20 km/h group, it was significantly higher at the 1% significance level. As for the 21–30 km/h group, it is observed that the no-neck-injury rate with an AHR was higher than that without an AHR, but no statistically significant difference can be confirmed because of the limited data. As a whole, it can be concluded that the no-neck-injury rate with an AHR was higher than that without an AHR even when the influence of the impact severity in the collision was eliminated.

Figure 14 presents the results for the no-neck-injury rate when a comparison was made by gender in relation to the presence of an AHR, after the 760 persons were distinguished by gender. For males, it was confirmed that the no-neck-injury rate with an AHR was higher than that without an AHR at the 1% significance level. As for females, the no-neck-injury rate with an AHR was higher than that without an AHR, though no statistically significant difference can be confirmed because of the limited data. Overall, it can be inferred that the no-neck-injury rate with an AHR was higher than that without an AHR even after excluding the influence of gender.

Figure 15 shows that the no-neck-injury rate with an AHR was higher than that without an AHR for each age group into which the 760 persons were divided according to age (Figure 11). A statistically significant difference was confirmed only for the 24-or-younger group at the 1% significance level, because of the limited data for the other groups. Considering the group from 25 to 64 years old, the no-neck-injury rate with an AHR was also higher than that without an AHR at the 5% significance level as shown in Figure 16. On the whole, it would appear that the no-neck-injury rate with an AHR was higher than that without an AHR even when the influence of age was removed.

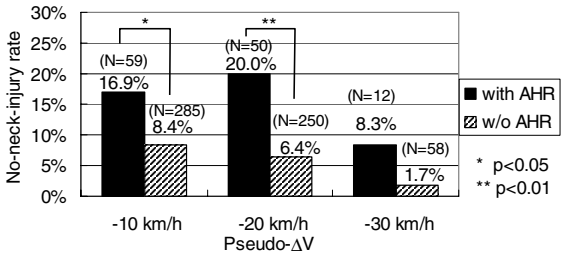

Figure 13. Influence of AHR on no-neck-injury rate by pseudo-ΔV.

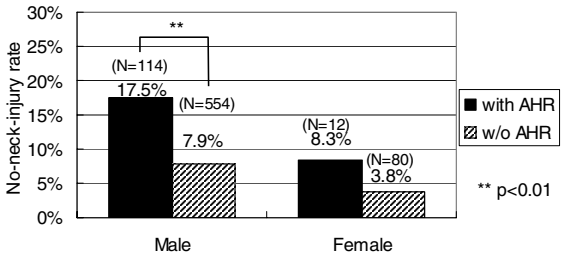

Figure 14. Influence of AHR on no-neck-injury rate by gender.

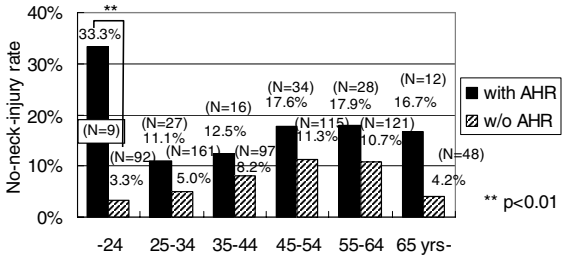

Figure 15. Influence of AHR on no-neck-injury rate by age (divided into six age groups).

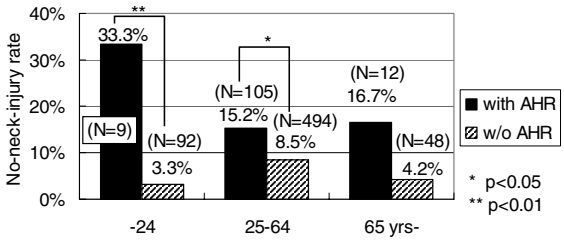

Figure 16. Influence of AHR on no-neck-injury rate by age (divided into three age groups).

Effect of an Anti-whiplash Device: Regression Analysis

Method and Data - In the preceding analysis, the influence of each factor was separately excluded when the no-neck-injury rate was calculated in order to analyze the effect of an AHR. A regression analysis was then conducted in which all of the factors, including the presence/absence of an AHR, were treated at the same time. As the neck injury severity is a qualitative variable and also a ranked variable, an ordered response model was used in the analysis [11]. It was decided to treat the neck injury severity as a binary response of neck injuries (fatalities, serious or slight injuries principally to the neck) or no injuries. An explanation is given here of the method for conducting a regression analysis using an ordered response model. With an ordered response model, it is assumed that there is a latent factor Y^*_i which is a continuous variable that determines whether the neck injury severity Y_i is 1 (neck injury) or 0 (no injury). In this analysis, it is assumed that there is a linear relation between the continuous latent factor Y^*_i indicating the neck injury severity and the explanatory variables, including $X_{k,i}$ (k=1,2,3, …), pseudo-ΔV, which are considered as independent variables. Then, Y^*_i can be expressed with the following equations.

$$Y^*_i = z_i + \varepsilon_i$$

$$z_i = \beta_0 + \beta_1 X_{1,i} + \beta_2 X_{2,i} + \beta_3 X_{3,i} + \ldots + \beta_k \text{PseudoΔV}$$

where,

$$Y_i = \begin{cases} 1 \text{ (neck injury): in the case of } Y^*_i > 0 \\ 0 \text{ (no injury): in the case of } Y^*_i \le 0 \end{cases}$$

z_i is a value which can be explained by $X_{1,i}$, $X_{2,i}$, $X_{3,i}$, …, $X_{k,i}$ and pseudo-ΔV. ε_i is a residual value. $X_{1,i}$, $X_{2,i}$, $X_{3,i}$, …, $X_{k,i}$ are explanatory variables and have a value of either 0 or 1 if they are dummy variables. β_0, β_1, β_2, β_3, …, β_k are constant values which express the degree of influence of each explanatory variable on Y^*_i. The cumulative distribution function F of $-\varepsilon_i$ is assumed to be the logistic distribution given in the following equation.

$$F = e^z / (1 + e^z)$$

Here, the explanatory factors are with/without an AHR, gender (male, female), age (24 years or younger, 25-34 years, 35-44 years, 45-54 years, 55-64 years, 65 years or older) and pseudo-ΔV. These factors, except pseudo-ΔV, are treated as dummy variables which have a value of either 0 or 1. A combination of without an AHR, male and 24 years or younger is assumed to be the standard combination, and the analysis is conducted. Concretely, k is set from 0 to 8, and $X_{1,i} = X_{2,i} = \ldots = X_{7,i} = 0$ in the standard combination. $X_{1,i} = 1$ with an AHR. $X_{2,i} = 1$ in the case the gender is female. $X_{3,i} = 1$ when the age is 25-34 years, $X_{4,i} = 1$ when 35-44 years, $X_{5,i} = 1$ when 45-54 years, $X_{6,i} = 1$ when 55-64 years, and $X_{7,i} = 1$ when the age is 65 years or older.

The data for 21 of the 760 persons extracted in the preceding analysis were omitted in this analysis because of uncertain pseudo-ΔV. The data of the remaining 739 persons were used in the regression analysis conducted with the ordered response model. The constant values of β_0, β_1, β_2, β_3, ..., β_8 were estimated by the maximum likelihood method, using the TSP 5.0 statistical analysis software [12].

Results - The results of the analysis are presented in Table 4 and Figure 17. The estimated values are the results of an estimation of the coefficient β_k. A likelihood ratio test was carried out to evaluate the null hypothesis, assuming that all the estimated values were equal to 0. The 2LL result of this test was 22.85, which was statistically significant because it was larger than 20.1 of the 1% chi-square of 8 degrees of freedom. The fraction of correct predictions was 0.912. Therefore, it can be concluded that the regression equation consisting of the explanatory variables such as with/without an AHR, gender, age and pseudo-ΔV is significant.

As for the effect of an AHR, the estimated coefficient with an AHR was negative at -0.871, and the t-statistic was -2.97, which satisfied the 1% significance level in the two-sided test. This indicates that Y^*_i becomes smaller and that the possibility of no injury increases when an AHR is installed.

Table 4.
Estimated results of regression analysis using an ordered response model (Standard=without AHR, male, 24 years or younger)

			Estimated	Std. Error	t-statistic	P-value	
Constant		β_0	2.417	0.472	5.115	0	
with AHR		β_1	-0.871	0.293	-2.970	0.003	**
Female		β_2	0.800	0.539	1.483	0.138	
Age	25-34 yrs	β_3	0.108	0.537	0.202	0.840	
	35-44 yrs	β_4	-0.514	0.542	-0.949	0.342	
	45-54 yrs	β_5	-0.785	0.497	-1.579	0.114	
	55-64 yrs	β_6	-0.564	0.504	-1.119	0.263	
	65 yrs or older	β_7	-0.018	0.678	-0.026	0.979	
Pseudo-ΔV(km/h)		β_8	0.036	0.019	1.834	0.067	

Number of observations = 739
Log likelihood L = -208.639
2LL= 22.85
Fraction of correct predictions = 0.912
Log likelihood L_0 = -220.063
** : p<0.01

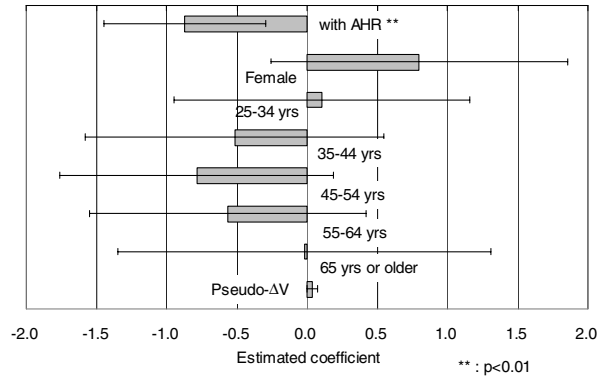

Figure 17. Estimated coefficients and 95% confidence intervals.

INFLUENCE OF HUMAN ATTRIBUTES OF STRUCK-VEHICLE DRIVERS

Regression Analysis

Method and Data - A regression analysis was conducted to examine the influence of human attributes, such as gender, age and trip purpose, on the incidence of neck injuries suffered by the drivers of the struck vehicles in rear-end collisions. The vehicles considered in the analysis were ordinary passenger cars of the Sedan-A class (engine displacement of under 1500 cc) in the passenger car classes (Table 2). The accidents analyzed were limited to rear-end collisions in 2004 between vehicles that met the following conditions:

- Struck vehicle: secondary party and struck in the entire rear-end area
- Striking vehicle: passenger car or truck, ordinary or light , and primary party

- Multiple collision: excluded
- Pseudo-ΔV of the struck vehicle: 30 km/h or less.

The Sedan-A class was selected as the target vehicle category for analysis because it accounted for the largest number of accidents of the above-mentioned type among the seven classes of ordinary passenger cars (excluding Family-Light) in Table 2. It was also confirmed that the pseudo-ΔV of the Sedan-A class was 30 km/h or less in more than 90% of the cases.

Among the rear-end collisions analyzed, there were a total of 18,718 cases in which the driver of the struck vehicle mainly suffered a neck injury or was not injured. In order to restrict neck injuries to those presumed to be whiplash or an extension thereof, as was done in the analysis of vehicle properties, the types of serious and slight injuries treated here were limited to sprains, dislocations or fractures.

Similar to the analysis of vehicle properties, an ordered response model was used to conduct a regression analysis of the data for the 18,718 struck-vehicle drivers. The objective variable used in the analysis was neck injury severity, which was treated in terms of a binary response of neck injuries or no injuries.

The explanatory variables used were gender (male or female), age group (six age groups of 24 years or younger, 25-34 years, 35-44 years, 45-54 years, 55-64 years, 65 years or older), trip purpose (private trip, business trip, commuting to work, commuting to school) and pseudo-ΔV. Twelve combinations of gender and age (2x6=12) were considered: male/24 years or younger, male/25-34 years, male/35-44 years, …, female/55-64 years, and female/65 years or older. These twelve combinations and trip purpose were treated as dummy variables having a value of either 0 or 1. A combination of male/24 years or younger and a private trip was regarded as the standard combination in conducting the analysis. Specifically, in the regression equation formulated for the analysis of vehicle properties, k was set at values from 0 to 15, and $X_{1,i} = X_{2,i} = \ldots = X_{13,i} = X_{14,i} = 0$ was set in the standard combination. For the combination of male/25-34 years, $X_{1,i} = 1$, for male/35-44 years, $X_{2,i} = 1$, …, for female/55-64 years, $X_{10,i} = 1$ and for female/65 years or older, $X_{11,i} = 1$. With respect to the trip purpose, $X_{12,i} = 1$ for a business trip, $X_{13,i} = 1$ for commuting to work and $X_{14,i} = 1$ for commuting to school.

Results - The results of the regression analysis are shown in Table 5 and Figure 18. A likelihood ratio test of the regression equation produced a 2LL result of 613.4, which satisfied the 30.6 value of the 1% chi-square for 15 degrees of freedom. It can be concluded therefore that the regression equation consisting of the explanatory variables of gender, age group, trip purpose and pseudo-ΔV was significant. The fraction of correct predictions was 0.936.

Table 5.
Estimated results of regression analysis using an ordered response model (Standard=male/24 years or younger, private trip)

			Estimated	Std. Error	t-statistic	P-value	
Constant		β_0	2.031	0.137	14.806	0.000	**
Gender, Age	Male, 25-34 yrs	β_1	0.133	0.149	0.893	0.372	
	Male, 35-44 yrs	β_2	-0.058	0.154	-0.373	0.709	
	Male, 45-54 yrs	β_3	-0.221	0.155	-1.426	0.154	
	Male, 55-64 yrs	β_4	-0.482	0.146	-3.293	0.001	**
	Male, 65 yrs or older	β_5	-0.704	0.147	-4.799	0.000	**
	Female, 24 yrs or younger	β_6	0.457	0.188	2.424	0.015	*
	Female, 25-34 yrs	β_7	1.191	0.183	6.503	0.000	**
	Female, 35-44 yrs	β_8	0.665	0.172	3.865	0.000	**
	Female, 45-54 yrs	β_9	0.629	0.163	3.858	0.000	**
	Female, 55-64 yrs	β_{10}	0.825	0.182	4.531	0.000	**
	Female, 65 yrs or older	β_{11}	1.037	0.290	3.573	0.000	**
Purpose	Business trips	β_{12}	0.954	0.132	7.250	0.000	**
	Commuting to work	β_{13}	1.665	0.151	11.013	0.000	**
	Commuting to school	β_{14}	1.536	1.013	1.516	0.129	
Pseudo-ΔV(km/h)		β_{15}	0.019	0.004	4.324	0.000	**

Number of observations = 18,718
Log likelihood L = -4142.53
2LL= 613.41
Fraction of correct predictions = 0.939
Log likelihood L_0 = -4449.24
* p<0.05 ** p<0.01

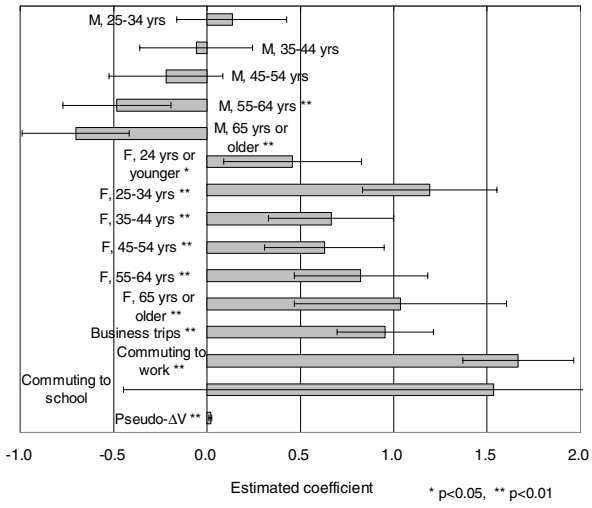

Figure 18. Estimated coefficients and 95% confidence intervals.

Comparisons were then made with the standard combination (male/24 years or younger) with respect to gender and age group. The estimated regression coefficients for male/55-64 years and male/65 years or older were negative at -0.482 and -0.704, respectively, and both values satisfied the 1% significance level in a two-sided test. This indicates that for males aged 55 years or older, Y^*_i becomes smaller, which means the possibility of no neck injury increases. The estimated regression coefficients for all the female age groups were positive, and all the values satisfied the 1% significance level in a two-sided test. Looking at the results for males and females in general, female drivers showed much larger, positive regression coefficients than their male counterparts, which suggests that female drivers of struck vehicles have a higher likelihood of suffering a neck injury in a rear-end collision. Focusing on differences attributable to the age group among females, no pronounced tendencies are seen. It can be inferred that age did not have any appreciable influence on the overall results.

Trip purposes were compared with the standard of private trips. Business trips and commuting to work showed positive estimated regression coefficients of 0.954 and 1.665 respectively. Both values satisfied the 1% confidence level in a two-sided test. These values indicate that Y^*_i becomes larger for business trips and commuting to work, compared with private trips, which means there is a greater possibility of suffering a neck injury. No significant difference was observed for commuting to school.

The foregoing analysis results can be summed up as follows:

a. Females are more likely to be injured than males.
b. Younger males are more likely to be injured than older ones.
c. Age does not have any influence in the case of females.
d. Drivers are more likely to be injured on business trips or when commuting to work than on private trips.

Cohort Analysis

Method and Data - It is known that when occupants are injured in a traffic accident, their likelihood of suffering a fatal or serious injury increases with age. The reason for that is attributed to an aging-related decline in the body's tolerance of the shock or force resulting from an impact [13-15]. Among the results of the regression analysis described above, the finding noted in (b) "younger males are more likely to be injured than older ones" would seem to run counter to that general trend. Nearly all of the accident cases analyzed involved slight neck injuries, which need not be viewed in the same light as fatal or serious injuries. Nonetheless, this contrary tendency aroused interest because of its seeming peculiarity. It was presumed that some other latent factor besides age was at work here. In order to examine that hypothesis, a cohort analysis was conducted separately for males and females.

The struck vehicles considered in the analysis were ordinary passenger cars of the Sedan-A class in the passenger car classes. The accidents analyzed were limited to rear-end collisions in 2004 between vehicles that satisfied the following conditions:

- Struck vehicle: secondary party and struck in the entire rear-end area
- Striking vehicle: passenger car or truck, ordinary or light , and primary party
- Multiple collision: excluded

The birth year of the struck-vehicle drivers was defined as the year obtained by subtracting the person's age at the time of the accident from the year in which the accident occurred. On the basis of their birth year, struck-vehicle drivers were divided into age groups in four-year increments. A time history of the no-neck-injury rate in rear-end collisions was found for each age group at four-year intervals of 1992, 1996, 2000 and 2004.

Results - The cohort analysis results are shown separately for males and females in Figures 19 and 20, respectively. A comparison of the results for the two genders shows that the no-neck-injury rate was lower for females in general. This provides additional confirmation of the regression analysis finding noted above in (a) "females are more likely to be injured than males".

For males with a birth year of 1951 or earlier (referred to here as the older generation), the time histories of their no-neck-injury rate did not show much change or revealed a rising trend. The histories nearly overlapped one another and showed continuity (circle A in Figure 19). Accordingly, it was concluded that, within this older generation, the time history patterns of the no-neck-injury rate did not differ appreciably from one age group to another.

On the other hand, for males having a birth year of 1952 or after (referred to here as the younger generation), the time histories of their no-neck-injury rate revealed a downward trend. The histories did not overlap and discontinuities were seen (circle B in Figure 19). The patterns differed from those of the older generation. In other words, the time histories of the no-neck-injury rate showed different patterns between the generations.

This suggests that one cannot make a simple assertion based only on age that "younger males are more likely to be injured than older ones", as mentioned in (b) in the summary above. It can be inferred that generational and time period differences, including related traffic and societal circumstances, also probably exert an influence on neck injuries in rear-end collisions. It is presumed that such influence gave rise to the tendencies seen in the cohort analysis results for the younger generation to have a lower no-neck-injury rate than the older generation and for that trend to become more pronounced with increasing age.

For females, the no-neck-injury rates in Figure 20 are nearly constant regardless of age or generation, excluding the results for those aged 69 years or older, for which large scatter is seen because of the small number of data. These results provide additional confirmation of the regression analysis finding mentioned above in (c) "age does not have any influence in the case of females". Moreover, the results also show virtually no influence of generation, a tendency that differs from the results seen for males.

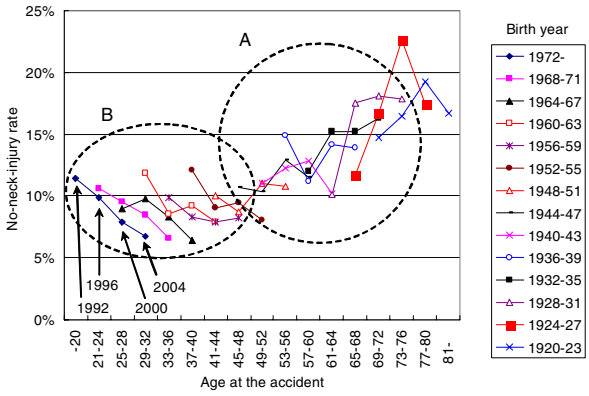

Figure 19. No-neck-injury rate by age and birth year for males (Sedan-A class, secondary parties).

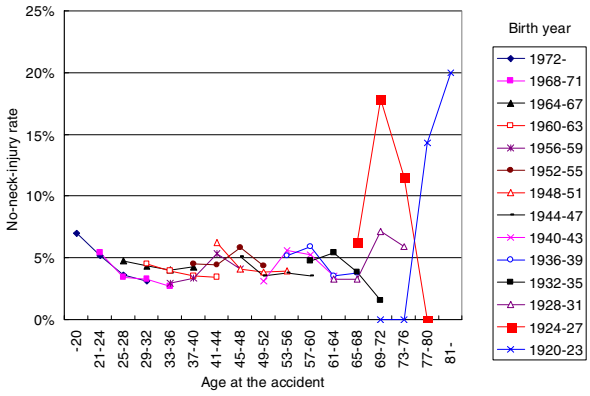

Figure 20. No-neck-injury rate by age and birth year for females (Sedan-A class, secondary parties).

For the sake of reference, nearly the same tendencies were found when the same analysis was performed for the other passenger car classes, with the exception of large scatter that was observed for a small number of cases.

Discussion of the Influence of Human Attributes of Struck-vehicle Drivers

Human attributes such as gender, age, generation and trip purpose were shown to influence the incidence of neck injuries in rear-end collisions. From a biomechanics perspective, it is easy to understand that gender or age might influence the incidence of neck injuries inasmuch as the body's tolerance of the resultant impact severity or force of a collision can vary depending on differences in these attributes. On the other hand, an attempt to discuss the influence of

generation from a biomechanics standpoint lacks persuasiveness, although one can consider, for example, that the body's tolerance may change depending on variation in such factors as the living environment or diet. Moreover, the influence of the trip purpose can no longer be discussed from a biomechanics perspective. It might be more appropriate to assume that the influence of generation or trip purpose is due to some reason other than biomechanics considerations.

This investigation focused on whether neck injuries occurred or not in rear-end collisions. Injuries requiring long-term care and those involving simply an examination by a doctor just to be on the safe side were both treated in the same manner. Consequently, the findings may have been influenced by the health consciousness of the parties involved. If that led to the results seen concerning the influence of generation or trip purpose on the incidence of neck injuries, it would make such tendencies easier to understand. Earlier studies [16-18] pointed out the possibility of results being influenced by the health consciousness of the parties involved, and such a possibility certainly cannot be ruled out in this study that looked at whether injuries occurred or not. However, it is a fact that many people incur neck injuries in rear-end collisions or suffer from subsequent complications. It is strongly felt that all of neck injuries should not be ascribed simply to the health consciousness of the parties involved in the accidents.

If the no-neck-injury rate tendency seen here for males of the younger generation continues in the future, it will cause the rate to decline for males in general. Unless measures are taken to prevent neck injuries in rear-end collisions, there is concern that the incidence of such injuries may increase in the coming years.

CONCLUSION

The following results were obtained in this analysis of neck injuries in rear-end collisions in Japan using the integrated accident database developed by ITARDA.

Regarding Struck-vehicle Properties

- It was shown that the no-neck-injury rate of struck-vehicle drivers did not tend to decrease with a later initial year of registration of the struck vehicles. On the contrary, in some passenger car classes, the no-neck-injury rate tended to increase with a later initial year of registration of the struck vehicles.
- After eliminating various factors which were thought to influence the incidence of neck injuries, it was found that an active head restraint (AHR) system, which is one type of anti-whiplash device, was effective in suppressing the incidence of neck injuries in struck-vehicle drivers, though the verification was based on just one vehicle model. The various factors eliminated were the crash characteristics of the struck vehicle, impact severity estimated from the weight and impact speed of the striking and struck vehicles, and drivers' gender, age and consciousness of whiplash.

Regarding the Human Attributes of Struck-vehicle Drivers

- Females were more likely to be injured than males.
- For males, age and generation influenced the incidence of neck injuries. The younger generation (those having a birth year of 1952 or later) were more likely to be injured than the older generation (having a birth year before 1952), and that tendency became even stronger as they grow older.
- For females, age and generation did not show any influence.
- The trip purpose exerted an influence in that drivers were more likely to be injured on business trips or while commuting to work than on private trips.
- Among these findings, the influence of generation and trip purpose was difficult to explain from a biomechanics perspective. There was a possibility that the health consciousness of the parties involved influenced whether some injuries were reported or not. However, it is indisputable that many people incur neck injuries in rear-end collisions or suffer from subsequent complications. There is a strong feeling that all of neck injuries should not be ascribable merely

to the health consciousness of the parties involved.

- If the tendency seen for the no-neck-injury rate of males continues in the future, there is concern that the incidence of neck injuries may increase in the coming years.

The incidence of no injuries in property damage accidents are not reflected in the no-neck-injury rate used in this study because of limitations of the integrated accident database. The accuracy of analyses based on the no-neck-injury rate could be further improved by using a database that included the incidence of no injuries in property damage accidents such as the database of the automobile insurance industry.

There is also a need to undertake studies based on data for more narrowly defined injury severity categories, such as investigations that focus on the number of days required for treatment, for example. Such an approach might yield insights that reduce the possible influence of the health consciousness of the parties involved.

ACKNOWLEDGMENTS

The authors wish to thank Dr. Munemasa Shimamura of the Chiba Institute of Science for his useful advice about conducting a regression analysis using an ordered response model.

REFERENCES

1. T Suzuki and K Hagita, Analysis of the reason the number of traffic fatalities decreased to 7,358 persons (in Japanese), Proceedings of 8th ITARDA Annual Seminar, p3-20, 2005

2. K Mashiko, H Matsumoto, Y Hara, Y Sakamoto, K Takei, Y Ueno and Y Tomita, Present status and future perspectives of emergency medical service system for traffic accident (in Japanese), Proceedings of Society of Automotive Engineers of Japan “Challenges for making traffic fatalities and casualties zero” in GIA dialogue 2005, p39-44, 20054653, 2005

3. Cabinet Office, WHITE PAPER on traffic safety in Japan 2005, 2005

4. H J Mertz and L M Patrick, Strength and Response of the Human Neck, SAE 710855, 1971

5. T Matsushita, T B Sato and K Hirabayashi, X-Ray Study of the Human Neck Motion Due to Head Inertia Loading, SAE 942208, 1994

6. K Ono, K Kaneoka, A Wittek and J Kajzer, Cervical injury mechanism based on the analysis of human cervical vertebral motion and head-neck-torso kinematics during low speed rear impacts, SAE 973340, 1997

7. O Bostrom, M Y Svensson, B Aldman, H A Hansson, Y Haland, P Lovsund, T Seeman, A Suneson, A Saljo and T Ortengren, A new neck injury criterion candidate - based on injury findings in the cervical spinal ganglia after experimental neck extension trauma, Proceedings of 1996 International IRCOBI conference on the Biomechanics of impact, p123-136, 1996

8. M Y Svensson, B Aldman, H A Hansson, P Lovsund, T Seeman, A Suneson and T Ortengren, Pressure effects in the spinal canal during whiplash extension motion; A possible cause of injury to the cervical spinal ganglia, Proceedings of 1993 International IRCOBI conference on the Biomechanics of impact, p189-200, 1993

9. Japan Automobile Manufacturers Association, Inc. (JAMA), Anti-whiplash head restraint (in Japanese), http://www.jama.or.jp/safe/technique/technique_6b.html

10. M Shimamura, M Yamazaki and G Fujita, Method to evaluate the effect of safety belt use by rear seat passengers on the injury severity of front seat occupants, Accident Analysis and Prevention Vol.37, issue1, p5-17, 2005

11. K Nawata, Probit Logit Tobit, A Maki, et al., Applied econometrics II (in Japanese), Section 4, p237-270, Taga-Shuppan, 1997

12. TSP Japan, Guide for TSP 5.0, 2005

13. Institute for Traffic Accident Research and Data Analysis (ITARDA), Injury situation of elderly drivers (in Japanese), ITARDA INFORMATION No.41, 2003

14. M Shimamura, H Ohhashi and M Yamazaki ,The effects of occupant age on patterns of rib fractures to belt-restrained drivers and front passengers in frontal crashes in Japan, Stapp Car Crash Journal, Vol. 47, p349-365, 2003-22-0016, 2003

15. E Bergeron, A Lavoie, D Clas, L Moore, S Ratte, S Tetreault, J Lemaire and M Martin, Elderly trauma patients with rib fractures are at greater risk of death and pneumonia, The journal of TRAUMA: injury, infection, and critical care, Vol.54, No.3, p478-485, 2003

16. S Nakagama, Y Kondoh and K Mori, Analysis of injuries with sequelae in Japanese traffic accidents (in Japanese), Proceedings of Society of Automotive Engineers of Japan, No.117-01, p17-20, 20015407, 2001

17. N Ichihara, Y kondoh and K Okamura, Analysis of insurance payment data by type of accident and kind of vehicle in Japan (in Japanese), Proceedings of Society of Automotive Engineers of Japan, No.7-03, p1-4, 20035094, 2003

18. T Ohori, Study of increase of slight injury accidents because of cervical sprains (in Japanese), Research report of Sagawa Traffic Society Foundation, Vol.21, p103-113, 2006

ASSESSING THE BioRID II REPEATABILITY AND REPRODUCIBILITY BY APPLYING THE OBJECTIVE RATING METHOD (ORM) ON REAR-END SLED TESTS

Linda Eriksson
Autoliv Sverige AB
Sweden
Harald Zellmer
Autoliv B.V. & Co. KG, Elmshorn
Germany
Paper Number 07-0201

ABSTRACT

The BioRID II seems to be the most biofidelic dummy for low-speed rear-end crash tests and is therefore included in several proposed test methods. However, to be broadly accepted, the repeatability and reproducibility of the BioRID II must be verified.

This study aims to assess the BioRID II repeatability and reproducibility by applying the Objective Rating Method (ORM) to rear-end sled tests. The ORM compares crash tests in terms of correlations between criteria, peak values, peak value occurrence times, and curve shapes. Correlations are calculated for all dummy readings and criteria, and for the complete dummy.

Thirty tests were included in this study. These were divided into twelve sets with two to four tests each. The tests within each set mirrored each other, and were used to assess the BioRID II repeatability and reproducibility. The tests were conducted at two crash-test sites. Four BioRID II dummies, five different seats, and three crash pulses were used. Both criteria and dummy readings were compared.

The BioRID II repeatability, in terms of ORM-values, ranged from 83 to 90% with a median value of 88%. Based on component tests with the Hybrid III, TNO/TASS has stated that high correlation is 65% or above. Hence, the BioRID II repeatability is very high. The BioRID II reproducibility ranged from 74 to 78% with a median value of 77%. Five of the nine comparisons included in the reproducibility study were conducted not only with different dummies, but also on different sites.

It can be concluded that the BioRID II shows high repeatability and reproducibility for all of the compared crash conditions. Furthermore, the BioRID II shows excellent repeatability for nearly all of the NIC, N_{km}, T1x, HC, F_x, and M_y criteria comparisons. The ORM-values for these criteria were predominantly above 90%.

INTRODUCTION

The BioRID II seems to be the most biofidelic dummy for low-speed rear-end crash tests ([1], [2], [3], [4], [5]) and it has been shown that the BioRID II is a good tool for predicting low-speed rear-end neck injuries ([6], [7], [8]). Therefore, the BioRID II is included several proposed test methods, among them the EuroNCAP Final Draft [9].

Several studies have been performed to evaluate the BioRID II repeatability. Good repeatability was shown already for early versions of the BioRID by [11] and [12]. [13] evaluated BioRID II (however not the actual version g) repeatability by exposing one dummy seated in four different seat designs three times to a 16 km/h crash pulse. Also the reproducibility was evaluated by using three different dummies on a rigid steel seat. The BioRID II showed sufficiently good repeatability and reproducibility, although these were somewhat better for the RID2 which was also included in the study.

[14] performed three repeated tests on three different seats using a 16 km/h crash pulse. To evaluate reproducibility, the same three seats were tested at five different test labs using two different crash pulses (16 and 25 km/h). The sleds used included both acceleration and deceleration types. Scattering was defined as difference between maximum and minimum values divided by the mean value. Repeatability was rated to be good – meaning scattering being about 20% – and reproducibility was rated acceptable at 16 km/h (scattering 10% to 40%). But the scattering at 25 km/h showed to be generally between 30% and more than 100% on biomechanical criteria. The authors mentioned that training in seat and dummy set-up will help to improve the results.

[15] carried out repeatability and reproducibility investigations using four BioRID dummies, two types of seats, and two crash pulses (16 and 24 km/h). All together thirty-eight tests were performed at one test facility. Almost the same NIC values were found for all four dummies. The repeatability

(maximum deviation from the mean value) for NIC was ±13%, the reproducibility (maximum deviation from the mean value of all four dummies) for NIC was ±3.5%. The repeatability for N_{km} was ±20% and the reproducibility ±11%. The repeatability for F_x was ±34 %, and the reproduceibility was ±27 % with clear dependency on dummy used. The repeatability for F_z was ±6 % and the reproducibility was ±8 %. The influence of pulse variation inside its corridors was studied but did not show apparent influence on the before mentioned measurement values.

[16] investigated repeatability and reproducibility of dummy response using the coefficient of variation (CV). Three BioRID dummies underwent five tests on a rigid seat design each. The CV for repeatability was expressed as percentage after dividing the standard deviation of the peak measurement values for each dummy by the average value. The CV for reproducibility was also expressed as percentage after dividing the standard deviation of differences among the three dummies by the average value. Repeatability in terms of CV showed to be below 5% for head acceleration and neck moment in flexion, between 5% and 10% for F_x, F_z, and T1 acceleration, and in some cases slightly above 10% in neck extension. Reproducibility in terms of CV was 6.3% for T1 acceleration, 5.0% for F_x, 13.7% for F_z, 3.3% for neck flexion, and 31.6% for neck extension.

METHOD

Twelve sets of rear-end sled tests were evaluated in this study. Each set of crashes contained two to four tests, and all tests within each set were designed to mirror each other. Altogether, thirty tests were included in the twelve sets. Tests with four different BioRID II dummies (all of version g), three different crash pulses, five different seats, and conducted at two different crash sites, were included in order to assess the BioRID II repeatability and reproduce-ibility. The crashes were conducted between November 2004 and August 2006. The test set-ups can be found in Table 1.

The seats used were standard seats with head restraints. However, some of them had added, excluded, or modified safety systems, or were tested during development. The three crash pulses used were those that are proposed for EuroNCAP, however all of them do not fulfil all pulse requirements specified in the EuroNCAP v2.3 Final Draft ([9]). The IIWPG pulse is triangular shaped with a peak of appr. 10g at 27 ms, mean acceleration of 5.5g, and Δv of 16 km/h. The Folksam/SRA low severity pulse (FV1) is trapezoidal shaped with mean acceleration of 4g and Δv of 16 km/h, and the Folksam/SRA high severity pulse (FV2) is trapezoidal shaped with mean acceleration of 6.5g and Δv of 24 km/h. The two crash sites used were those located at Autoliv in Vårgårda, Sweden (ALS) and at Autoliv in Elmshorn, Germany (ANG). At ALS a hydraulic accelerator sled was used, and at ANG a deceleration sled with a hydraulic brake system was used.

Seventeen pairs of tests were conducted with exactly the same set-up and these were used to assess the BioRID II repeatability. Set 4 contained four tests with two different dummies, while all other variables were similar. These tests were used to assess the BioRID II reproducibility. Set 11 contained two tests conducted at different tests sites and with different dummies and showed a combined correlation for dummy reproducibility and test repeatability at different sites. Set 12 also contained two pairs of tests conducted at different sites and with different dummies, and were used to assess both repeatability and reproducibility.

Table 1.
Included tests

Set	Test	Dummy	Seat	Pulse	Site	Test Date
1	**a**	B1	A	IIWPG	ALS	Dec. 2004
	b	B1	A	IIWPG	ALS	Dec. 2004
2	**a**	B1	B	FV3	ALS	April 2005
	b	B1	B	FV3	ALS	April 2005
	c	B1	B	FV3	ALS	April 2005
3	**a**	B1	A	FV3	ALS	April 2005
	b	B1	A	FV3	ALS	April 2005
	c	B1	A	FV3	ALS	April 2005
4	**a**	B2	A	IIWPG	ALS	Feb. 2006
	b	B2	A	IIWPG	ALS	Feb. 2006
	c	B1	A	IIWPG	ALS	Feb. 2006
	d	B1	A	IIWPG	ALS	Feb. 2006
5	**a**	B1	A	IIWPG	ALS	Sept. 2005
	b	B1	A	IIWPG	ALS	Sept. 2005
6	**a**	B1	A	FV1	ALS	Sept. 2005
	b	B1	A	FV1	ALS	Sept. 2005
7	**a**	B1	A	FV3	ALS	Nov. 2005
	b	B1	A	FV3	ALS	Nov. 2005
8	**a**	B3	C	FV3	ANG	Aug. 2006
	b	B3	C	FV3	ANG	Aug. 2006
9	**a**	B3	C	FV1	ANG	Aug. 2006
	b	B3	C	FV1	ANG	Aug. 2006
10	**a**	B3	C	IIWPG	ANG	Aug. 2006
	b	B3	C	IIWPG	ANG	Aug. 2006
11	**a**	B1	D	IIWPG	ALS	Nov. 2004
	b	B4	D	IIWPG	ANG	Nov. 2004
12	**a**	B1	E	IIWPG	ALS	Nov. 2004
	b	B1	E	IIWPG	ALS	Nov. 2004
	c	B4	E	IIWPG	ANG	Nov. 2004
	d	B4	E	IIWPG	ANG	Nov. 2004

Within each set, the same dummy positioning procedure was used. The compared dummy records were the x- and z-accelerations in the head, C4, T1, T8, L1 and pelvis, and the upper neck shear force (F_x), tension (F_z) and bending moment (M_y). The filter classes used were those specified in the Euro-NCAP v2.3 Final Draft ([9]): CFC 1000 for head z-acceleration, F_x and F_z, CFC 600 for M_y, and CFC 60 for all other. However, for test 10b, the C4, T1, T8, L1, and pelvis accelerations were filtered with CFC 180 and the head x-acceleration with CFC 1000. In

test 10b the T1 z-acceleration was missing, and in tests 11b and 12c the T8 z-accelerations were missing. Further, the crash pulses (filtered with CFC 60) were compared for all sets with the exception of set 9, since the crash pulse in test 9a was missing. The NIC, the N_{km}, the maximum T1 x-acceleration, the head restraint contact time, the maximum upper neck shear force, and the maximum upper neck tension force were calculated for all tests according to the EuroNCAP v2.3 Final Draft ([9]).

The Objective Rating Method, ORM, ([10]) was used to assess the correlation between the tests in each set. The ORM correlates one comparison test to one reference test. Therefore, the ORM was applied to all possible pairs in those sets that contained more than two tests. The ORM enables comparison between scalars, such as criteria, minimum and maximum peak values, and their occurrence times, and between curve shapes.

In this study the criteria and signals listed in Table 2 were included. The acceleration and the neck load maximum peak values and their occurrence times were compared, and for the M_y also the minimum peak value and its occurrence time were compared. The peak value comparisons were limited to peaks occurring during the first 200 ms of the crashes. Further, the curve shapes of the signals were compared during the first 200 ms of the crashes, and the crash pulse shapes were compared during the first 100 ms of the crashes.

Table 2.
Compared criteria and signals

Group	Component
Criteria	NIC (max. before end of head contact) N_{km} (max. before end of head contact) T1x (max. before end of head contact) HC (head restraint contact time) F_x (max. before end of head contact) F_z (max before end of head contact)
Acceleration	Head x-acc Head z-acc C4 x-acc C4 z-acc T1 x-acc T1 z-acc T8 x-acc T8 z-acc L1 x-acc L1 z-acc Pelvis x-acc Pelvis z-acc
Neck Loads	F_x F_z M_y
Crash pulse	Crash pulse

The ORM scalar correlations are calculated according to Equation 1. This expression is called the Factor Method and calculates the correlation between the reference test and the comparison test. The results range from 0 to 100%, where 100% represents a perfect match.

The curve shape correlation is calculated according to Equation 2. This expression is called the Weighted Integrated Factor Method and is a combination of the Factor Method and the Root Mean Square Addition Method. This means that the correlation in each time step contributes to the total correlation just as the function value would contribute to the total area underneath the curve. The δ is very small and used to avoid division by zero. *r* and *c* are used as abbreviations for *reference* and *comparison*, respectively.

$$ORM_{scalar} = \frac{\max(0, reference \cdot comparison)}{\max(reference^2, comparison^2)} \quad (1)$$

$$ORM_{shape} = 1 - \sqrt{\frac{\int \left(\max\left(|r(t)|,|c(t)|\right) \cdot \left(1 - \frac{\max(0, r(t) \cdot c(t))}{\max\left(\delta, r(t)^2, c(t)^2\right)}\right)^2 \right) dt}{\int \max\left(|r(t)|,|c(t)|\right) dt}} \quad (2)$$

In order to simplify comparison between tests, ORM-values are calculated not only for the scalars and the curve shapes, but also for groups of scalars and curve shapes. The contribution of each ORM-value in its group is defined by a weight factor (W). Equation 3 is used to calculate the ORM-value for each group. Further, the groups are arranged into one single ORM-value that is the correlation for the complete system. The contribution of the group ORM-values to the complete ORM-value is defined by weight factors (W). Equation 4 is used to calculate the ORM-value for the complete system.

$$ORM_{group} = 1 - \sqrt{\frac{\sum \left(W_{scalar\ or\ shape} \cdot \left(1 - ORM_{scalar\ or\ shape}\right)^2 \right)}{\sum W_{scalar\ or\ shape}}} \quad (3)$$

$$ORM_{complete} = 1 - \sqrt{\frac{\sum \left(W_{group} \cdot \left(1 - ORM_{group}\right)^2 \right)}{\sum W_{group}}} \quad (4)$$

In this study, the criteria were collected in the group Criteria, the head, the spine, and the pelvis accelerations were collected in the group Acc, and the neck loads were collected in the group Neck Loads. The weight factors (W) used for the scalars and curve shape to form the ORM-values for the groups are listed in Table 3. The weight factors used for the complete ORM-value were 6 for the Criteria since this group included six criteria, 12 for the Acc since this group included signals from six accelerometers in two directions (x and z), and 3 for the Neck Loads since this group included three signals from the upper neck load cell (see Table 3). For tests with one missing acceleration signal (10b, 11b, and 12c), the

weight factor used for the group Acc was 11. The tests in the set 9 and 10 did not have any positive F_x peaks, and consequently no ORM-values for the maximum peak or its occurrence time could be used. Therefore, the weight factor for the group Neck Loads was reduced by 2/3 to 2.333 for set 9 and 10. The crash pulses were not included in the complete ORM-values, since these were aimed to show the BioRID II repeatability or reproducibility.

Table 3
Weight factors used

Group	W_{group}	Component		$W_{scalar\ or\ shape}$
Criteria	6	NIC		0.167
		N_{km}		0.167
		T1x		0.167
		HC		0.167
		F_x		0.167
		F_z		0.167
Acc	12	Head x-acc	Max peak	0.028
			Max peak time	0.028
			Curve shape	0.028
		Head z-acc	Max peak	0.028
			Max peak time	0.028
			Curve shape	0.028
		C4 x-acc	Max peak	0.028
			Max peak time	0.028
			Curve shape	0.028
		C4 z-acc	Max peak	0.028
			Max peak time	0.028
			Curve shape	0.028
		T1 x-acc	Max peak	0.028
			Max peak time	0.028
			Curve shape	0.028
		T1 z-acc	Max peak	0.028
			Max peak time	0.028
			Curve shape	0.028
		T8 x-acc	Max peak	0.028
			Max peak time	0.028
			Curve shape	0.028
		T8 z-acc	Max peak	0.028
			Max peak time	0.028
			Curve shape	0.028
		L1 x-acc	Max peak	0.028
			Max peak time	0.028
			Curve shape	0.028
		L1 z-acc	Max peak	0.028
			Max peak time	0.028
			Curve shape	0.028
		Pelvis x-acc	Max peak	0.028
			Max peak time	0.028
			Curve shape	0.028
		Pelvis z-acc	Max peak	0.028
			Max peak time	0.028
			Curve shape	0.028
Neck Loads	3	F_x	Max peak	0.028
			Max peak time	0.028
			Curve shape	0.028
		F_z	Max peak	0.028
			Max peak time	0.028
			Curve shape	0.028
		M_y	Max peak	0.014
			Max peak time	0.014
			Min peak	0.014
			Min peak time	0.014
			Curve shape	0.028

RESULTS

BioRID II Repeatability

Seventeen pairs of tests were used to assess the BioRID II repeatability. The ORM-values for the complete system correlation range from 83 to 90% (median value 88%) and are shown in Figure 1. The ORM-values of the group Criteria for the same sets range from 89 to 97% and are shown in Figure 2, and their components are listed in Table 4. Among the Criteria components the F_x shows the largest spread, from 78 to 100%, and the lowest median value of 91%. The other five criteria have median values of 95% or above.

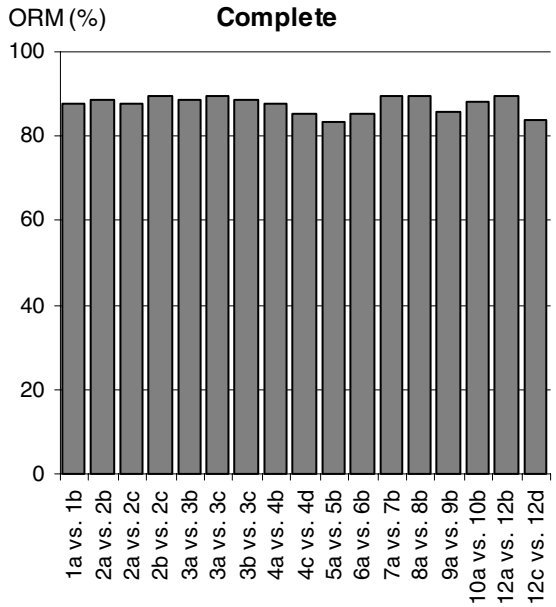

Figure 1. BioRID II repeatability tests: ORM-values in percent for the complete system

The ORM-values of the group Acc range from 82 to 90% and are shown in Figure 3. The ORM-values for the group Neck Loads range from 77 to 92 and are shown in Figure 4. In general, the peak value correlations are high; the median ORM-values for all peaks are shown in Figure 5. The ORM-values for the peak occurrence times are in general very high; the median values are shown in Figure 6. In total, the peaks for 268 pairs were compared. Of these, 23 match perfectly and only one peak ORM-value was below 65%. Among the peak value occurrence times 45 pairs match perfectly and three pairs have ORM-values less than 65%. Two of these three pairs have double peaks of almost the same magnitude in the T8 z-acceleration signals that cause the low correlation values: in both reference tests the first peak is the highest one and in the both comparison test the latter peak is the highest. For the third pair, there are double peaks in the M_y signals.

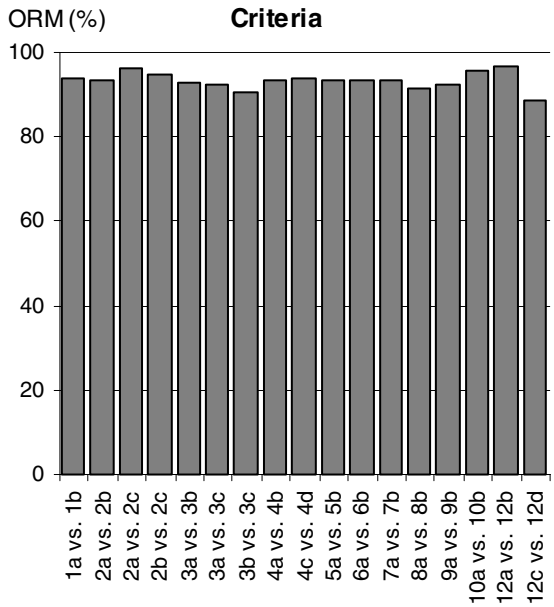

Figure 2. BioRID II repeatability tests: ORM-values in percent for the group Criteria.

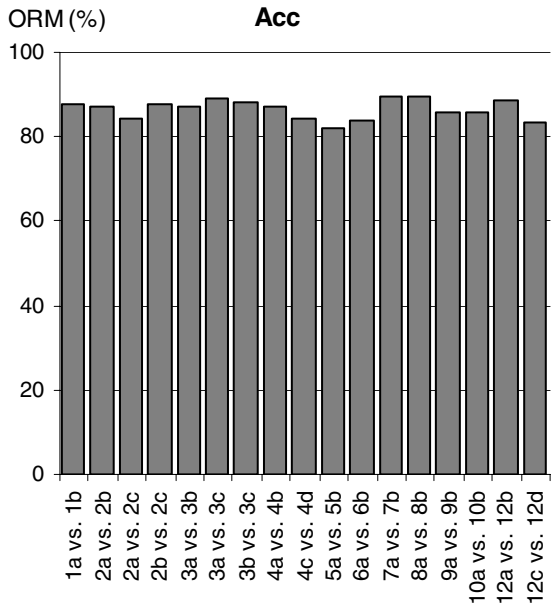

Figure 3. BioRID II repeatability tests: ORM-values in percent for the group Acc.

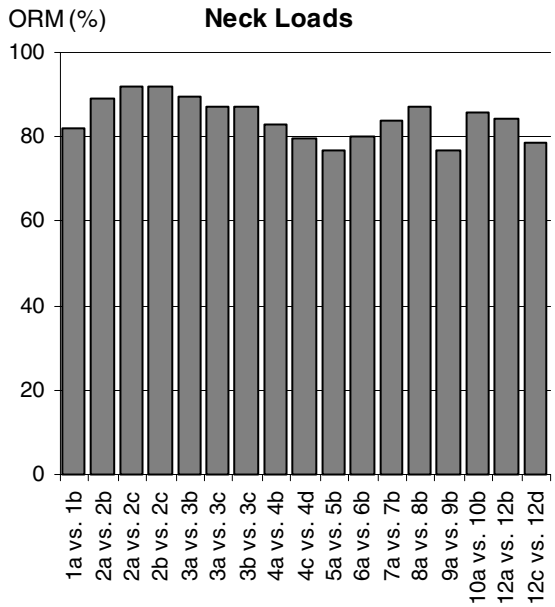

Figure 4. BioRID II repeatability tests: ORM-values in percent for the group Neck Loads.

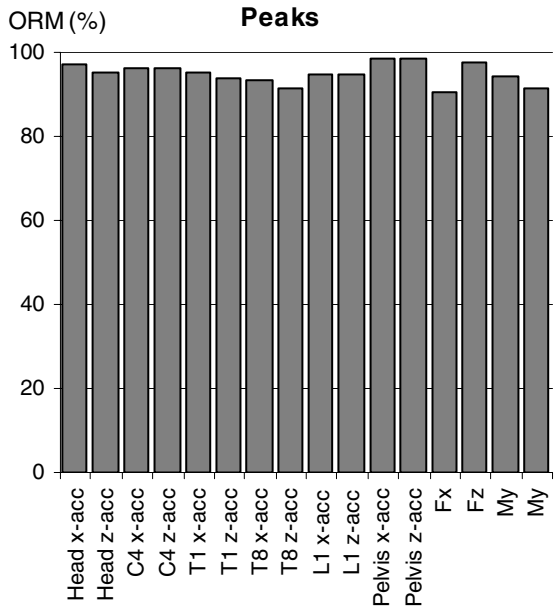

Figure 5. BioRID II repeatability tests: median ORM-values in percent for the maximum acceleration and neck load peak values, the last bar is the median minimum M_y peak value.

Table 4
BioRID II repeatability tests: ORM-values in percent for the components in the group Criteria

Tests	NIC	N_{km}	T1x	HC	F_x	F_y
1a vs. 1b	99	92	88	99	96	99
2a vs. 2b	92	92	95	96	90	98
2a vs. 2c	99	95	93	98	100	97
2b vs. 2c	93	97	98	98	91	99
3a vs. 3b	87	100	94	98	91	95
3a vs. 3c	91	97	98	100	85	94
3b vs. 3c	96	97	96	98	78	98
4a vs. 4b	99	91	95	100	88	96
4c vs. 4d	98	100	92	98	87	98
5a vs. 5b	96	86	95	97	95	96
6a vs. 6b	99	89	97	89	94	99
7a vs. 7b	90	96	89	100	96	99
8a vs. 8b	98	92	97	100	82	95
9a vs. 9b	86	95	98	95	100	90
10a vs. 10b	93	95	98	94	100	97
12a vs. 12b	99	93	98	99	97	98
12c vs. 12d	79	92	93	97	85	99
Min value	79	86	88	89	78	90
Median value	96	95	95	98	91	98
Max value	99	100	98	100	100	99

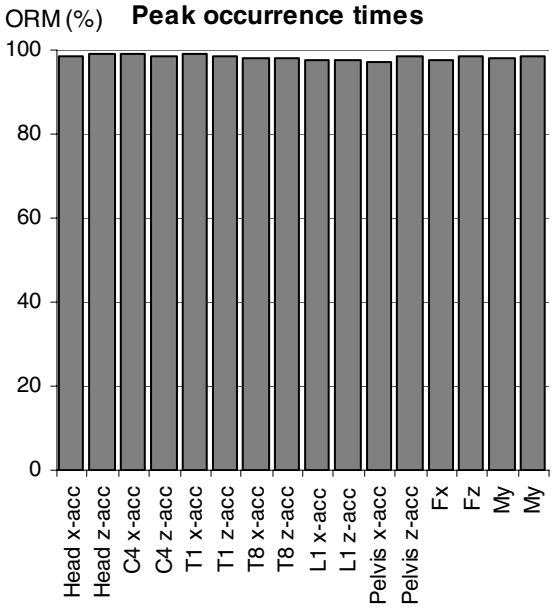

Figure 6. BioRID II repeatability tests: median ORM-values in percent for the occurrence time for the maximum acceleration and neck load peak values, the last bar is the median occurrence time for the minimum M_y peak value.

Figure 7 shows the ORM-values for the median curve shape correlations. The lowest median ORM-values can be found for T1 z-acceleration, T8 z-accelerations, and M_y. These, together with F_x, are the only signals for which the lowest curve shape ORM-values are below 65%. Still, all median ORM-values are above 65%.

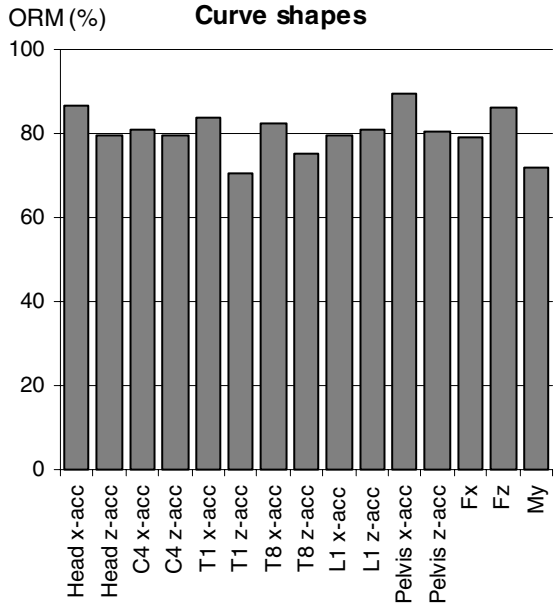

Figure 7. BioRID II repeatability tests: median ORM-values in percent for the acceleration and neck load curve shapes.

For the seventeen pairs of tests used to assess the BioRID II repeatability the corresponding ORM-values for the crash pulse shapes are shown Figure 8.

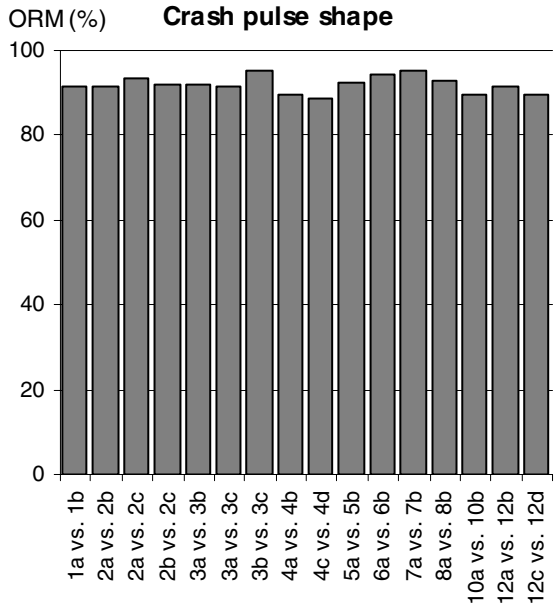

Figure 8. ORM-values in percent for the crash pulse shapes for the tests included in the BioRID II repeatability assessment. There is no ORM-value for set 9 because of a missing crash pulse.

BioRID II Reproducibility

Three sets can be used to assess the BioRID II reproducibility: Set 4, Set 11, and Set 12. In Figure 9 the ORM-values for the crash pulse shapes are given. The correlations of the crash pulse shapes are high for all pairs in Set 4 but somewhat lower for the reproducibility tests in Set 11 and Set 12. Set 4 was designed to evaluate the repeatability and these tests were conducted at ALS. In Set 11 and Set 12, not only two dummies were used, also two crash sites were used.

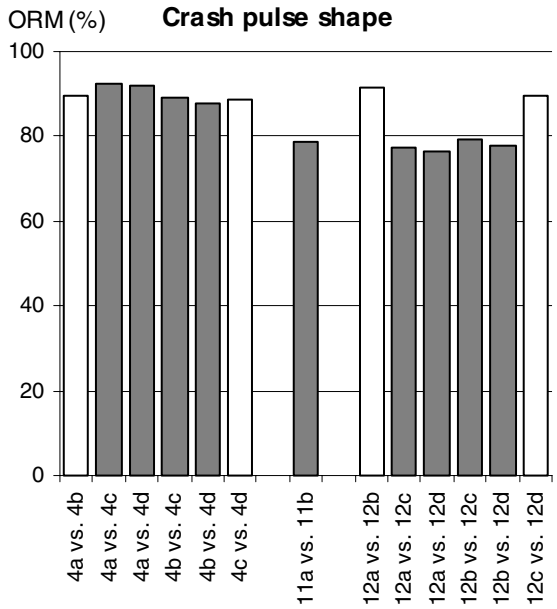

Figure 9. ORM-values in percent for the crash pulse shape. White bars are used for the BioRID II repeatability tests, and grey bars are used for the BioRID II reproducibility tests.

The ORM-values for the complete BioRID II reproducibility are shown in Figure 10. The reproducibility are lower than the repeatability, nevertheless well above 65%. The BioRID II reproducibility ORM-values range from 74 to 78%, with a median value of 77%. This should be compared with the range from 83 to 90% (median value 88%) for the BioRID II repeatability (Figure 1).

The ORM-values for the groups are shown in Figure 11 (Criteria), Figure 12 (Acc), and Figure 13 (Neck Loads). As can be seen, for the groups only one ORM-value is below 65%. That is the group Neck Loads for test 4b versus 4d that has a ORM-value of 62%, mainly because of low curve shape ORM-values for F_x and M_y. The ORM-values for the components in the groups Criteria are given in Table 5. The F_x is below 65% for there of the nine cases, the median value for this criteria is 68%. The corresponding value was 91% for the BioRID II repeatability tests. The other five criteria shows much better correlations than the F_x do, however the median values for all criteria are less good than for the BioRID II repeatability tests. The differences for these five criteria are between 2 and 9 percent units.

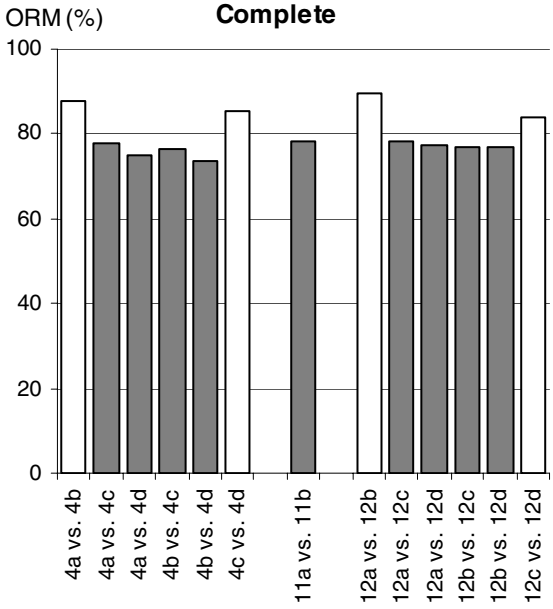

Figure 10. ORM-values in percent for the complete systems. White bars are used for the BioRID II repeatability tests, and grey bars are used for the BioRID II reproducibility tests.

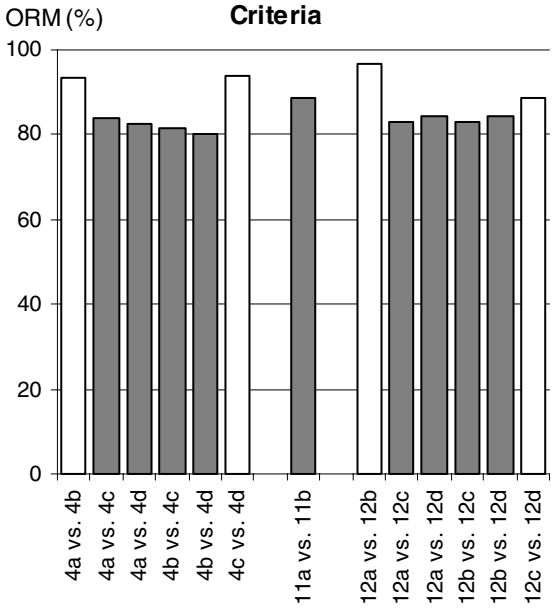

Figure 11. ORM-values in percent for the groups Criteria. White bars are used for the BioRID II repeatability tests, and grey bars are used for the BioRID II reproducibility tests.

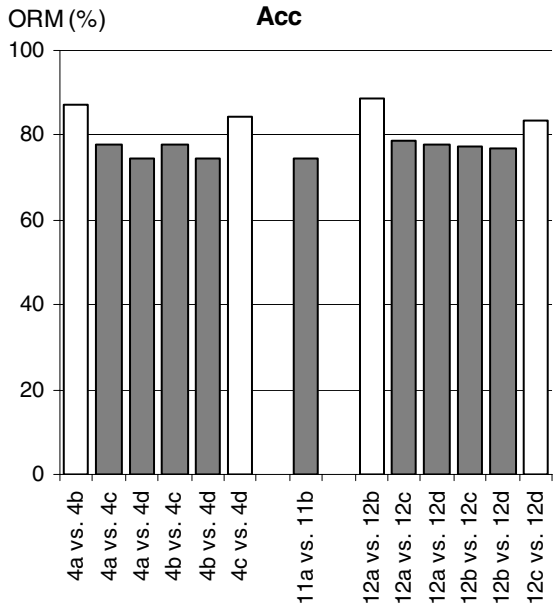

Figure 12. ORM-values in percent for the groups Acc. White bars are used for the BioRID II repeatability tests, and grey bars are used for the BioRID II reproducibility tests.

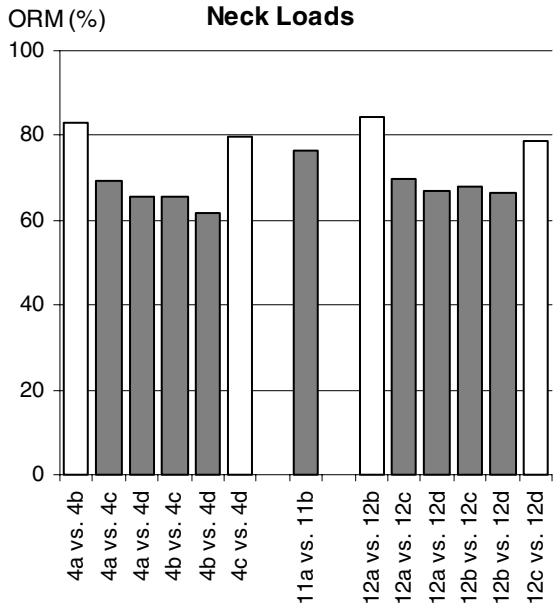

Figure 13. ORM-values in percent for the groups Neck Loads. White bars are used for the BioRID II repeatability tests, and grey bars are used for the BioRID II reproducibility tests.

Table 5.
BioRID II reproducibility tests: ORM-values in percent for the components in the group Criteria

Tests	NIC	N_{km}	T1x	HC	F_x	F_y
4a vs. 4c	88	83	80	98	77	87
4a vs. 4d	86	83	88	95	67	89
4b vs. 4c	89	92	76	98	68	84
4b vs. 4d	87	92	84	95	59	86
11a vs. 11b	87	78	95	98	96	92
12a vs. 12c	96	89	86	96	64	91
12a vs. 12d	82	82	92	93	75	90
12b vs. 12c	96	89	86	96	64	91
12b vs. 12d	82	88	90	94	73	88
Min value	82	78	76	93	59	84
Median value	87	88	86	96	68	89
Max value	96	92	95	98	96	92

The median ORM-values for the peak values in the BioRID II reproducibility tests are shown in Figure 14. The median ORM-values for the peak values are considerably lower for the T1 z-acceleration and the F_x compared to the other. However, taking the ranges into account, also the M_y values are low. Three cases match perfectly for the peak values. The numbers for the peak value occurrence times are somewhat better, for fifteen pairs the peak time correlated with 100%. The median ORM-values for peak occurrence times are given in Figure 14. These are nearly as high as those for the BioRID II repeatability tests (Figure 6). Only the median ORM-values for the T1 z-acceleration and the M_y negative peak occurrence times are significantly lower.

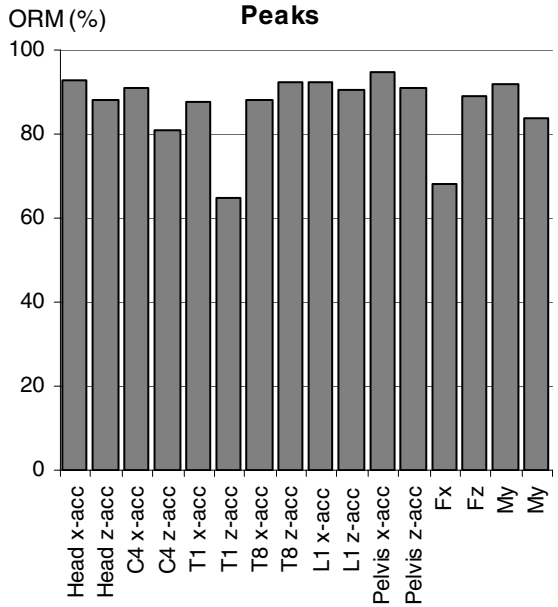

Figure 14. BioRID II repoducibility tests: median ORM-values in percent for the maximum acceleration and neck load peak values, the last bar is the median minimum M_y peak value.

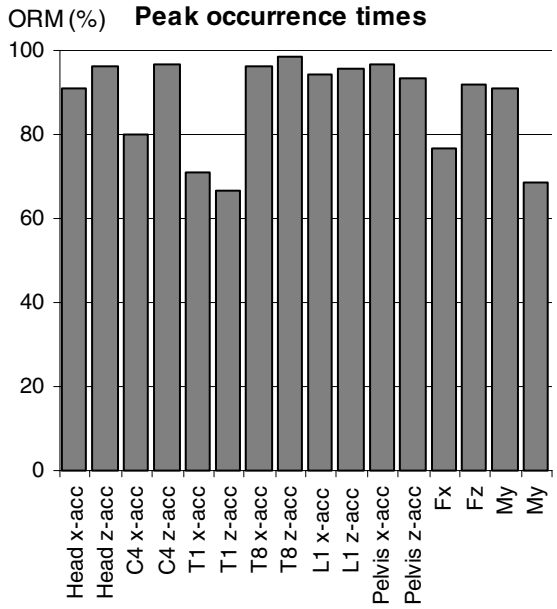

Figure 15. BioRID II reproducibility tests: median ORM-values in percent for the maximum acceleration and neck load peak value occurrence times, the last bar is the median minimum M_y peak value occurrence time.

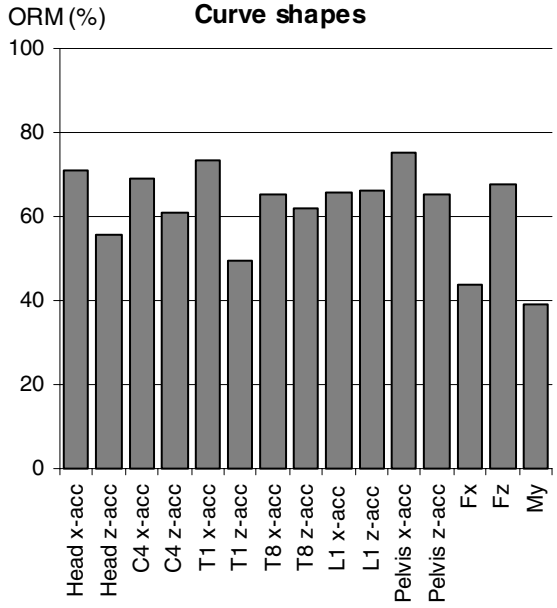

Figure 16. BioRID II reproducibility tests: median ORM-values in percent for the acceleration and neck load curve shapes.

The median ORM-values for the curve shapes are much lower for the reproducibility tests compared to the repeatability tests. The z-accelerations for the head, C4, T1, and T8, and the F_x and M_y median curve shape ORM-values are below 65%; for the repeatability tests all were above. In general the curve shape trends are similar for all compared pairs, but the magnitudes for the peaks differ and that results in somewhat lower ORM-values. Predominantly, the least correlating parts of the curves occur between 150 ms and 200 ms.

DISCUSSION

Repeatability and reproducibility studies

The values for repeatability and reproducibility from the studies conducted by [11], [12], [13], [14], [15], [16] cannot be directly compared to each other or to this study since each study calculate repeatability and reproducibility with different methods. [14] assessed good repeatability in general, acceptable reproducibility at 16 km/h, and unacceptable reproducibility at 25 km/h. It has to be mentioned that all biomechanical values were largely exceeding common thresholds in the 25 km/h tests. [15] and [16] both did tests resulting in low to medium bio-mechanical values but showing just opposite trends in F_x and F_z reproducibility. In this study, good overall repeatability and reproducibility were assessed for the BioRID II. However, the F_x was below the limit for good reproducibility in three of nine comparisons, but it showed good repeatability for all seventeen comparisons.

High Repeatability: ORM > 65%

The Objective Rating Method (ORM) was published in 2005 ([10]) as a tool for assessing the correlation of Madymo simulation models to mechanical tests. They stated that high correlation is 65% or above repeatability for mechanical tests. This statement was based on component tests on one Hybrid III 50%-ile without arms and lower legs. Ten different tests were repeated ten times, and in each test thirty signals were recorded. All signals of the repeated tests were then compared to the first test in each test series. However, which signals that were compared, or their weight factors, are not specified. According to the authors, special attention was taken in positing the dummy before each test to ensure good repeat-ability and a well-defined environment was used in the tests. In this study, the ORM-values for the BioRID II repeatability ranged between 83 and 90% with a median value of 88%. This is much better numbers than those presented by [10] for Hybrid III component tests. Take into consideration that for the BioRID II tests, not only the BioRID II spread are measured, also the spread in the seats and test environments are included. Hence, it can be assessed that the BioRID II repeatability is very high.

The BioRID II repeatability assessment was based on seventeen pairs of test. In these tests four different BioRID II dummies, four seats, three pulses, and two sites were used (Table 1). The specific influences of these parameters on the ORM-values cannot be assessed since seventeen pairs are

too few to measure significant differences. Further, the spread is between 83 and 90%, and twelve of the seventeen pairs have ORM-values of 88, 89 or 90%. Consequently, there are only minor differences between most of the pairs in terms of repeatability ORM-values. Although no significant influences can be assessed, the BioRID II repeatability ORM-values are presented sorted according to dummies (Figure 17), seats (Figure 18), pulses (Figure 19), and sites (Figure 20) used. The unsorted data can be found in Figure 1. The B2 and B4 BioRID II dummies were only used for one test each. Therefore, no conclusions should be draw regarding these dummies. The median ORM-values for B1 and B3 are almost the same. The spread when using the same dummy appear to be somewhat wider than the spread between different dummies (Figure 17). The spread in ORM-values do not likely depend on the seat (Figure 18) or the site (Figure 20). Further, the spread is much smaller between the tests conducted with FV3 pulse than for the other pulses (Figure 19).

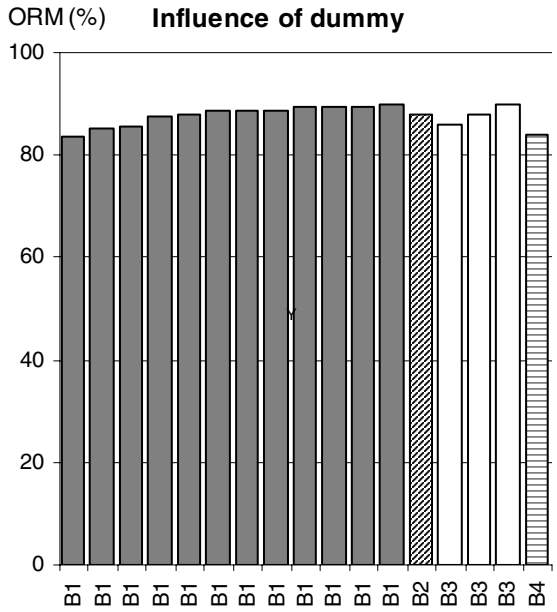

Figure 17. BioRID II repeatability tests: ORM-values for the complete system sorted according to seat used.

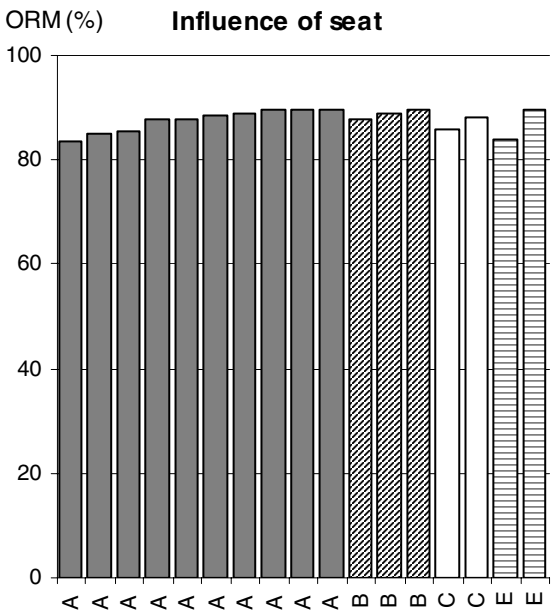

Figure 18. BioRID II repeatability tests: ORM-values for the complete system sorted according to seat used.

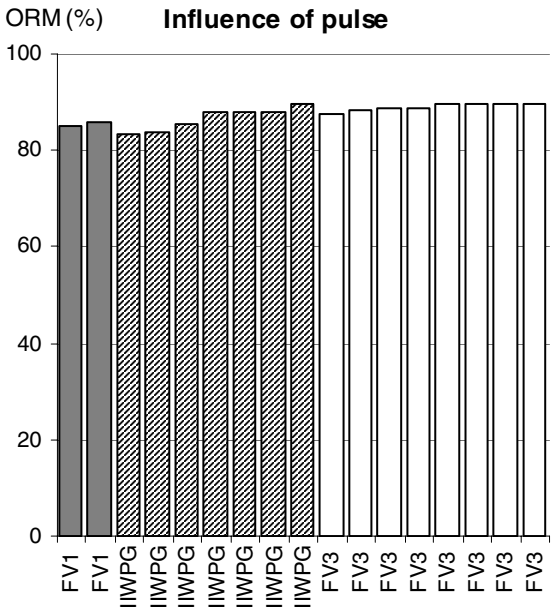

Figure 19. BioRID II repeatability tests: ORM-values for the complete system sorted according to pulse used.

Set 2 and Set 3 contained three tests each that were set-up to mirror each other. The NIC, the N_{km}, the T1x, the HC, the F_x, and the M_y values for these sets were analyzed in order to find out if these values increased or decreased with the number of tests. Only the T1x values for Set 2 shows continues decrease, and none shows continues increase. Hence, nothing in this study indicates that the BioRID II responses changes due to the number of conducted tests.

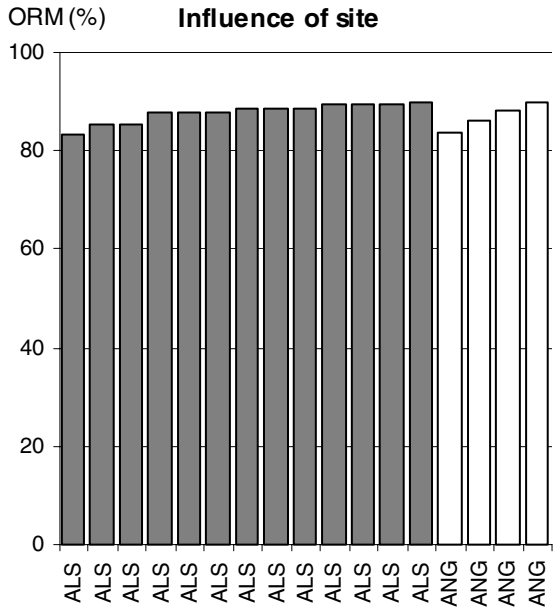

Figure 20. BioRID II repeatability tests: ORM-values for the complete system sorted according to site used.

Three sets were used to assess the BioRID II reproducibility. Of these, only Set 4 were designed with the aim to evaluate the reproducibility. Set 11 and Set 12 were parts of a seat improvement study that were conducted at two sites. Therefore, not only the dummies used differed, also the crash sites differed. As can be seen in Figure 9, the crash pulses shapes were less similar for the reproducibility tests conducted at two different sites (Set 11 and 12) than those conducted at the same site (Set 4). A comparison between the pulses used in Set 11 is given in Figure 21. Likely, the differences between these crash pulses only influence the outcome negligible. However, there are other differences that may have influenced the outcome. The gap between the dummy and the head restraint differed between the sites. Therefore, it can not be excluded that the dummy positions influenced the outcome. For Set 11, the gap was 5 mm wider for the dummy at ALS, and for Set 12 the gaps were 7 and 9 mm wider at ALS. Furthermore, the crash tracks used at ALS and ANG differ. At ALS a hydraulic acceleration sled is used: the dummy is at rest when the crash starts and by the aid of a hydraulic system the dummy is accelerated with a pre-defined pulse. At ANG a Hydro-Brake sled is used: prior to the crash the dummy is moving and a hydraulic system is then used to brake the sled with a pre-defined deceleration pulse. According to Figure 10 the ORM-values for the BioRID II reproducibility tests are in the same range for all three sets. Hence, it is likely that the dummy influence in much larger than influence from the positioning and the test conditions.

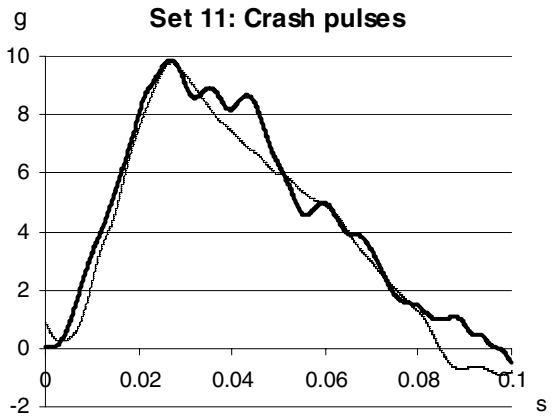

Figure 21. The crash pulses used in Set 11. The reference test (thick line) was conducted at ALS and the comparison test (thin line) at ANG.

The ORM-values for the criteria values, the peak values, and the peak value occurrence times are generally higher than ORM-values for curve shapes. However, both equation 1 and 2 will result in the same ORM-value if they are applied to the same scalars. Nevertheless, our demands are often much higher on scalars than on curves. Hence, different rule of thumbs may be used when deciding if scalars or curves correlate well. Up to date, too few correlation evaluations have been performed to assess if different type of tests and measured signals require different ORM threshold values.

The ORM

An example from Set 4 will be presented in detail in order to provide a feeling for the ORM scale. This set contains four tests: 4a and 4b were conducted with one BioRID II dummy, and 4c and 4d were conducted with another BioRID II. Comparing 4a to 4b, and 4c to 4d, will show the BioRID II repeatability. Comparing 4a to 4c and 4d, and 4b to 4c and 4d, will show the BioRID II reproducibility. NIC and N_{km} values and their corresponding ORM-values are given in Table 6. Table 7 shows the ORM-values that correspond to the signals shown in Figure 22 to Figure 26.

Table 6.
NIC and N_{km} values and their corresponding ORM-values in percent for Set 4

Tests	NIC Values	NIC ORM	N_{km} Values	N_{km} ORM
4a vs. 4b	10.2 vs. 10.3	99	0.20 vs. 0.22	91
4a vs. 4c	10.2 vs. 11.6	88	0.20 vs. 0.24	83
4a vs. 4d	10.2 vs. 11.8	86	0.20 vs. 0.24	83
4b vs. 4c	10.3 vs. 11.6	89	0.22 vs. 0.24	92
4b vs. 4d	10.3 vs. 11.8	87	0.22 vs. 0.24	92
4c vs. 4d	11.6 vs. 11.8	98	0.24 vs. 0.24	100

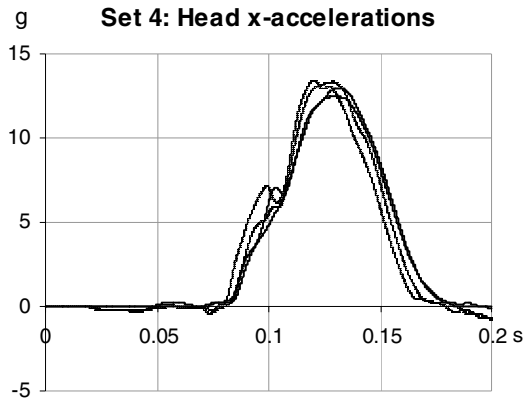

Figure 22. Head x-accelerations for all tests in Set 4. The two thick lines correspond to test 4a and 4b, and the two thin lines to test 4c and 4d.

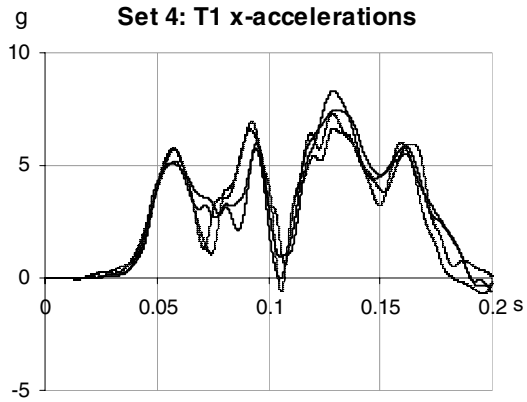

Figure 23. T1 x-accelerations for all tests in Set 4. The two thick lines correspond to test 4a and 4b, and the two thin lines to test 4c and 4d.

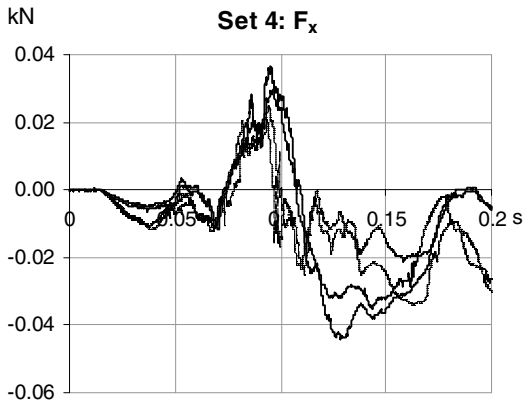

Figure 24. F_x for all tests in Set 4. The two thick lines correspond to test 4a and 4b, the two thin lines to test 4c and 4d.

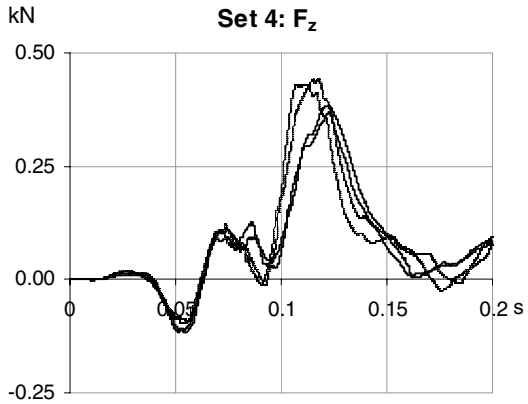

Figure 25. F_z for all tests in Set 4. The two thick lines correspond to test 4a and 4b, and the two thin lines to test 4c and 4d.

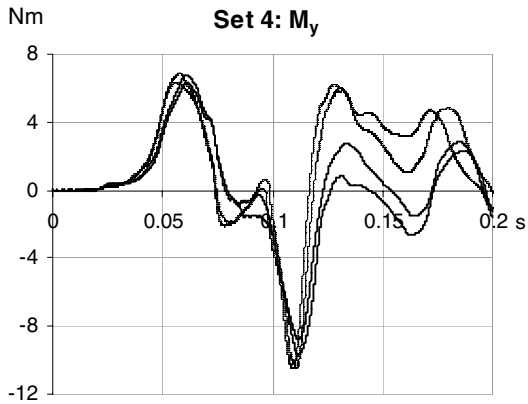

Figure 26. M_y for all tests in Set 4. The two thick lines correspond to test 4a and 4b, the two thin lines correspond to test 4c and 4d.

Table 7.
ORM-values in percent for some of the signals evaluated in Set 4

Signals		4a vs. 4b	4a vs. 4c	4a vs. 4d	4b vs. 4c	4b vs. 4d	4c vs. 4d
Head x-acc	Max peak	96	97	97	93	93	100
	Max peak time	100	98	91	98	92	93
	Curve shape	88	77	67	78	70	81
T1 x-acc	Max peak	90	93	98	84	88	95
	Max peak time	99	71	99	72	100	72
	Curve shape	86	74	72	73	71	76
Fx	Max peak	89	77	67	68	60	88
	Max peak time	99	97	95	99	97	98
	Curve shape	76	42	38	40	34	59
F_z	Max peak	96	87	89	84	86	98
	Max peak time	99	97	92	96	92	95
	Curve shape	84	66	58	62	56	74
M_y	Max peak	92	92	100	100	92	92
	Max peak time	100	95	91	95	91	96
	Min peak	90	84	84	93	93	100
	Min peak time	100	99	97	99	97	98
	Curve shape	61	46	39	35	31	66

CONLUSIONS

The Objective Rating Method (ORM) was applied to twenty-six pairs of tests in order to assess the BioRID II repeatability and reproducibility. The tests were conducted at two crash-test sites. Four BioRID II dummies, five different seats, and three crash pulses were used. Both criteria and dummy readings were compared. The BioRID II repeatability, in terms of ORM-values, ranged from 83 to 90% with a median value of 88%, and the reproducibility ranged from 74 to 78% with a median value of 77%. Based on component tests with the Hybrid III, TNO/TASS has stated that high correlation is 65% or above. Hence, the BioRID II repeatability and reproduce-ibility are very high.

REFERENCES

[1] Davidsson, J., Lövsund, P., Ono, K., Svensson, M. Y., Inami, S. (1999) *Proceedings of the 1999 International IRCOBI Conference on the Biomechanics of Impacts*, September 23-24, Sitges, Spain, pp. 165-178.

[2] Philippens, M., Cappon, H., van Ratingen, M., Wismans, J., Svensson, M., Sirey, F., Ono, K., Nishimoto, N., Matsuoka, F. (2002) Comparison of the Rear Impact Biofidelity of the BioRID II and RID2. *Stapp Car Crash Journal 46*, pp. 461-476.

[3] Roberts, A. K., Hynd, D., Dixon, P. R., Murphy, O., Magnusson, M., Pope, M. H. (2002) Kinematics of the Human Spine in Rear End Impact and the Biofidelity of Current Dummies. *Proceedings of Vehicle Safety 2002 ImechE Conference*, May 28-29, London, United Kingdom, Paper No. 2002-04-0067.

[4] Willis, C., Carroll, J., Roberts, A. (2005) An Evaluation of a Current Rear Impact Dummy against Human Response Corridors in both Pure and Oblique Impact. *Proceedings of the 19th International Technical Conference of the Enhanced Safety of Vehicles*, June, Washington, DC, USA, Paper No. 05-0061.

[5] Yaguchi, M., Ono, K., Kubota, M., Matsuoka, F. (2006) Comparison of Biofidelic Responses to Rear Impact of the Head/Neck/Torso among Human Volunteers, PMHS, and Dummies. *Proceedings of the 2006 International IRCOBI Conference on the Biomechanics of Impacts*, September 20-22, Madrid, Spain, pp. 183-197.

[6] Boström, O., Fredriksson, R., Håland, Y., Jakobsson, L., Krafft, M., Lövsund, P., Muser, M., Svensson, M. Y. (2000) Comparison of Car Seats in Low Speed Rear-End Impacts using the BioRID Dummy and the New Neck Injury Criterion (NIC). *Accident Analysis and Prevention*, Vol. 32, No. 2, pp. 321-328.

[7] Muser, M., Hell, W., Schmitt, K.-U. (2003) How Injury Criteria Correlate with the Injury Risk – A Study Analysing Different Parameters with Respect to Whiplash Injury. *Proceedings of the 18th International Technical Conference of the Enhanced Safety of Vehicles*, May 19-21, Nagoya, Japan, Paper No. 68-W.

[8] Eriksson, L., Kullgren, A. (2006) Influence of Seat Geometry and Seating Posture on NIC_{max} Long-Term AIS 1 Neck Injury Predictability. *Traffic Injury Prevention*, Vol. 7, pp 61-69.

[9] Euro NCAP – The Dynamic Assessment of Car Seats for Neck Injury Protection. Version 2.3 Final Draft. Status by 11/05/06.

[10] Hovenga, P. E., Spit, H. H., Uijldert, M., Dalenoort, A. M. (2005) Improved Prediction of Hybrid-III Injury Values using Advanced Multibody Techniques and Objective Rating. Proceedings of the SAE 2005 World Congress & Exhibition, April, Detroit, MI, USA. Paper No. 05AE-222.

[11] Davidsson, J., Flogård, A., Lövsund, P., Svensson, M. Y. (1999) BioRID P3 – Design and Performace Compared to Hybrid III and Volunteers in Rear Impacts at dv = 7 km/h. *Proceedings of the 43th Stapp Car Crash Conference*, October 25-27, San Diego, Ca, USA, Paper No. 99SC16, pp. 253-265.

[12] Ishikawa, T., Okano, N., Ishikura, K., Ono, K. (2000) An Evaluations of Prototype Seats using BioiRID-P3 and Hybrid III with TRID neck. *Proceedings of the 2000 International IRCOBI Conference on the Biomechanics of Impacts*, September, Montpellier, France, pp. 379-391.

[13] Bortenschlager, K., Kramberger, D., Barnsteiner, K., Hartlieb, M., Ferdinand, L., Leyer, H., Muser, M., Schmitt, K.-U. (2003) Comparison Tests of BioRID II and RID-2 with Regard to Repeatability, Reproducibility and Sensitivity for Assessment of Car Seat Protection Potential in Rear-End Impacts. *Stapp Car Crash Journal 47*, pp. 473-488.

[14] Adalian, C., Sferco, R., Fay, P. (2005) The Repeatability and Reproducibility of Proposed Test Procedures and Injury Criteria for Assessing Neck Injuries in Rear Impact. *Proceedings of the 19th International Technical Conference of the Enhanced Safety of Vehicles*, June, Washington, DC, USA, Paper No. 05-0340.

[15] Hartlieb, M. (2006) Study on Repeatability and Reproducibility of BioRID-Dummy Measurements for Whiplash Assessment. *Presented at 7th BioRID Users' Meeting*, March 1-2, Kaiserslautern, Germany, URL: http://groups.iihs.org/bioridusers/

[16] Ishii, M., Ono, K., Kubota, M. (2006) Factors Influencing the Repeatability and Reproducibility of the Dummies Used for Rear-End Impact Evaluation. *Proceedings of the 2006 International IRCOBI Conference on the Biomechanics of Impacts*, September 20-22, Madrid, Spain, pp. 405-408.

STUDY ON STATIC AND QUASI-DYNAMIC EVALUATION METHOD FOR ASSESSING WHIPLASH-ASSOCIATED DISORDERS IN REAR IMPACTS

Hiroyuki Asada
Mitsubishi Motors Corporation,
Japan
Katsumi Nawata
Toyota Motor Corporation,
(on behalf of the JAMA Working Group for WAD in rear impacts)
Japan
Paper number 07-0264

ABSTRACT

Studies are underway in JAMA on appropriate static (height of head restraint and backset) and quasi-dynamic (dynamic head rotation angle of Hybrid III dummy and dynamic backset) seat & head restraint evaluation methods for assessing whiplash-associated disorders in rear impacts. For various types of seats, the following items were evaluated for each index: i) road accident & whiplash phenomena, ii) reproducibility and repeatability, iii) correlation with dynamic evaluation results on BioRID II, iv) suitability for various seat types. The results revealed new findings as follows:

1) As for height of head restraint, if the height of head CG + ramping up is secured, a further increase in height does not provide much support for reducing injury.
2) As for backset, due to poor reproducibility in measurements on conventional HRMD, a new measuring method on the basis of SRP is effective. A decrease in backset reduces injury, however, since an excessively small backset impairs comfort, the balance between safety and comfort was examined.
3) As for dynamic head rotation angle of the neck of the Hybrid III dummy, because of poor biofidelity of the dummy, the angle is not considered to be good for a proper dynamic evaluation, however, thanks to good reproducibility and repeatability of the dummy as well as some correlation between head rotation angle and injury criteria, the angle can be used as a tool for alternative evaluation of the backset.
4) The dynamic backset was proposed as an alternative test to the static backset. However, the evaluation uses only the neck behavior of the dummy, and reproducibility and repeatability are still low. Consequently, the backset is not regarded as an appropriate evaluation method at this time.

INTRODUCTION

The death toll in traffic accidents is falling in Japan; however, the number of traffic accidents remains unchanged. Rear-end accidents in particular are significantly increasing (See Figure 1). About 90% of injuries caused by rear-end accidents are light injuries of the neck such as whiplash flagellum and about 90% of victims are the driver or the passenger occupant (See Figure 2). Therefore, the Ministry of Land, Infrastructure and Transport of Japan announced in September 2002 that it would take countermeasures against whiplash-associated disorders (WAD) in rear impacts (WAD reduction seat) as a candidate for the next safety standardization [(1)].

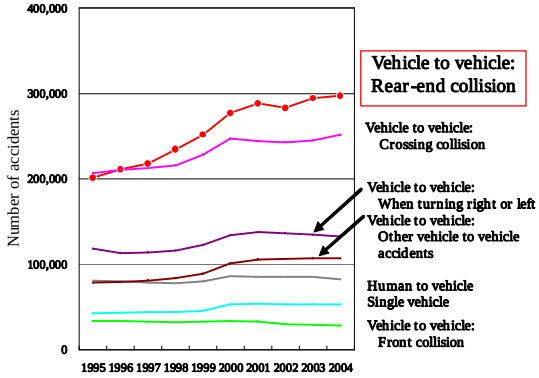

Figure 1. Trends of number of accidents by accident type in Japan (as of end of December of each year).

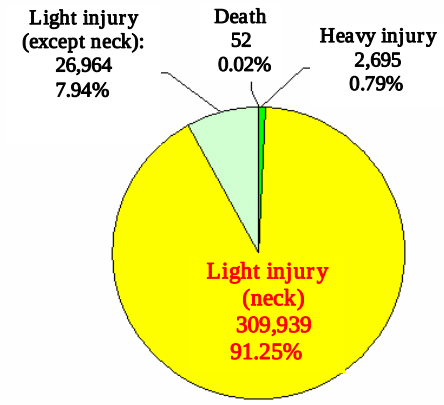

Figure 2. Breakdown of injuries caused by rear-end collisions in Japan.

WAD in rear impacts is attracting global attention. In the World Forum for the Harmonization of Vehicle Regulations (WP.29) held in March 2005, the establishment of global technical regulations (gtr)

based on the FMVSS202a head restraint regulation issued that year was approved[2]. In accordance with the MLIT announcement, in June 2003 the Japan Automobile Manufacturers' Association (JAMA) established a working team for examining with MLIT the standardization of whiplash reduction seats. JAMA has also participated in the informal head restraints gtr meeting, which began in February 2005. Moreover, in July 2005, a working group for WAD in rear impacts was established to start studying an appropriate dynamic evaluation method. This paper outlines the static and quasi-dynamic evaluation methods for the seat and head restraint for reducing WAD in rear impacts on the front outboard seats, which were examined by JAMA.

Causes of WAD

To examine an appropriate method for evaluating WAD in rear impacts, it is necessary to understand the mechanism by which whiplash flagellum is generated. However, since the mechanism is not clarified yet, this study employed the following latest hypothesis proposed by Ono[3] to examine the evaluation method.

As shown in Figure 3, the behavior of the passengers when a car is hit at low speed can be roughly categorized into three stages: (1) Straightening of the spine and extending it up to the neck, (2) S-shaped deformation of the neck by the forward displacement of the trunk and subsequent shearing, and (3) Hyperextension of the neck. The mechanism of whiplash flagellum seems to be caused by the S-shape deformation of cervical vertebrae, tucking synovium into the intervertebral joint when extending the cervical vertebrae, and flexure of the articular capsule around the joint. Therefore, an evaluation and indicator that lead to suppression of the S-shape deformation and extension are considered to be appropriate.

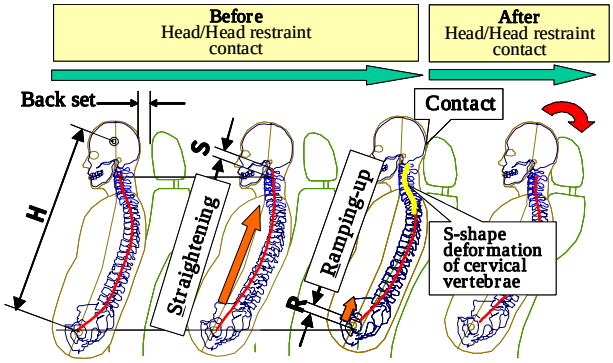

Figure 3. Behavior of passenger's head and neck during a rear impact.

STATIC EVALUATION

To statically evaluate the WAD reduction seat, "Height of head restraint" and "Backset" are considered to be important indexes as the International Insurance Whiplash Prevention Group (IIWPG) is conducting an assessment[4].

Height of Head Restraint

To reduce the S-shaped deformation of passengers with various physical frames, the height of the head restraint must be appropriate for the occupant's head. If the head restraint is too high, it may disturb the field of rear vision and impede an emergency escape since it causes an obstacle to the head when getting in and out of the rear seat of a two-door vehicle. Therefore, the required height should be minimized.

Maximum Height - First, JAMA examined the height of the head restraint necessary for properly protecting the head of the passenger from AF5%ile to AM95%ile. As the occupant's behavior in Figure 3 shows, the maximum head restraint height (Hmax) must be higher than the height reached when straightening of the spine in a rear-end collision (S) and ramping up of the trunk (R) are added to the height from the H-point to the center of gravity of the head at the time of seating (H)[5][6]:

$$Hmax = H+S+R \text{ of AM95\%ile} \quad (1).$$

The length S is 34–38mm and the length R is about 15mm based on experience, however, data that demonstrates the length R is not sufficient. Hmax for US 95%ile male was calculated as 813mm[5][6].

IIWPG also determined their own evaluation threshold by examining the required height of the head restraint obtained from past accident analyses (See Figure 4). The statistics in the figure show that reduction of injury cannot be expected even if the head restraint is higher than the height to the center of gravity of the head, and that taller women tend to be more affected by the height of the head restraint [3].

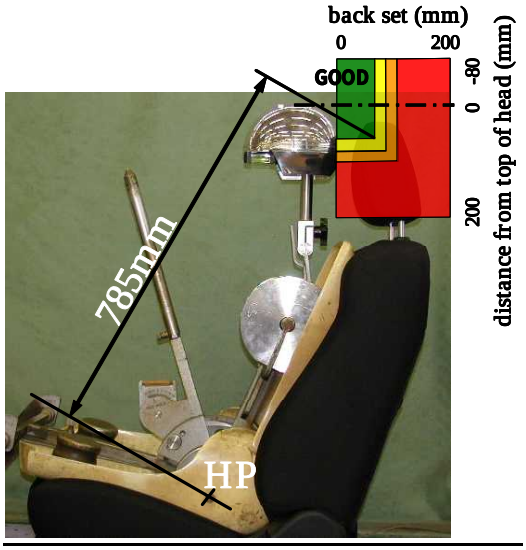

Figure 4. IIWPG head restraint height evaluation.

JAMA examined these hypotheses with an actual car seat in experiments. In the experiments, various changes in injury value were confirmed by changing the height of the head restraint of the existing seat and by IIWPG's dynamic evaluation method. As the results in Figure 5 show, the injury value was not improved even when the height was higher than that proposed by IIWPG. Our test has shown the same tendency as IIWPG accident research. The BioRID II dummy was used for this evaluation. The height of BioRID II is equivalent to the AM50%ile. From these results, an appropriate head restraint height for AM95%ile equivalent passengers is considered to be 820mm, because the height difference to the center of gravity between AM50%ile and AM95%ile is 35mm. The value is almost the same as that calculated from human height.

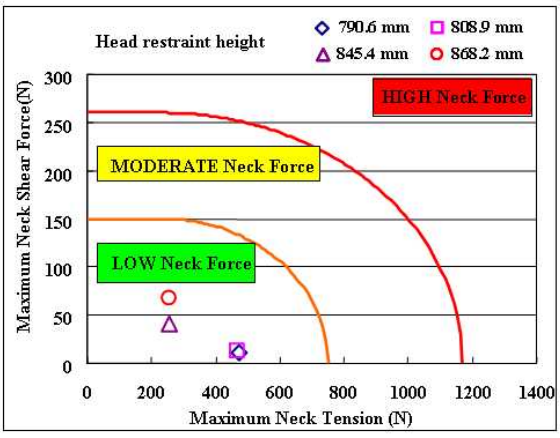

Figure 5-1. Relationship between head restraint height and IIWPG dynamic evaluation.

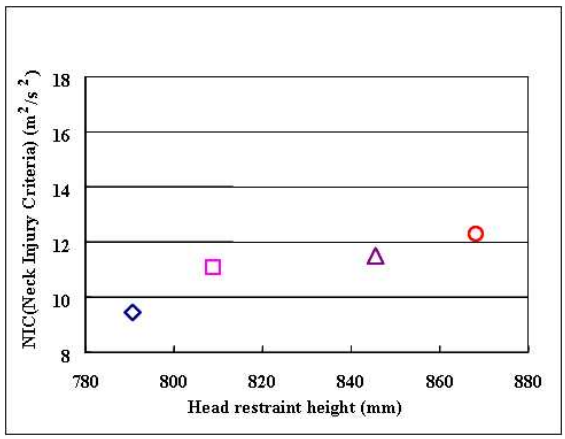

Figure 5-2. Relationship between head restraint height and NIC.

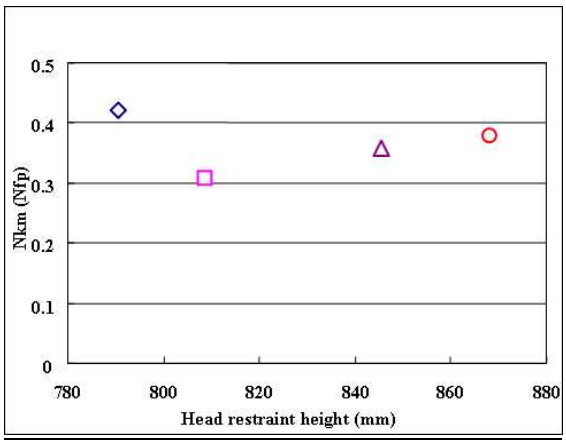

Figure 5-3. Relationship between head restraint height and Nkm.

<u>Rear Visibility Effect</u> - Next, we evaluated the influence of maximum head restraint height on the field of rear vision for a Japanese mini car, which is considered to be significantly affected by head restraint height, because the width of cars in this class must be 1480mm or less, and the distance between driver and passenger seats is almost the smallest in the world. For the evaluation, a vehicle with the head restraint integrated into the seat back was used, as this is common among reasonably priced compact cars, to evaluate the influence of the head restraint height on the direct and indirect field of rear vision and the feelings of passengers. As a result, in the case of such narrow vehicles, it was found that a head restraint height of 850mm or higher might affect the direct rear-diagonal field of vision and the indirect field of vision through the inside rearview mirror (See Figure 6). In the case of 800 to 820mm height, both direct and indirect vision were marginal.

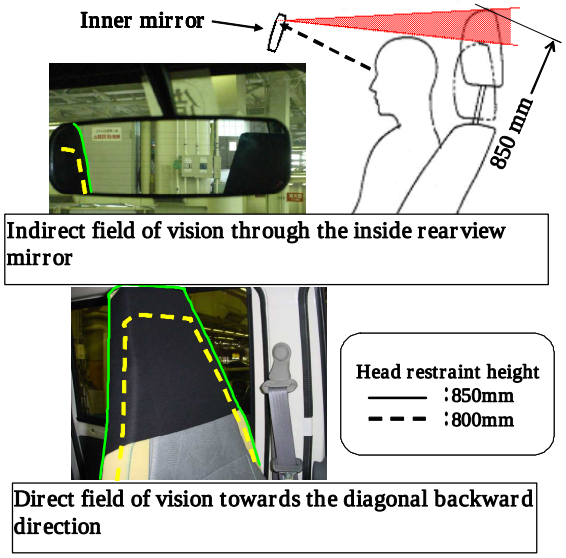

Figure 6. Relationship between the height of head restraint and field of view on the mini car.

Backset

The backset between the head and head restraint was examined as another important requirement. The backset measurement method using HRMD, which was developed by the Research Council for Automobile Repairs (RCAR)[7] and quoted in the assessment of IIWPG and FMVSS202a, has been shown to have problems regarding repeatability and reproducibility during measurement[8]. Accordingly, we examined repeatability and reproducibility in order to seek a more precise measurement method, and studied reasonable requirement values for the measurement method.

Repeatability and Reproducibility – Variation measurements of backset using HRMD were evaluated with four typical seats (See Table 1). The repeatability was evaluated from three to five measurements for the fixed seat reclining position by the same evaluator for each seat. The results were evaluated by maximum variation and coefficient of variation (C.V):

$$\text{Repeatability C.V} = \left[\frac{S_d}{\overline{X}}\right] 100\ (\%) \qquad (2).$$

$\overline{X}$ = Average value of each measurement

S_d = Standard deviation of each measurement

Admissible level: C.V $\leq$ 10%

Maximum variation was within ±2mm and C.V was within 1.75%, showing sufficient precision (See Figure 7 and Table 3). The reproducibility was evaluated for two or three measurements with variable seat reclining positions, which could maintain a torso angle of 25 degrees. The result was also evaluated by maximum variation and C.V:

$$\text{Reproducibility C.V} = \left[\frac{S_b}{\overline{X}_G}\right] 100(\%) \qquad (3).$$

$\overline{X}_G$ = Average value of all measurements

$$S_B = \left[\frac{MSB - MSW}{n}\right]^{1/2}$$

MSB: Average square between measurers

MSW: Average square within a measurer

n: Number of repetitions of test

Admissible level: C.V $\leq$ 10%

The maximum variation was up to ±14.5mm and the C.V diverged towards infinity, thus making it uncalculatable (See Figure 7 and Table 3). This was an unacceptable variation.

Table 1.
Conditions of repeatability and reproducibility evaluation by using HRMD

	Seat		No. of measur-ers	No. of measure-ments	No. of measurering device	Reclining angle
	Type	No.				
Repeatability	A	3	3	3	1	Fixed
	B	3	3	3	1	
	C	3	3	3	1	
	D	1	4	1 to 4	1	
Reproducibility	B	3	3	4	1	Variable
	C	3	3	4	1	
	D	1	4	1 to 5	1	

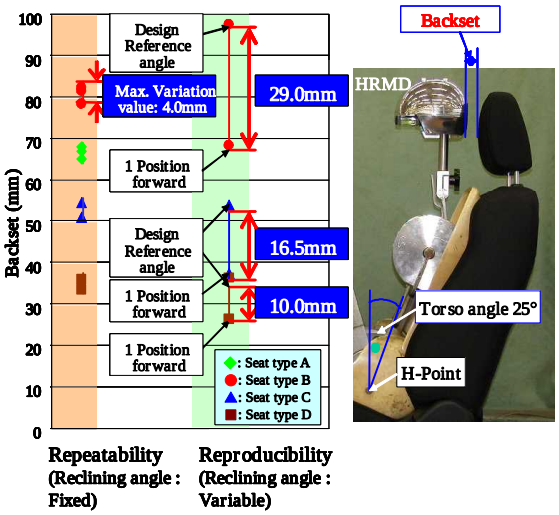

Figure 7. Repeatability and reproducibility for backset by using HRMD.

The three major causes of the deviation are:

(1) Variation of the seatback angle when aligning the seat torso angle to 25 degrees
(2) Variation of H-point when seating the 3DM manikin with HRMD
(3) Variation of vehicle configuration at the time of measurement

The variation, which occurs when mounting the 3DM manikin with multiple joints on a soft seat, has long been a common problem. Therefore, the torso angle of ±5 degrees and H-point of ±25mm have been approved by ECE regulations. In the case of ECE regulation R17, the seating reference point (SRP) and design seat back angle are used as a datum of seat dimensional measurement such as height if the measurement value is within this variation range. Then, we examined applying this idea to the backset measurement. We modified and experimentally manufactured equipment to measure the backset based on SRP and the design seat back angle (See Figure 8), and then evaluated the measurement variation of the backset using the same two types of seats, which were evaluated by the HRMD method, and one new type seat (See Table 2). Since the load by the back pan was applied to the seat back during measurement with the traditional 3DM manikin, we also checked the effect of this. We did not evaluate repeatability because there is almost no potential repeatability variation. The reproducibility was evaluated by using different equipment. The maximum variation was drastically improved from ±14.5mm to ±2.3mm, and C.V from uncalculatable to within 4.41%. The absolute value also became close to the design value (See Figure 9 and Table 3). The value without the back pan was closer to the design value. Similar research conducted by Alliance found that this phenomenon occurred because of excessive back pan load on the seat back due to the difference between SRP and H-point[9]. Within proper load such as back pan load from the normal 3DM manikin, the difference of head restraint position that affects the measurement value of the backset was very minor. Therefore, measurement without the back pan is more appropriate for the new measurement method. On the other hand, some consider that the true value of the vehicle cannot be measured with the new measurement method. Our examination of the difference between SRP and the design standard back angle, and actual measurements on various vehicle seats, showed that the variation is almost even, centered on the reference value (See Figure 10). Therefore, SRP and the design standard back angle are considered to be generally representative of the true value.

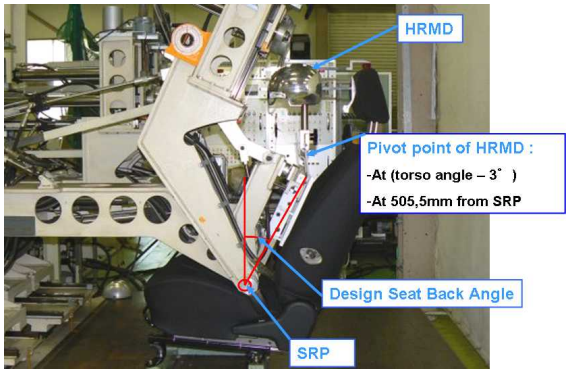

Figure 8. New backset measurement method based on SRP and design seat back angle.

Table 2.
Conditions of repeatability and reproducibility evaluation by using new backset measurement method

	Seat		No. of measur-ers	No. of measure-ments	No. of measurering device	Reclining angle
	Type	No.				
Reproducibility	A	3	1	1	3	Fixed
	C	2	1	1	2	
	E	1	1	1	3	

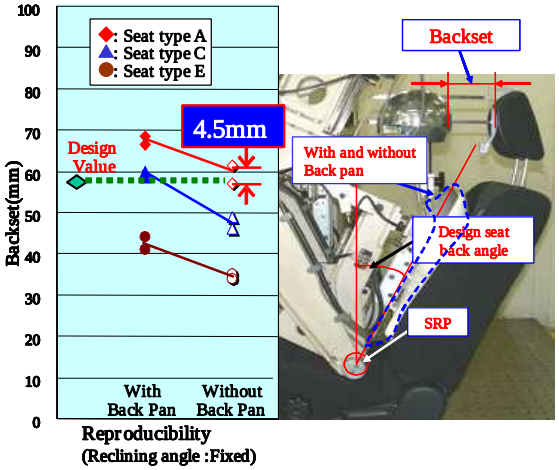

Figure 9. Reproducibility with new backset measurement method.

Table 3.
Comparison of backset repeatability and reproducibility between HRMD method and New method

Seat Type	Repeatability		Reproducibility					
	HRMD Method				New Method with Back pan		New Method w/o Back pan	
	Variation (mm)	C.V.	Variation (mm)	C.V.	Variation (mm)	C.V.	Variation (mm)	C.V.
A	±1.50	0.99	-	-	±1.00	1.70	±2.25	4.41
B	±2.00	1.36	±14.50	∞	-	-	-	-
C	±1.75	1.75	±8.25	∞	±0.75	1.46	±1.50	3.61
E	-	-	-	-	±1.75	4.39	±0.50	1.68

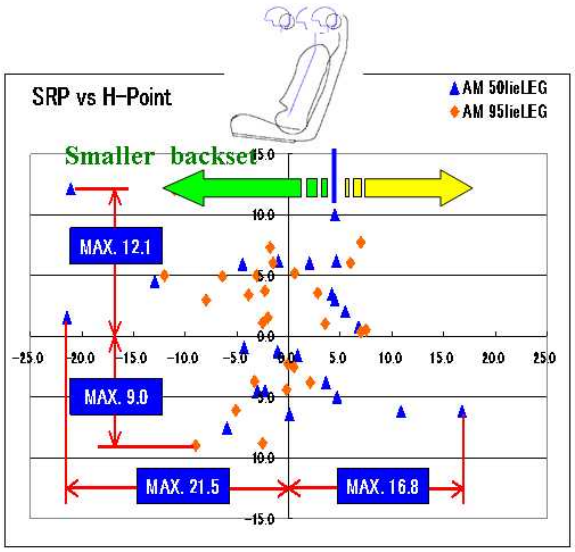

Figure 10-1. Relationship between SRP and H-point.

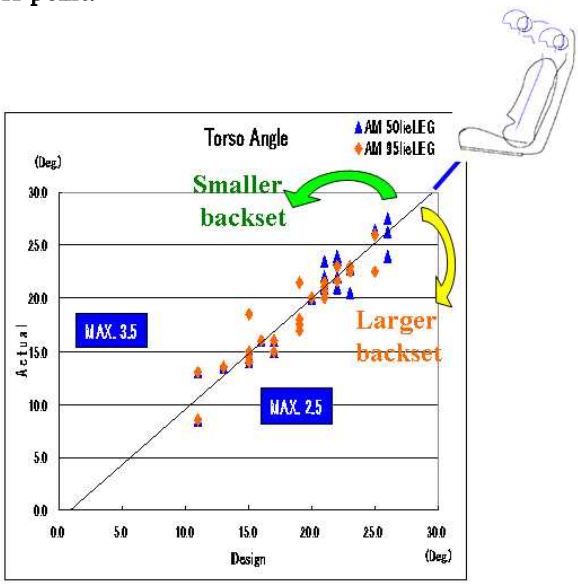

Figure 10-2. Relationship between design torso angle and actual measurement angle.

Comfort - To reduce whiplash flagellum, an effective backset value is 100mm or less and a smaller value produces a larger effect [3]. However, it is known that if the backset is too small, it impairs sitting comfort [10]. For these reasons, we examined backset values that balance safety and comfort. UMTRI summarized the correlation between backset and comfort, but there was not enough data for values smaller than 70mm (with hair margin). Accordingly, we examined whether correlation data for smaller than 70mm could be a substitute. In the examination, we modified the backset of the head restraint of a typical seat to be variable and then determined the actual backset length that made drivers with various frames feel uncomfortable through a sensory evaluation. We found that the evaluation results of UMTRI could extend to the backset range smaller than 70mm. Hence, the backset value could be 40mm or more to secure about 70% comfort (See Figure 11).

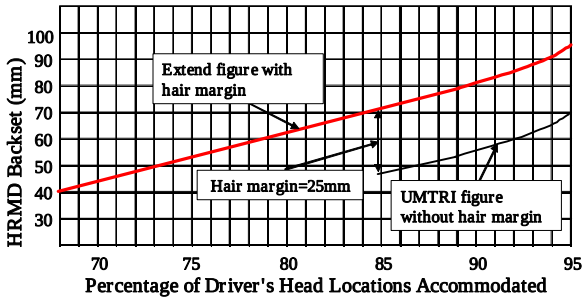

Figure 11. Relationship between comfort and backset.

QUASI-DYNAMIC EVALUATION METHOD

Normally, WAD must be evaluated by the dynamic test, which represents typical rear crash accident conditions. The test must take into consideration the vehicle crash pulse of an actual accident, a dummy with high biofidelity, and injury indicators. However, there was no standardized dynamic evaluation method for regulatory use. On the other hand, it is difficult to measure the static backset value of an active head restraint, in which the seat moves the head restraint forward using the pushing force of the passenger or another drive force at the time of a rear-end collision. The active seat has been increasingly adopted recently to reduce WAD. Therefore, a quasi-dynamic evaluation method with the Hybrid-III dummy was proposed in FMVSS202a as an alternative method of evaluating static backset. We examined the validity and possibility of this method and alternative test methods.

Assessment Dummy

BioRID II, which was developed for evaluating rear-end collisions, is considered to be suitable since it can simulate the behavior aforementioned (knocking up by straightening of the entire spine, S-shaped deformation, etc.) and has high biofidelity, however, it is incomplete as measurement equipment. Therefore, we confirmed a comparison test with Hybrid-III, which has been proven in many proposed collision tests. K. Ono et al. examined the repeatability and reproducibility of two types of dummies [11].

Test Conditions – The evaluation method was as follows (See Figures 12 and 13).

Figure 12. Sled test using BioRID II.

Figure 13. Sled test using Hybrid-III.

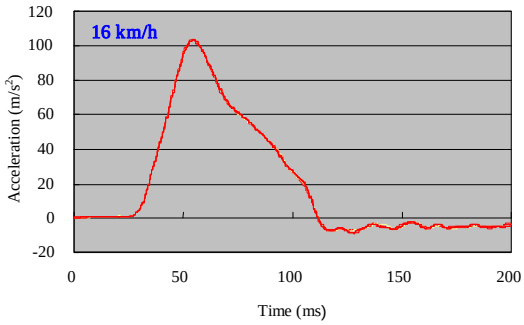

Figure 14. Sled pulse.

- HYGE sled test that simulates the rear-end collision
- Pulse wavelength is △V = 16km/h (See Figure 14)
- Rigid seat
- Test conducted five times under the same conditions
- Dummy: BioRID II (A, B, C), Hybrid-III (A, B, C)
- Features of the dummy, standard calibration description, and measurement items are as follows.

BioRID-II Level F
Dummy A: Owner A (With standard calibration)
Dummy B: Owner B (Without calibration)
Dummy C: Owner C (With standard calibration)

Hybrid-III
Dummy A: Owner A (With standard calibration)
Dummy B: Owner D (With standard calibration)
Dummy C: Owner E (With standard calibration)

Evaluation Indicators
BioRID-II
- Acceleration of the first thoracic vertebra (T1) (T1_Acc)
- Shearing load to the neck (Fx)
- Axial load to the neck (Fz) (Reference evaluation)
- Acceleration of the head (Head_Acc)
- Neck moment (My)
- Rearward rotation angle of the head (HA-TA)

Hybrid-III
- Rearward rotation angle of the head (HA-TA) (Reference evaluation)
- Acceleration of the first thoracic vertebra (T1) (T1_Acc)
- Shearing load to the neck (Fx)
- Axial load to the neck (Fz)
- Acceleration of the head (Head_Acc)
- Neck moment (My)

Method and Criteria for Evaluating Repeatability – The definition of the C.V value used as an evaluation indicator was as follows:

$$\text{Repeatability C.V} = \left[\frac{S_d}{\overline{X}}\right] 100\ (\%) \qquad (4).$$

$\overline{X}$ = Average value of each dummy
S_d = Standard deviation of each dummy
Admissible level: C.V $\leq$ 10%

For both BioRID II and Hybrid-III, the repeatability of the evaluation indicators was within the limit of tolerance (See Figures 15 and 16).

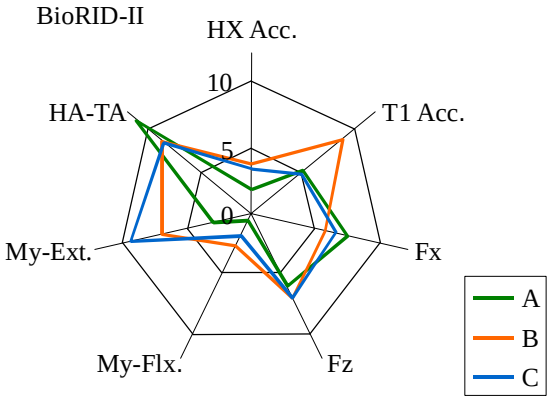

Figure 15. Repeatability C.V for BioRID II.

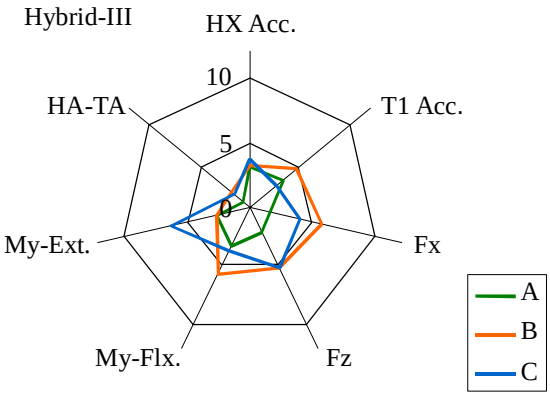

Figure 16. Repeatability C.V for Hybrid-III.

Method and Criteria for Evaluating Reproducibility – The respective three dummies of BioRID II and Hybrid-III of different owners were used and the C.V value to evaluate the reproducibility was calculated as follows:

$$\text{Reproducibility C.V} = \left[\frac{S_b}{\overline{X_G}}\right] 100(\%) \qquad (5).$$

$\overline{X_G}$ = Average value of 3 dummies

$$S_B = \left[\frac{MSB - MSW}{n}\right]^{1/2}$$

MSB: Average square between dummies
MSW: Average square within a dummy
n: Number of repetitions of test
Admissible level: C.V $\leq$ 10%

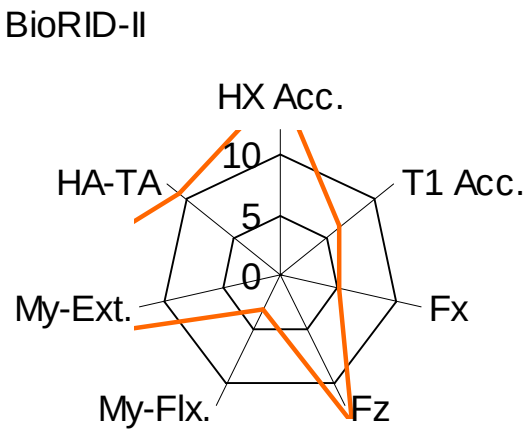

Figure 17. Reproducibility C.V for BioRID II.

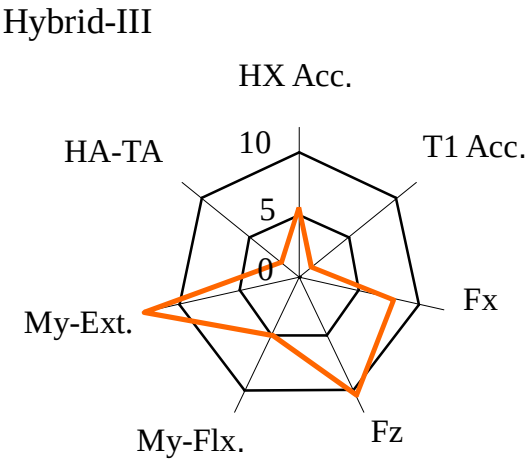

Figure 18. Reproducibility C.V for Hybrid-III.

For Hybrid-III, the reproducibility of the evaluation indicators was within the limit of tolerance (See Figure 17). On the other hand, some of the indicators of BioRID II exceeded the evaluation reference value of the reproducibility (See Figure 18). This occurred because the calibration method for the dummies differed.

Criterion

The backward rotation angle of the head was proposed as an evaluation criterion for Hybrid-III for head restraint gtr, the same as FMVSS202a. The threshold of the rotation angle was also proposed as 12 degrees or less [(12)]. JAMA conducted a comparison sled test between BioRID II and Hybrid-III to evaluate the validity of the indicators aforementioned.

Test Condition – The test was conducted under certain conditions (using Hybrid-III dummy, thread test, $\triangle$V=16km/h, measurement of backward rotation angle of the head) proposed in gtr with the same type of seat as tested by IIWPG that has already been evaluated with BioRID II. The results of the test and IIWPG were then compared

Test Result – As shown in Figure 19, the results are roughly correlated. However, since even the seat with a "Good" evaluation in IIWPG is slightly above the proposed criterion, 12 degrees, the proposed criterion is slightly too severe to compare IIWPG criteria.

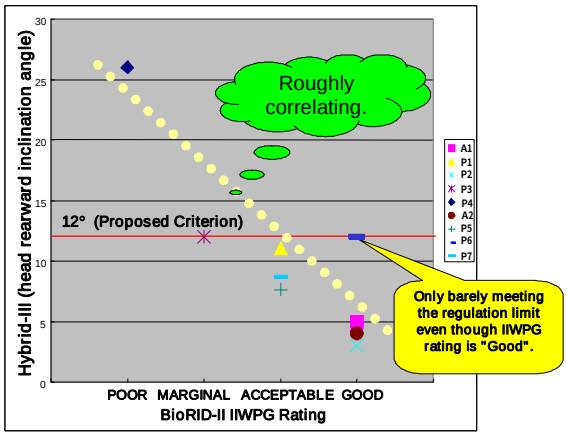

Figure 19. Correlation between IIWPG (BioRID II) and FMVSS 202a (Hybrid-III) evaluations.

Test Variation – The results of backward rotation angle of the head when the thread test was conducted five times under the same conditions with three types of Hybrid-III dummies are shown in Table 4. The difference between the maximum and minimum value is about 4 degrees. Therefore, the criterion should have this ±2 degrees variation margin.

Table 4.
Head rear rotation angle variation

	Dummy	Speed (km/h)	Value 1st	2nd	3rd	4th	5th	Value max	min
HA-TA (deg)	Hybrid-III A	16	48.6	48.9	48.0	48.4	48.4	48.9	48.4
	Hybrid-III B		50.3	48.1	49.4	48.7	48.4	50.3	48.1
	Hybrid-III C		48.3	46.5	47.2	47.4	46.8	48.3	46.5

DISCUSSION

We have examined the static and quasi-dynamic evaluation methods and requirements concerning the effects of head restraints and seats for WAD in rear impacts. These static requirements mainly affect only the part of first stage of the whiplash phenomenon (the stage before the head contacts the head restraint) as shown in Figure 3. To evaluate the S-shaped deformation of cervical vertebrae, which is a major factor of whiplash flagellum, the difference of behavior between the trunk and head before and after contacting the head restraint and the degree of load applied to the neck must be evaluated. To do so, a dynamic evaluation using a dummy for the rear-end accident simulation is effective, and many studies and assessments have already been conducted. In fact, the correlation between the IIWPG backset value and result of the dynamic evaluation in terms of only the seats with sufficient head restraint heights is extremely low (See Figure 20). Therefore, to properly evaluate the seat and head restraint performance for WAD, it is essential to introduce the dynamic evaluation.

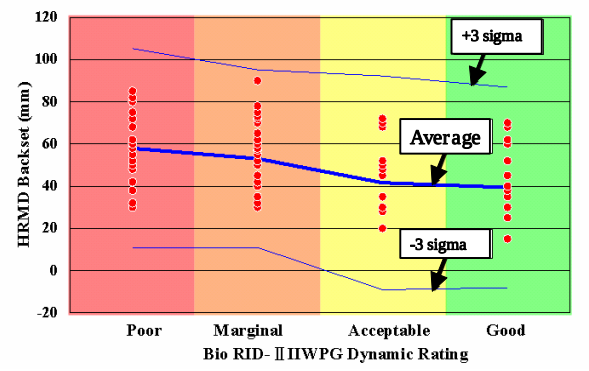

Figure 20. Correlation between IIWPG backset and dynamic evaluation score for proper height of non active seat.

Proposal from JAMA – A new workgroup must be established to examine the proper dynamic test and evaluation method. The results of the tests and method must be fed back to the head restraint gtr as phase two which was agreed in GRSP held in December 2006. This workgroup should clarify the following items.
Agenda Items for WG

- Sled pulse conditions:
  Reflecting accident realities
- Assessment dummy:
  Biofidelity level, Test method, Seating method, etc.
- Assessment criteria:
  Reflecting injury phenomena; Assessed in terms of injury values
- Limit value:
  An appropriate value based on injury risk analyses and feasibility studies
- Effect assessment:
  Determining the injury-reducing effect on real-world accidents

CONCLUSIONS

From the evaluation results described in this paper, JAMA recommends the following description as the static and quasi-dynamic evaluation method and the evaluation standard on the front outer seat and head restraint.

Height

The appropriate required maximum height (Hmax) is 820mm for both protection and visibility.
We could not find any further benefit of setting the head restraint higher than 820mm for up to AM95%ile.
We also found by our internal review that most of the current head restraints, complying with the 800mm

requirement regulated in ECE R17, are already higher than 820mm; therefore, the current regulation requirement, Hmax = 800mm, virtually already covers the required height.

Backset

To achieve a good balance between competing requirements, WAD reduction performance and comfort, the backset value should be made as small as possible without sacrificing comfort. To achieve this, the variation of the evaluation method should be minimized. In this regard, our study showed that the new backset evaluation method is the most appropriate method. Since even this test method cannot eliminate manufacturing variations of the seat itself (±10mm), we propose that the limit of the backset requirement value with the new measurement method be as follows:

Backset requirement =Comfort boarder [40mm]
+ Measurement variation [4.5]
+ Manufacturing variation [10mm]
=[54.5mm] (6).

QUASI-DYNAMIC

This test method is an alternative to the backset evaluation for the active head restraint in which the head part moves at the time of a rear-end collision. As well as the active head restraint, the test method that measures the backward rotation angle of the neck of the Hybrid-III dummy was also considered to be effective since the variation is smaller than that of the traditional HRMD backset measurement method. However, since Hybrid-III has less biofidelity during a rear-end collision, it was found that they were evaluated differently from the BioRID II dummy having high biofidelity on some seats. Therefore, it is difficult to introduce the dynamic evaluation with severer criterion unless a highly reproducible method that can properly reproduce the actual phenomenon with a dummy with high biofidelity is established. For these reasons, for the time being, a Hybrid-III dynamic test with slightly less severe criterion or the new backset measurement method incorporating the activation margin of the active headrest are considered to be effective in the case of the active head restraint.

ACKNOWLEDGEMENTS

We thank JARI (Japan Automobile Research Institute), JAMA, and twelve member companies of these organizations for their assistance with this study.

REFERENCES

[1] Third Symposium for Automobile Safety (Ministry of Land, Infrastructure and Transport, September 2002)

[2] TRANS/WP.29/1039 - Report of the 135th session of WP.29 (8 - 11 March 2005)

[3] IIHS Status Report Vol. 34, No. 5 (IIHS, May 22, 1999)

[4] K. Ono et al.: Motion Analysis of Cervical Vertebrae During Whiplash Loading, Spine Vol. 24, Number 8, pp. 763-770 (1999)

[5] GRSP Informal Group on Head Restraints, 4th Meeting (USA, HR4-2, 7-9 September 2005)

[6] GRSP Informal Group on Head Restraints, 5th Meeting (Japan, HR5-18, 23-26 January 2006)

[7] Procedure for Evaluating Motor Vehicle Head Restraints, Issue 2 (RCAR, Feb. 2001)

[8] Céline Adalian et al.: The Repeatability and Reproducibility of Proposed Test Procedures and Injury Criteria for Assessing Neck Injuries in Rear Impact (19th ESV, 05-0340, June 2005)

[9] GRSP Informal Group on Head Restraints, 5th Meeting (OICA/Alliance, HR7-4, 12 -14 September 2006)

[10] Matthew P. Reed et al.: Response to NPRM on FMVSS 202, Docket No. NHTSA-2000-8570 (UMTRI, March 3, 2001)

[11] Mitsuru Ishii et al.: Factors Influencing the Repeatability and Reproducibility of the Dummies Used for Rear-end Impact Evaluation(IRCOBI Conference, September 2006)

[12] GRSP Informal Group on Head Restraints, 1th Meeting (USA, HR1-2, 1-2 February 2005)

APPLICATION OF REAR HEAD AIRBAG TO MITIGATE REAR IMPACT INJURIES

Jörg Hoffmann
Toyoda Gosei Europe N.V.
Germany
Shigeyuki Suzuki
Masaya Sakamoto
Kenji Hayakawa
TOYODA GOSEI CO., LTD.
Japan
Paper Number 07-0315

ABSTRACT

In the real world, the accident ratio of rear impact is high. The injury scheme in those accident scenarios is mainly caused by whiplash. The intrusion of the rear end of the vehicle during impact combined with movement by occupants seated on rear seats plays a significant roll. This paper discusses an airbag which deploys from the roof header along the rear window. By means of numerical simulations and tests, the mitigation of biomechanical injuries of passengers seated on rear seats during rear impact was observed. Significant occupant protection was assessed under high-speed rear-impact conditions.

Keywords: Airbag, Rear impact

INTRODUCTION / ACCIDENT RESEARCH

When evaluating NASS/CDS (National Automotive Sampling System / Crashworthiness Data System) data, according to rear-impact injuries covering the years 1996 to 2005, it can be observed that in 47 % of all AIS1+ injuries, 40 described accidents in which passengers seated on rear seats sustained head injuries and 53 % concerned neck injuries. A significant increase in this injury ratio is observed when evaluating the data from NASS/CDS according to the AIS2+ injury scale for the head and neck region (5 accidents described). Injuries to the head account for 80 % of all injuries to this body region in rear impacts. Figure 1 depicts the ratio of head and neck injuries in vehicle rear impact for AIS1+ and AIS2+.

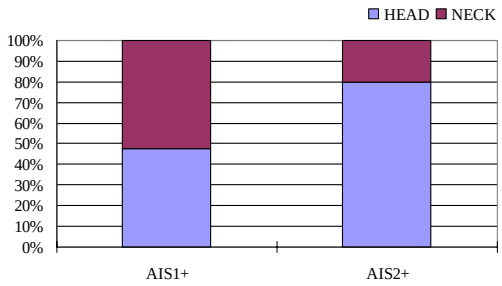

Figure 1. Injury ratio of head and neck (NASS/CDS, AIS1+: 40 cases, AIS2+: 5 cases)

The NASS/CDS data base also permits derivation and evaluation of the sources of these injuries. The sources for AIS1+ injuries are varied. During a rear-impact accident, the passenger's head can come into contact with various vehicle body parts such as the C-pillar, rear window, seat-back, rear header, head rest and roof. The distribution of these injury sources affecting AIS1+ head injuries is depicted in Figure 2. Contact is most frequent with the C-pillar (23 %), rear window (18 %) and the seat back (17 %).

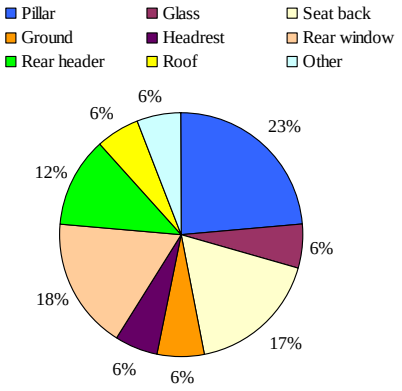

Figure 2. Injury sources for head injuries in rear-end collisions (NASS/CDS, AIS1+: 20 cases)

The injury sources causing head injuries according to the Abbreviated Injury Scale AIS2+ are limited. The accident data analysis shows three main contact points that lead to severe head injuries. Besides C-pillar and roof contact, each of which accounts for about 20 %, contact of the head with the rear header is most frequent. The ratio of the injury scenario is 40 % of all injury sources. Figure 3 depicts the breakdown of injury sources producing AIS2+ head injuries.

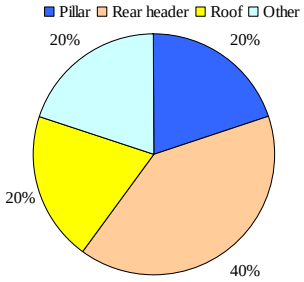

Figure 3. Injury sources for head injuries in rear-end collisions (NASS/CDS, AIS2+: 5 cases)

Rear passengers in which vehicle group are exposed to the most danger? This can also be derived from the NASS/CDS data base. The data indicates that 45 % of all head injuries occur in small cars. It suggests that the smaller the vehicle, the more likely a head injury will occur in an vehicle rear-end accident. Figure 4 illustrates that the ratio of mini cars is 25 % and those of compact cars is 20 %. The percentage attributable to intermediate cars is also 20 %.

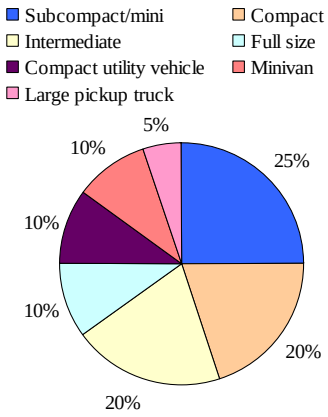

Figure 4. Ratio of car classes relating to head injuries (NASS/CDS, AIS1+: 20 cases)

The impact velocities delta v (km/h) of rear impact in real-life accidents can also be derived from the NASS/CDS data base. When evaluating the impact scenarios, it is remarkable that the impact velocity affecting this head injury of AIS1+ level is between 16 and 35 km/h. Rear-end collision velocities higher than 40 km/h cause injuries to the rear passengers of AIS2+. Figure 5 illustrates the various rear-impact velocities for AIS1 and ASI2+.

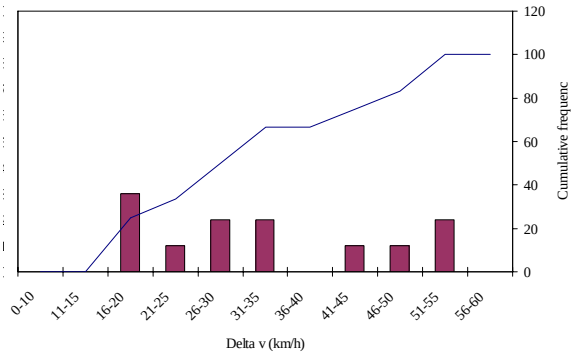

Figure 5. Rear-impact velocities relating to the injury scale (NASS/CDS)

When evaluating the same accident data based on rear occupant weights, no significant difference can be observed. The following Figure 6 presents the occupant weights sustaining head injuries AIS1+.

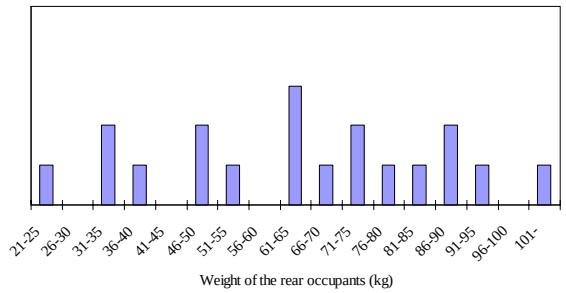

Figure 6. Weight of rear passengers in rear-end collisions (NASS/CDS)

Accident research has shown that occupants seated in rear seats can sustain severe head injuries in rear-impact accidents. The risk of passengers being injured in small vehicles is significant. Independent of weight respective to height, the occupants have hardly any contact to vehicle body parts such as the rear header, C-pillar and roof.

OCCUPANT PROTECTION CONCEPT IN HIGH-SPEED REAR IMPACT

Based on rear-impact research, a procedure has been designed to evaluate the risk of head and neck injuries in rear-end collisions. In this low-speed rear-impact test procedure, the equivalent of a stationary vehicle being struck by a vehicle of the same weight at a velocity of 32 km/h is applied. A BioRID 2 dummy is placed on the front seat measuring the loads during the rear-impact crash. Application of this test procedure will evaluate introduction of safety features mostly integrated into the seat back or head rest of frontal seats. These technical solutions are introduced to enhance the protection of front seat occupants in low-speed rear-impact crashes.

Front-seated vehicle occupants can be protected by headrest systems, which lower the gap between the head and the headrest. By means of crash-absorbing seat structures and a rocker system which uses the occupant's seat intrusion to displace the headrest or pyrotechnical actuators, the kinematics of the occupant head can be optimised. The protection concepts introduced are mainly designed for protecting front-seated passengers.

For rear-seated passengers, an airbag concept covering the area of rear header, roof and C-pillar could be the key to the technical solution. The technology is similar to curtain airbag technology for vehicle side protection. The airbag covers both the rear header and window area to provide space for absorbing the energy of the occupant's head during impact. The principle layout of this airbag technology is illustrated in Figure 7.

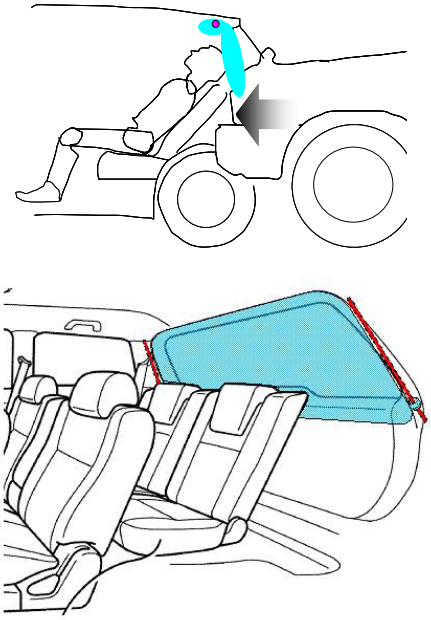

Figure 7. Principle layout of back seat head airbag concept for rear-end collisions

A gas inflator and a folded airbag are placed in the roof of the car. In the case of a rear impact, the hybrid gas inflator with a 220 kPa tank pressure characteristic starts to inflate the gas into the 20-litre silicon-coated rear row airbag. The upper part of the airbag deploys to cover the rear header of the car and the lower part turns into a rear deployment portion which is presented below in Figure 8.

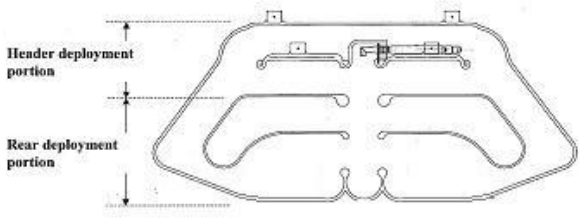

Figure 8. Rear row head airbag design

Based on this initial design, the airbag concept has been set up as a prototype. Deployment tests were performed to check the proper deployment behaviour in a real vehicle environment. The following Figure 9 depicts a video sequence of the rear row head airbag deploying in a compact car.

Figure 9. Video sequence of a static deployment test with the rear row head airbag concept

In addition to static deployment tests, impactor tests were performed to generate deceleration data for validating the numerical simulation airbag model.

INVESTIGATION OF THE PROTECTION CONCEPT BY NUMERICAL SIMULATION

On the basis of a mass production vehicle, a numerical simulation mock-up was set up. The rear end geometry of the mock-up corresponds to a compact class vehicle. Hybrid III dummies sized AF05 and AM50 were used in the simulations. A detailed seat model was introduced representing dummy-seat interactions. The dummies were not belted. According to the results of the evaluated NASS/CDS data, a rear-impact crash pulse was used in the simulation representing a 50 km/h rear-impact to a compact car.

Evaluation of protection performance - The validated rear row head airbag model was incorporated into the vehicle simulation mock-up. The two different scenarios AM50 and AF05 were simulated with the validated airbag concept. Figures 10 and 11 depict the simulation mock-up modelled using Madymo simulation software [1].

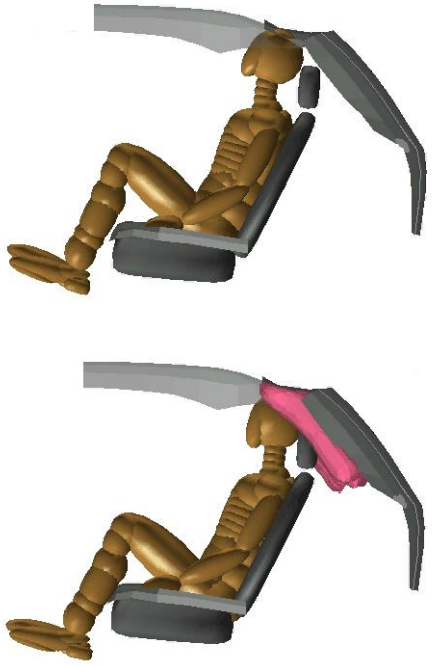

Figure 10. Video sequence of rear impact where v = 50 km/h, an AM50 dummy (top) and with rear row head airbag (bottom)

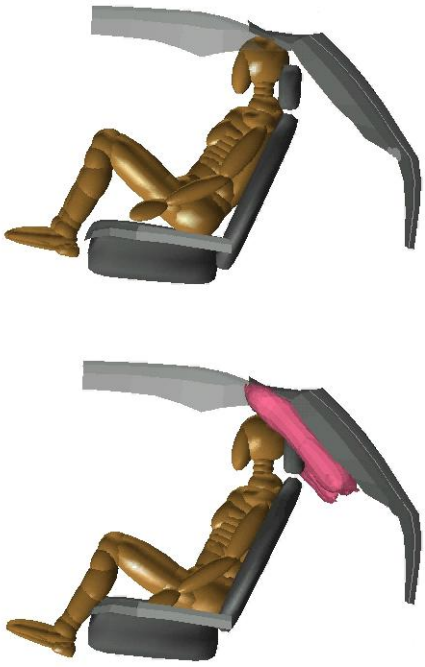

Figure 11. Video sequence of rear impact where v = 50 km/h, an AF05 dummy (top) and with rear row head airbag (bottom)

When evaluating the results derived from the 50 km/h rear-impact crash simulation, the contact between the dummy head and rear header was observed. In this case, the biomechanical loads AM50 and AF05 in the head and neck area are well above acceptable limits. The impact of the collision causes the dummy seated on rear seats to slip slightly upwards. At about 25 ms, the head hits the rear header. The hard contact ends up in a load peak. The rear airbag concept prevents the occupant's head from making such hard contact with the car. Head acceleration and neck forces are thereby reduced. The following Figures 12 to 15 show the results of the simulation.

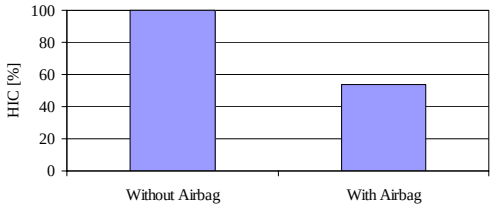

Figure 12. Comparison of HIC_{15} results with and without airbag for AM50 dummy

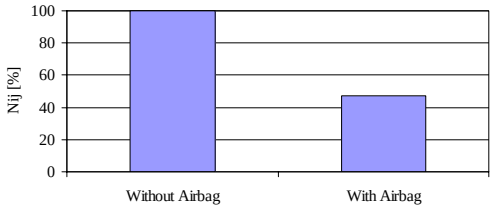

Figure 13. Comparison of Nij results with and without airbag for AM50 dummy

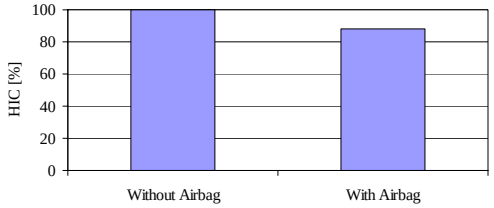

Figure 14. Comparison of HIC_{15} results with and without airbag for AF05 dummy

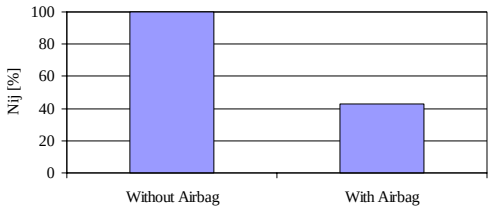

Figure 15. Comparison of Nij results with and without airbag for AF05 dummy

CONCLUSIONS

The numerical simulation discussed in this paper illustrate the importance of protecting rear row-seated occupants from hard contact with the vehicle rear header, in order to avoid significant loads on the head and the neck.

This computer-simulated investigation into rear-impact protection demonstrated that an airbag concept covering a vehicle's rear header area is very effective in preventing the rear passenger's head from sustaining severe injuries during high velocity rear impact.

REFERENCE

[1] Madymo 6.2.2 Reference / Theory Manual. TNO Madymo BV. Delft, The Netherlands. August 2006

A COMPARATIVE STUDY OF DUMMY SENSITIVITY TO SEAT DESIGN PARAMETERS

Michael Kleinberger
Liming Voo
Andrew Merkle
Rafal Szczepanowski
Bethany McGee
Johns Hopkins University Applied Physics Laboratory
United States
Paper Number 07-0366

ABSTRACT

Whiplash injuries and their associated cervical symptoms are a critical problem resulting from rear impact motor vehicle collisions. Although the exact injury mechanisms remain elusive, recent biomechanical research has suggested that relative motion between the head and torso, or more precisely between adjacent vertebrae of the neck, may be the primary cause for such injuries. Currently available test dummies have limited biofidelity and functionality in the assessment of head restraint performance. The challenge to the automotive safety community is to select a dummy that can discriminate between seat designs with varying levels of performance in terms of their whiplash injury mitigation. The objective of this study was to evaluate the responses of various 50th-percentile male dummies, namely the BioRID II, Hybrid III, RID III, and THOR, under rear impact conditions to determine their sensitivities to seat design parameters believed to be critical to the mitigation of whiplash injuries. Seat and head restraint design features studied included seatback recliner stiffness, head restraint height, and head restraint backset. A variety of biomechanical measurements related to whiplash injury risk were used in the comparison of dummy responses, including relative head-to-torso extension rotations, extension moments measured in the lower neck, and tension and shear forces measured in the upper neck. Results indicated significant differences between the dummy responses and their sensitivities to critical seat design features. Sensitivity was also found to vary greatly depending on the specific dummy and injury measure selected.

INTRODUCTION

Although typically classified as AIS 1, whiplash injuries can result in long-term and even permanent disabilities, with an annual societal cost in the US of approximately $2.7 billion associated with rear impacts as estimated by the National Highway Traffic Safety Administration (NHTSA) [1]. Although these injuries can occur in any crash direction, rear impact collisions produce a higher incidence rate than other types of crashes.

During a typical rear impact collision an occupant will initially move rearward with respect to the vehicle interior as the vehicle is accelerated forward. The occupant's head and torso will contact the head restraint and seatback, respectively, causing the seatback to rotate and deform rearward. The occupant will then rebound off the seatback and begin to move forward relative to the vehicle interior. For a belted occupant, the forward rebound motion is stopped by the force of the seatbelt acting across the torso and hips. Motion of the occupant depends on a number of parameters, including their height and weight, position and design of the head restraint, seatback recliner stiffness, seatbelt usage, and motion of the vehicle. The entire sequence of events typically takes less than 200 milliseconds, or two-tenths of a second.

Loading on the body during a rear impact collision is a complex, multi-directional event, even for an in-line bumper-to-bumper collision. As the seat moves forward and makes contact with the occupant's back, the normal kyphotic curve of the thoracic spine is straightened, resulting in a compressive load applied to the spine. This spinal compression was noted by Ono and Kaneoka [2,3] during their volunteer studies using high-speed x-ray imaging. Shear forces and localized flexion and extension bending moments are also sustained by the spine, resulting in a complex combination of forces and moments incurred at each level of the spine and on the head.

Although there is currently no consensus on cervical spine injury criteria, most researchers agree that whiplash injuries are related to the relative motion between the head and torso, and that the reduction of this relative motion will lead to a decrease in the incidence and severity of these injuries. Further, it has been shown that the relative motion between the head and torso is greatly affected by various seat

design parameters, including the position of the head restraint relative to the head [4] and the seatback recliner stiffness [5]. Head restraint position is typically quantified using the height and backset (horizontal distance between the head and head restraint) as measured in accordance with the FMVSS 202a standard using the SAE J826 manikin and the ICBC Head Restraint Measuring Device (HRMD), respectively. Recliner stiffness is typically measured in accordance with the procedures established in the FMVSS 207 standard.

Injury Criteria

Several different injury criteria have been proposed by researchers in an attempt to predict the occurrence of whiplash injuries. Bostrom *et al* [6] proposed the Neck Injury Criterion (NIC), which is based on the Navier Stokes equations and the assumption that fluid flow within the spinal canal causes pressure gradients that are injurious to the nerve roots. Kleinberger *et al* [7] proposed the N_{ij} neck injury criteria, which combines the effects of forces and moments acting at the occipital condyles normalized by a set of critical threshold values. Schmitt *et al* [8] proposed a modified version of the Nij criteria, called the N_{km} Criteria, which combines the effects of shear force and flexion-extension moment acting in the upper cervical spine. Prasad *et al* [9] suggested using extension moments measured at the lower neck load cell because it was found to be more sensitive to seat design and crash severity. Viano *et al* [10] proposed a Neck Displacement Criterion (NDC), which is based on the relative displacement and rotation between the occipital condyles and the T1 vertebrae as compared with the natural range of motion. This criterion was proposed as a supplement to other existing criteria until the mechanisms of whiplash injury are better understood. More recently, Kuppa *et al* [11] proposed a relative head-to-torso extension rotation criterion, which has been adopted in the newly upgraded FMVSS 202a standard.

It is important to note that each of the proposed injury criteria mentioned above has been developed using a specific anthropomorphic test device (ATD). Application of these criteria to other ATDs would require the determination of a new set of critical values or thresholds, which would be a difficult task due to significant differences in dummy designs.

The objective of this study was to evaluate the relative performance of various ATDs currently being used to investigate occupant responses to rear impact. Dummy performance was compared using measures of the relative head-to-torso extension rotation, lower neck extension moment, upper neck tension force, and upper neck posterior shear force (head moving posteriorly relative to the neck) for various combinations of head restraint position and recliner stiffness.

EXPERIMENTAL METHODS

A production automotive seat (1999 Toyota Camry) was modified to allow the rotational recliner stiffness, head restraint height, and backset to be adjustable over a wide range. The normal recliner mechanism was replaced with a simple pin joint to provide free rotation at the hinge joint. Rotational stiffness was provided by two spring-damper assemblies externally mounted to the rear of the seatback. Stiffness was varied by changing the set of coil springs and/or their location relative to the hinge joint. To provide a repeatable test system and avoid any permanent deformation, the seatback frame was structurally reinforced with steel channels to provide attachment points for the spring assemblies. The head restraint supports were also modified to allow adjustment in both the horizontal and vertical directions. Figure 1 shows the modified seat with the attached spring-damper assemblies.

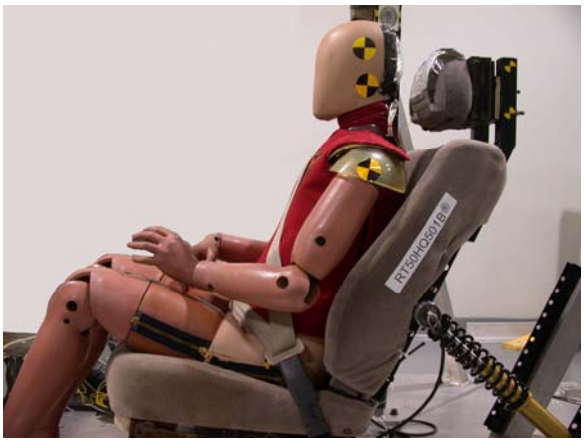

Figure 1. Modified seat providing adjustable recliner stiffness and head restraint position.

Rear impact tests were conducted on a Via Systems deceleration sled using four different mid-sized male ATDs, including the Hybrid III, BioRID2, THOR, and RID3. A sinusoidal sled pulse with a nominal impact speed of 17 kph was used that fit within the FMVSS 202a dynamic testing corridor. The nominal peak acceleration and duration of the pulse was 9.0 g's and 90 msec, respectively. Seatback angle was initially set at 25 degrees relative to vertical; head restraint height was set at either 750 mm or 800 mm;

and head restraint backset was set at either 50 mm or 75 mm. Head restraint height is the distance from the H-point to the top of the head restraint measured parallel to the torso line, as prescribed in FMVSS 202a. Backset is defined as the horizontal distance between the posterior aspect of the head and the front surface of the head restraint. This distance was measured using the ICBC's HRMD attachment to the SAE J826 manikin. Seatback recliner stiffness was set at either a baseline value of 35 Nm/deg or at 105 Nm/deg (300%). The baseline recliner stiffness value of 35 Nm/deg represents a relatively compliant single recliner automotive seat [12].

Sensor arrays for the various dummies varied slightly due to differences in dummy design. However, all tests included a core suite of instrumentation, including triaxial accelerometers at the head CG and thorax CG, a single accelerometer at T1, angular rate sensors mounted in the head and upper spine, 6-axis load cells in the upper and lower neck, and a 3-axis load cell in the lumbar spine. All sensor data were collected using an on-board TDAS-Pro data acquisition system. In addition to the sensor output, dummy kinematics were recorded for each test using an on-board IMC Phantom 4 digital video camera operating at 1000 frames per second. The two components of a custom designed head contact switch were attached to the posterior surface of the head and front surface of the head restraint to serve as a switch to determine head contact times.

RESULTS

Measured responses for the different ATDs varied considerably under identical test conditions. In addition, the sensitivity of each dummy to changes in the critical seat design parameters varied greatly. An overall comparison of the dummy responses to rear impact is shown below in Figures 2-5 for tests with a baseline recliner stiffness and a relatively good head restraint position with a height of 800 mm and a backset of 50 mm. Clear differences in responses are readily observable between dummies. Relative head-to-torso extension rotations (Figure 2) range from a maximum of 11 degrees for the Hybrid III down to almost zero for both the BioRID2 and THOR. Lower neck extension moments (Figure 3) also varied considerably from 96 Nm for the Hybrid III down to almost zero for THOR. Upper neck tension forces (Figure 4) ranged from roughly 1100 N to 1700 N, but the differences were not as dramatic between dummies. Upper neck posterior shear forces (Figure 5) varied from 287 N for the RID3 down to almost zero for THOR.

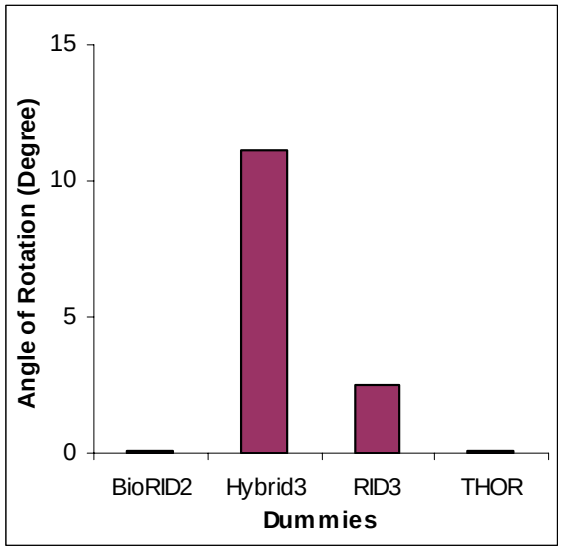

Figure 2. Measured relative head-to-torso rotation for the various dummies at baseline stiffness and good head restraint position.

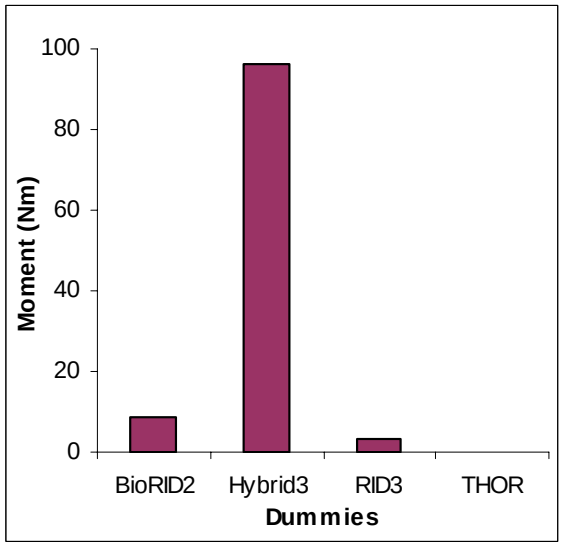

Figure 3. Measured lower neck extension moment for the various dummies at baseline stiffness and good head restraint position.

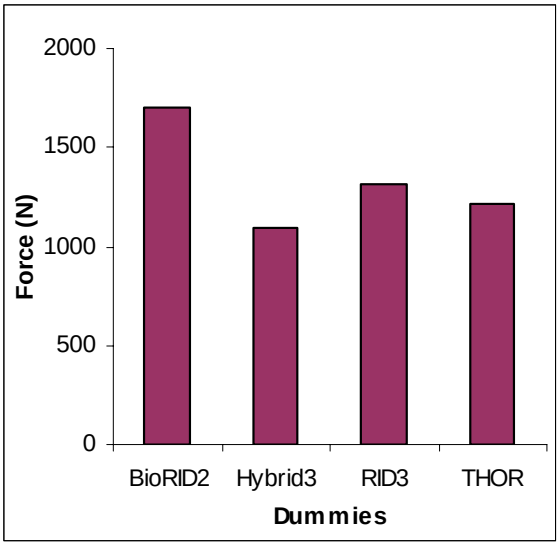

Figure 4. Measured upper neck tension force for the various dummies at baseline stiffness and good head restraint position.

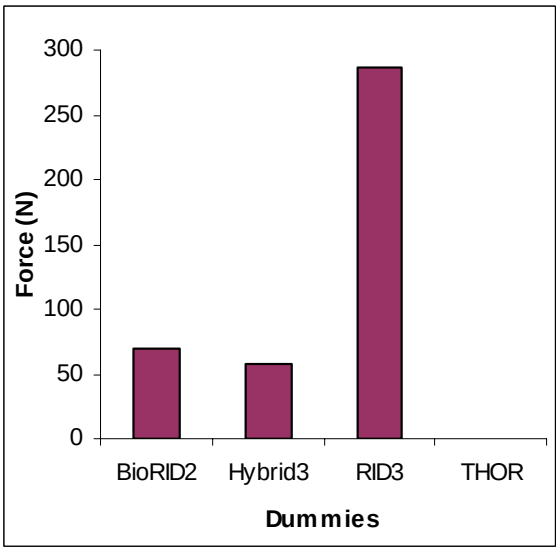

Figure 5. Measured upper neck posterior shear force for the various dummies at baseline stiffness and good head restraint position.

The time until the initial contact between the head and head restraint was also found to vary significantly between the various dummies, ranging from 83 ms for the THOR dummy to 113 ms for the BioRID2 dummy. Figure 6 shows a comparison of these initial contact times, and Figure 7 shows the position of each dummy at the point of contact. It should be noted that the contact location on the posterior surface of the head is different for each dummy, and is affected by the overall dummy design. For example, the BioRID2 and THOR dummies were found to have a higher initial seated height than the Hybrid III and RID3 dummies, which resulted in head contact on the inferior aspect of the skull cap.

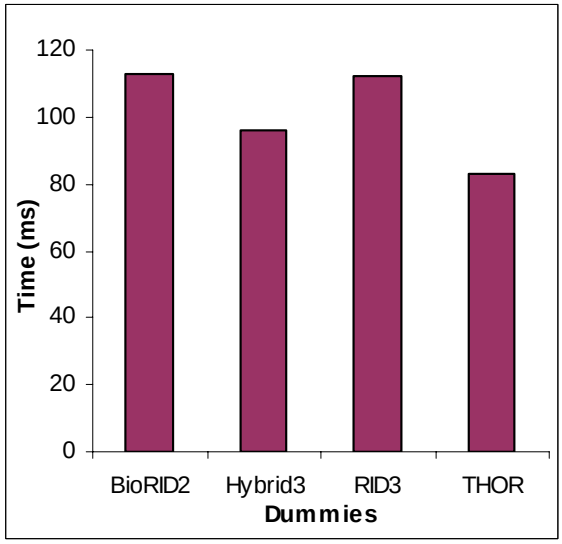

Figure 6. Measured initial head contact times for the various dummies at baseline stiffness and good head restraint position.

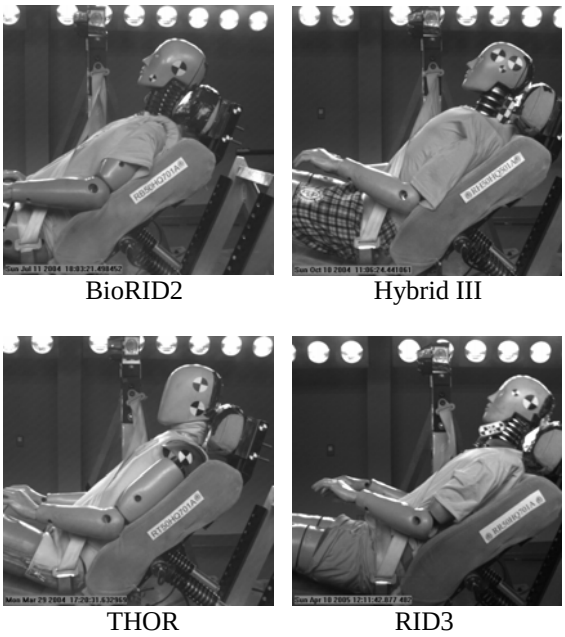

Figure 7. Dummy positions at point of initial head to head restraint contact.

The effects of head restraint position are shown in Figures 8-11 for each of the dummies. In these figures, the head restraint positions are shown on the horizontal axes, where H represents the "High" height of 800 mm and L represents the "Low" height of 750 mm. Similarly, the backset position is represented by the number, where "5" represents a backset of 50 mm and "7" represents a backset of 75 mm. Therefore, in these figures, H5 represents the best case head restraint position with an 800 mm height and 50 mm backset, while L7 represents the worst case head restraint position with a 750 mm height and 75 mm backset.

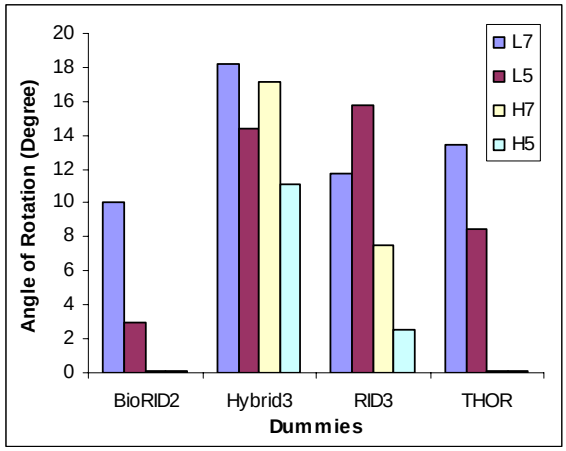

Figure 8. Effect of head restraint position on measured head-to-torso rotation for a baseline stiffness.

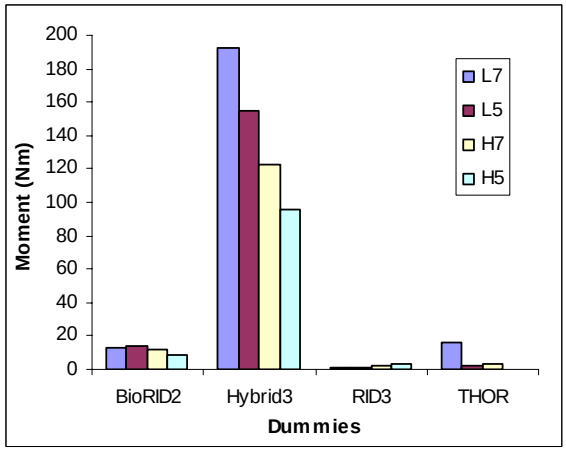

Figure 9. Effect of head restraint position on measured lower neck extension moment for a baseline stiffness.

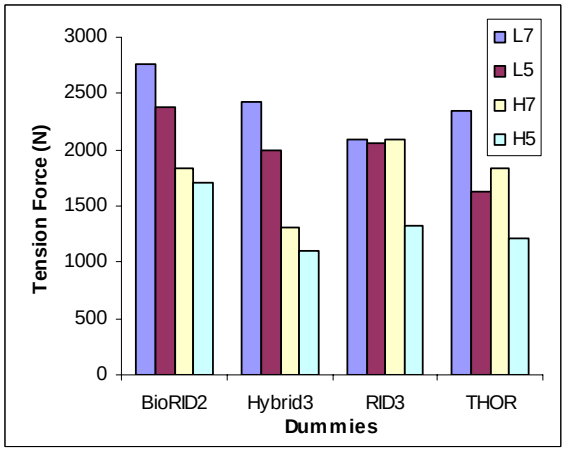

Figure 10. Effect of head restraint position on measured upper neck tension force for a baseline stiffness.

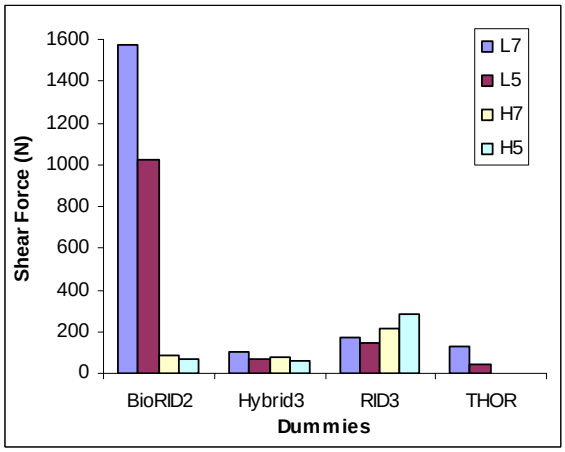

Figure 11. Effect of head restraint position on measured upper neck shear force for a baseline stiffness.

The effects of seatback recliner stiffness are shown in Figure 12 for each of the dummies using the best case head restraint position (H5) with a height of 800 mm and a backset of 50 mm. The baseline (100%) recliner stiffness of 35 Nm/deg represents a relatively compliant single recliner automotive seat, while the 105 Nm/deg recliner stiffness represents a seat that is nominally three times stiffer (300%). Figure 13 shows similar data for the worst-case head restraint position (L7) with a height of 750 mm and a backset of 75 mm. It is important to note in Figure 12 that even though the relative head-to-torso rotations measured with the Hybrid III dummy were larger than the other dummies, the values were below the 12-degree threshold established for the dynamic option within the FMVSS 202a standard for both the baseline and 300% recliner stiffnesses with the best head restraint position. Conversely, the head-to-torso

rotations of the Hybrid III dummy exceeded the 12-degree threshold for the worst-case head restraint position as shown in Figure 13.

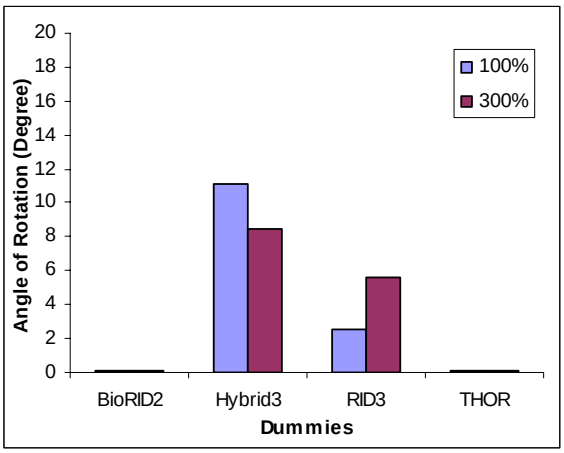

Figure 12. Effect of seatback recliner stiffness on measured head-to-torso rotation for best-case (H5) head restraint position.

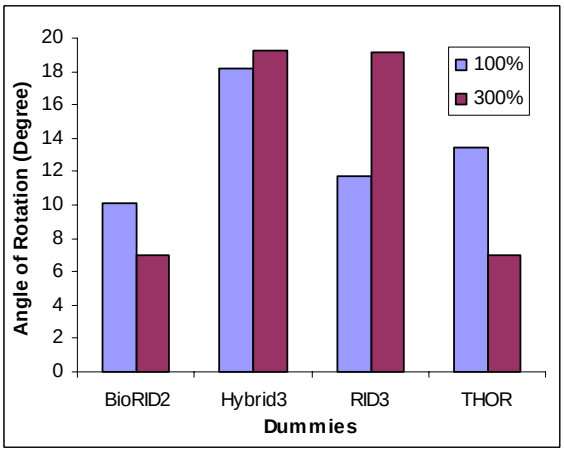

Figure 13. Effect of seatback recliner stiffness on measured head-to-torso rotation for worst-case (L7) head restraint position.

Data from all of the tests in this study are shown in the Appendix in Table A1. This includes a summary of results from a total of 32 tests, including all combinations of four dummies, two head restraint heights, two head restraint backsets, and two recliner stiffness levels.

DISCUSSION

Results from this series of testing clearly demonstrate the complexity of the occupant response to rear impact, and also the difficulty of designing an automotive seat when there is no consensus on injury criteria and thresholds, or even on which dummy is most appropriate. However, history has shown us that effective vehicle design does not require an absolutely biofidelic dummy, rather a dummy and test protocol that can distinguish between good and bad vehicle and component designs. Therefore, the analysis of these results will focus on the sensitivity of each dummy and associated injury criteria to the seat design parameters that have been shown to be important to providing protection against whiplash injuries to the occupants. The three seat design parameters that will be evaluated include head restraint height, head restraint backset, and seatback recliner stiffness. For the purpose of these analyses, a head restraint position that is higher and closer to the occupant's head is considered to be preferable to one that is lower with a larger backset.

In an attempt to quantify the sensitivity of the various dummies and injury criteria to the critical seat design parameters, a "sensitivity score" was used to rank the dummy responses. This score quantifies the percent difference in measured response for each dummy as one of the design parameters is modified. Sensitivity values are assigned for each test comparison using the criteria shown below in Table 1.

Table 1. Definition of Sensitivity Values

Percent Change	Sensitivity Value
< 15 percent	0
15 – 50 percent	1
> 50 percent	2

The Sensitivity Score for each injury criteria is obtained by adding up the individual sensitivity values for each seat design parameter, while the remaining parameters are held constant. This Sensitivity Score will therefore be based on the summation of four individual test comparisons, representing the different combinations of the remaining two design parameters. Since each individual sensitivity value can range from 0 to 2, the Sensitivity Score for each injury criteria can range from 0 to 8 for each dummy. An Overall Sensitivity Score is also calculated for each dummy as the sum of the four individual Sensitivity Scores for each injury criteria, namely head-to-torso rotation, lower neck extension moment, upper neck tension, and upper neck shear. The value of the Overall Sensitivity Score can therefore range from 0 to 32.

Effects of Head Restraint Height

To obtain the Sensitivity Score for a particular dummy and injury criteria to head restraint height, a total of four individual sensitivity values will be added. Responses will be compared for data from tests with High versus Low head restraint heights for each combination of head restraint backset and recliner stiffness. This process is repeated for each of the four injury criteria under consideration to obtain the Overall Sensitivity Score. Table 2 shows a summary of the sensitivity results with respect to head restraint height.

Table 2. Dummy Sensitivity Scores for head restraint height.

Criteria	L5-H5 (100)	L7-H7 (100)	L5-H5 (300)	L7-H7 (300)	SS
BioRID II Dummy					
Rotation	2	2	2	2	8
LN Ext.	1	0	0	0	1
Tension	1	1	1	1	4
Shear	2	2	2	2	8
Overall Height Sensitivity Score					21
Hybrid III Dummy					
Rotation	1	0	1	0	2
LN Ext.	1	1	1	1	4
Tension	1	1	1	1	4
Shear	0	1	1	0	2
Overall Height Sensitivity Score					12
RID-III Dummy					
Rotation	2	1	2	1	6
LN Ext.	0	0	0	0	0
Tension	1	0	2	2	5
Shear	0	0	0	0	0
Overall Height Sensitivity Score					11
THOR Dummy					
Rotation	2	2	2	2	8
LN Ext.	2	2	0	0	4
Tension	1	1	1	2	5
Shear	2	2	0	0	4
Overall Height Sensitivity Score					21

Based on the analysis of test results for the sensitivity of each dummy to head restraint height, it can be seen that the BioRID II and THOR dummies were found to be the most sensitive ATDs to distinguish this seat design parameter. It is important to once again note that the objective of these analyses is not to make a determination relative to the biofidelity of each dummy, but only to determine which dummies are suitable to distinguish between differences in critical seat design parameters. It is also important to note that the calculated sensitivities depend on the injury criteria selected, and that the values presented in Table 2 are specific for the four criteria under investigation. Figure 14 shows the sensitivity of each dummy to head restraint height.

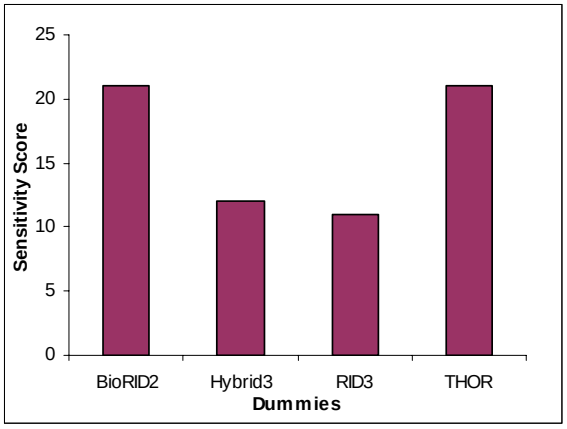

Figure 14. Overall sensitivity of various dummies to changes in head restraint height.

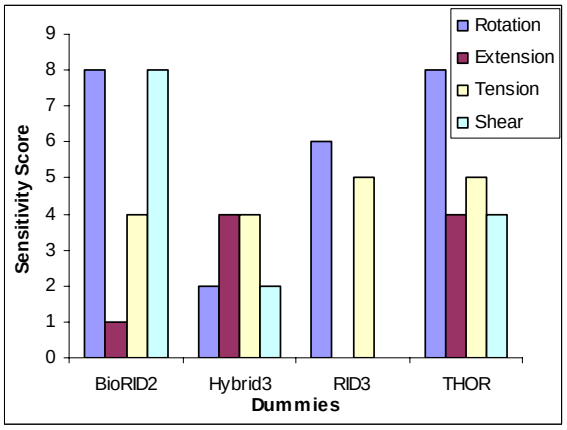

Figure 15. Breakdown of head restraint height sensitivity by injury criteria.

The results presented in Table 2 can also be analyzed to examine the sensitivity of each dummy to head restraint height based on the individual injury criteria. Figure 15 shows a breakdown of the height sensitivity scores for each injury criteria. It can be clearly seen from this breakdown of the data that the selection of a specific dummy does not guarantee sufficient sensitivity to the seat design parameters. The selection of a particular injury criterion is also an important determinant. For example, even though the BioRID II dummy was found to have one of the highest sensitivities to head restraint height, this dummy would not be a good choice if lower neck extension was selected as the distinguishing injury criteria. Likewise, although the RID-III dummy was

found to be the least sensitive dummy overall to head restraint height, it might prove to be a useful dummy if head-to-torso rotation or upper neck tension was selected as the injury criteria.

As shown in Table 2 and Figure 15, the BioRID II and THOR dummies had the highest sensitivities to relative head-to-torso rotations. This may be due largely to the fact that these dummies had higher initial seated heights than the other dummies. Since the 750 mm head restraint height is located roughly at the CG of the Hybrid III 50th percentile male dummy head, this height should be sufficient to effectively limit the rearward movement of the Hybrid III head and neck. Increasing the height to 800 mm with no change in backset would offer only slight improvements in limiting the rearward movement of the head and neck. In contrast, since the 750 mm head restraint height may be located below the head CG for the BioRID II and THOR dummies due to their higher initial seated heights, an increase in height to 800 mm would be expected to significantly increase the level to which the head restraint limits the rearward motion of the head and neck.

Effects of Head Restraint Backset

In a manner similar to the analysis of head restraint height, the sensitivity of each dummy to head restraint backset can be calculated by comparing data from tests with Far (75 mm) versus Close (50 mm) head restraint backsets for each combination of head restraint height and recliner stiffness. This process is repeated for each of the four injury criteria under consideration to obtain the Overall Sensitivity Score. Figure 16 and Table 3 show a summary of the sensitivity results for head restraint backset. A breakdown of sensitivities by injury criteria is shown in Figure 17.

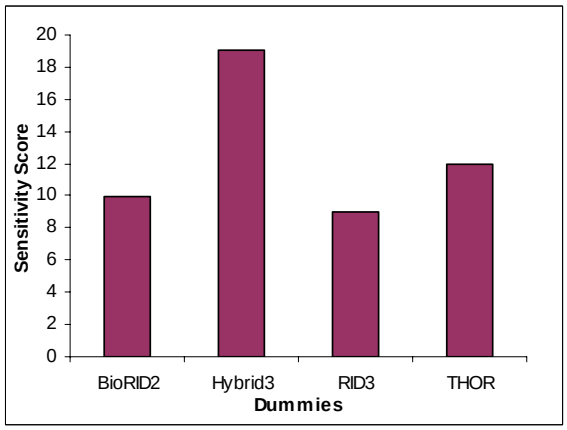

Figure 16. Overall sensitivity of various dummies to changes in head restraint backset.

Table 3. Dummy Sensitivity Scores for head restraint backset.

Criteria	L7-L5 (100)	H7-H5 (100)	L7-L5 (300)	H7-H5 (300)	SS
BioRID II Dummy					
Rotation	2	0	2	0	4
LN Ext.	0	1	1	1	3
Tension	0	0	0	0	0
Shear	1	1	1	0	3
Overall Backset Sensitivity Score					10
Hybrid III Dummy					
Rotation	1	1	1	2	5
LN Ext.	1	1	1	1	4
Tension	1	1	2	1	5
Shear	1	1	1	2	5
Overall Backset Sensitivity Score					19
RID-III Dummy					
Rotation	0	2	1	2	5
LN Ext.	1	0	0	0	1
Tension	0	1	0	2	3
Shear	0	0	0	0	0
Overall Backset Sensitivity Score					9
THOR Dummy					
Rotation	1	0	2	0	3
LN Ext.	2	2	0	0	4
Tension	1	1	1	0	3
Shear	2	0	0	0	2
Overall Backset Sensitivity Score					12

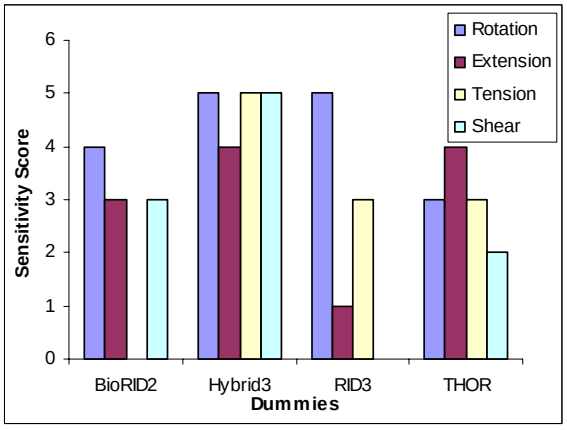

Figure 17. Breakdown of head restraint backset sensitivity by injury criteria.

Based on the analysis of test results for the sensitivity of each dummy to head restraint backset, it can be seen that the Hybrid III dummy is most sensitive to this seat design parameter. Furthermore, the sensitivity of the Hybrid III dummy for backset was

fairly consistent across the four different injury criteria. The RID-III dummy was equally sensitive to relative head-to-torso extension rotation but had low sensitivity to lower neck extension moment and upper neck shear force. The BioRID-II dummy was reasonably sensitive to backset, except for the case where upper neck tension force is selected as the criteria. The THOR dummy had the second highest sensitivity to backset with a relatively consistent response to all four injury criteria.

CONCLUSIONS

Results from this study clearly demonstrate the difficulty of selecting an optimal dummy and injury criteria by which to evaluate the performance of automotive seats in rear impact. Each of the tested dummies showed differences in sensitivities for the various seat design parameters and injury criteria under consideration. Since there is currently no consensus on injury criteria, nor on which design parameter is most critical, the selection of the most appropriate dummy should be based on which one provides the best overall sensitivity to all of these factors. Combining the results from Tables 2 and 3, we can determine the Combined Sensitivity Score for each dummy, which has a potential range from 0 to 64. These results are shown in Table 4.

Table 4. Combined Sensitivity Scores for the various dummies.

Dummy	Sensitivity		
	Height	Backset	Combined
BioRID II	21	10	31
Hybrid III	12	19	31
RID-III	11	9	20
THOR	21	12	33

Based on these combined findings, it appears that the BioRID II, Hybrid III, and THOR dummies are all suitable ATDs for the evaluation of seat design parameters. Again, it must be pointed out that these sensitivity scores are dependent on the injury criteria selected and may change if other criteria are chosen. Of these three potential dummies, the Hybrid III had the least number of test comparisons with a low level of sensitivity (<15% difference). In fact, the Hybrid III dummy showed at least a moderate level of sensitivity (15+ percent) for 28 out of the total 32 individual test comparisons, although only three of these 28 cases showed a high level of sensitivity (>50%). This finding implies that the Hybrid III dummy may be suitable for the evaluation of rear impact protection for a broader set of test conditions than the other dummies despite the fact that it may not have the same level of sensitivity to certain variables as the BioRID II or THOR dummies.

The THOR dummy showed reasonably consistent Overall Sensitivity Scores for each of the various injury criteria considered, although this dummy showed low sensitivity (<15%) values in 12 of the 32 individual test comparisons. Another 13 of the 21 comparisons showed a high level of sensitivity, with the remaining 7 showing moderate sensitivity.

The BioRID II dummy showed reasonably good sensitivity to the various injury criteria, except for the cases of lower neck extension moment during the evaluation of head restraint height and upper neck tension during the evaluation of head restraint backset. The finding that this dummy showed a sensitivity value of zero for tension during backset evaluation may be a consequence of the more flexible spine design of this dummy. Additional testing is needed to further explore this finding.

If we consider the suitability of the various dummies and injury criteria for ranking the different seat design parameters, assuming again that increased height and decreased backset provide increased rear impact protection, then we find that the combination of the Hybrid III dummy with head-to-torso rotation correctly ranks the various seat designs for all combinations of height, backset, and recliner stiffness. In fact, our data suggests that the Hybrid III dummy can properly rank seat designs using all four of the injury criteria under consideration in this study. This is based on a comparison of the specific values in Table A1 of the Appendix without consideration of the relative sensitivities of the measured responses. In contrast, the BioRID II and THOR dummies are able to properly rank the seat designs only using the upper neck tension criteria, which may again be related to the fact that these dummies have a higher initial seating height. The RID III dummy was not able to properly rank the seat designs using any of the injury criteria considered in this study.

REFERENCES

[1] NHTSA Final Rule. 2006. "Federal Motor Vehicle Safety Standards: Head Restraints." Docket No. NHTSA-2004-19807, RIN 2127-AH09.

[2] Ono K, Kaneoka K, Wittek A, and Kajzer J. 1997. Cervical injury mechanism based on the analysis of human cervical vertebral motion and head-neck-torso kinematics during low speed rear impacts. Proc. 41st Stapp Car Crash Conference.

[3] Kaneoka K, Ono K, Inami S, and Hayashi K. 1999. Motion analysis of cervical vertebrae during simulated whiplash loading. Proceedings of the World Congress on Whiplash Associated Disorders, pp. 152-160, Vancouver, BC, Canada.

[4] Voo L, Merkle A, and Kleinberger M. 2003. "Effective head restraint height in whiplash injury prevention." ASME International Mechanical Engineering Congress and R&D Expo, Paper No. IMECE2003-43155, November.

[5] Kleinberger M, Voo L, Merkle A, Bevan M, Chang SS, and McKoy F. 2003. "The role of seatback and head restraint design parameters on rear impact occupant dynamics." 18th International Technical Conference on the Enhanced Safety of Vehicles, Nagoya, Japan, May.

[6] Bostrom O, Svensson MY, Aldman B, Hansson HA, Haland Y, Lovsund P, Seeman T, Suneson A, Saljo A, and Ortengren T. 1996. A new neck injury criterion candidate based on injury findings in the cervical spinal ganglia after experimental neck extension trauma. Proc. of the IRCOBI Conference.

[7] Kleinberger M, Sun E, Eppinger R, Kuppa S, and Saul R. 1998. Development of improved injury criteria for the assessment of advanced automotive restraint systems. NHTSA Docket No. 98-4405, Notice 1, September.

[8] Schmitt KU, Muser MH, and Niederer P. A new neck injury criterion candidate for rear-end collisions taking into account shear forces and bending moments. Proc. 17th Int. Technical Conference on the Enhanced Safety of Vehicles, 2001.

[9] Prasad P, Kim A, Weerappuli DPV, Roberts V, and Schneider D. 1997. Relationships between passenger car seat back strength and occupant injury severity in rear end collisions: Field and laboratory studies. Proceedings of the 41st Stapp Car Crash Conference, SAE Paper No. 973343.

[10] Viano DC, Olsen S, Locke GS, and Humer M. 2002. Neck biomechanical responses with active head restraints: Rear barrier tests with BioRID and sled tests with Hybrid III. Society of Automotive Engineers, SAE World Congress Paper No. 2002-01-0030.

[11] Kuppa S, Saunders J, and Stammen J. 2003. Kinematically based whiplash injury criterion. Proceedings of the 18th International Technical Conference on the Enhanced Safety of Vehicles, Nagoya, Japan.

[12] Molino L. 1998. Determination of moment-deflection characteristics of automobile seat backs. NHTSA Docket No. 1998-4064-26, November 25.

APPENDIX

Table A1. Summary of results for all tests in this study.

Recliner Stiffness	Dummy	Head-To-Torso Rotation (Degrees)				Lower Neck Ext. Moment (Nm)†				Upper Neck Tension Force (N)				Upper Neck Post. Shear Force (N)			
		L7	L5	H7	H5	L7	L5	H7	H5	L7	L5	H7	H5	L7	L5	H7	H5
100%	BioRID2	10.1	2.9	*	*	13.0	13.7	11.6	8.6	2766.3	2379.6	1830.7	1700.3	1571.0	1020.7	89.5	69.8
	Hybrid3	18.2	14.4	17.1	11.1	192.9	155.0	122.5	96.2	2423.5	1990.6	1306.0	1097.0	102.0	64.9	75.1	57.2
	RID3	11.7	15.8	7.5	2.5	1.3	1.0	1.8	3.2	2093.0	2055.2	2097.8	1317.5	169.5	146.4	213.9	286.8
	THOR	13.4	8.5	*	*	15.9	2.3	2.9	*	2339.1	1628.5	1836.4	1217.6	129.5	41.2	*	*
300%	BioRID2	7.0	3.0	*	*	11.4	8.7	12.0	8.3	2227.3	2145.8	1411.9	1275.1	1463.2	1144.2	20.6	22.7
	Hybrid3	19.3	12.2	17.4	8.5	131.2	69.6	81.5	46.5	1589.8	774.7	809.9	466.9	127.9	69.7	115.5	48.2
	RID3	19.1	15.6	15.9	5.6	6.5	6.8	5.7	6.4	1625.1	944.1	750.1	304.3	275.4	284.0	264.7	325.4
	THOR	7.0	2.9	*	*	*	*	*	*	1247.1	675.9	502.4	480.1	*	*	*	*

† = Lower neck extension moment values are as recorded by the load cell and have not been corrected to the T1 location.

* = These measured values were either zero or negative, indicating that the measured response was in the opposite direction. (Flexion rotation, flexion moment, or anterior shear)

Notes:

1. Recliner Stiffness:
   100% = baseline stiffness of 35 Nm/deg
   300% = Nominal 3 times increase from baseline stiffness at 105 Nm/deg
2. Head Restraint Positions:
   L7 = 750 mm height with 75 mm backset
   L5 = 750 mm height with 50 mm backset
   H7 = 800 mm height with 75 mm backset
   H5 = 800 mm height with 50 mm backset

A MULTI-BODY MODEL OF THE WHOLE HUMAN SPINE FOR WHIPLASH INVESTIGATIONS

Volkan Esat
Memis Acar
Loughborough University
United Kingdom
Paper Number 07-0437

ABSTRACT

This paper presents whiplash simulations and analyses under various impact conditions and acceleration levels by employing a rigorously validated biofidelic multi-body (MB) model of the whole human spine. The novel MB model possesses highly advanced material properties such as viscoelastic behaviour, active-passive muscles, and geometric nonlinearities. Validation is carried out comparing the motion segment responses, the MB model responses for frontal and lateral impacts, the vertical loading results, and the responses of thoracolumbar region in rear-end impact. The model successfully reproduces the characteristic motion of the head and neck when subjected to rear-end crash scenarios. Whiplash simulations involve not only the responses of the ligamentous spine model, but also predictions of the model with active/passive musculature. The MB model simulation results and model predictions such as head translations and rotations, muscle and ligament forces, and intervertebral angles show good agreement with experiments. The study is limited to presenting the kinematics and kinetics of the cervical spine. The biofidelic whole human spine model proves to be a highly capable and versatile platform to simulate various traumatic whiplash injury situations.

INTRODUCTION

Multi-body/discrete parameter models possess the potential to simulate the kinematics and kinetics of the human spine, both entirely and partially. Multi-body models have advantages such as less complexity, less demand on computational power, and relatively simpler validation requirements when compared to FE models. Williams and Belytschko [1] constructed a three-dimensional human cervical spine model for impact simulation, which included a special facet element which allows the model to simulate both lateral and frontal plane motions. In a similar but an advanced manner, van Lopik and Acar [2] generated and validated a three dimensional multi-body model of the human head and neck using the dynamic simulation package MSC.visualNastran 4D. The model of the head-neck complex involves rigid bodies representing the head and 7 vertebrae of the neck interconnected by linear viscoelastic disc elements, nonlinear viscoelastic ligaments, frictionless facet joints and contractile muscle elements describing both passive and active muscle behaviour. Using a different approach, the emphasis is more on the lumbar spine in Jaeger and Luttmann's work [3]. Monheit and Badler [4] constructed a kinematic model of the human spine and torso based on the anatomy of the physical vertebrae and discs, range of movement of each vertebra, and effect of the surrounding ligaments and muscles. Broman et al. [5] generated a model of the lumbar spine, pelvis and buttocks to observe transmission of vibrations from the seat to L3 in the sitting posture. De Zee et al. [6] built a multi-body human spine model partially, in which only the lumbar spine part was completed, consisting of seven rigid segments as pelvis, the five lumbar vertebrae and a thoracic part, where the joints between each vertebra set of two was modelled as a three degrees-of-freedom spherical joint. Ishikawa et al. [7] developed a musculoskeletal dynamic multi-body spine model in order to perform Functional Electrical Stimulation (FES) effectively as well as to simulate spinal motion and analyse stress distributions within the vertebrae. The muscles were incorporated to the skeletal model by using 3D analysis software MSC.visualNastran 4D.

This paper reports a rigorously validated biofidelic multi-body (MB) model of the whole human spine including whiplash simulations and analyses under various impact conditions and acceleration levels. The main advantage associated with the model lies in incorporating the whole spinal components such as vertebrae, ribs, muscles, intervertebral discs, and ligaments, which helps to simulate and validate more realistically. The MB model devoid of muscles is validated against Panjabi and colleagues' experiments conducted using a bench-top trauma sled and isolated cervical spine specimens [8, 9]. These studies used cadaveric cervical spine specimens devoid of all non-ligamentous soft tissues fixed to a bench top sled device where an acceleration pulse is applied to the base of the specimen to reproduce whiplash trauma. These tests constitute an alternative to experiments using volunteers or whole body

cadavers. They have been successfully used for developing computational models that simulate whiplash trauma and provide valuable insights into the complex events and interactions that cause injuries to the cervical spine [10].

METHOD

The MB model utilised in the simulations is recently developed by the authors [11, 12]. The model embodies highly advanced material properties such as viscoelastic behaviour, active-passive muscles, and geometric nonlinearities.

Multi-Body Model Characteristics

The multi-body model developed is constructed by employing a similar methodology to the cervical spine multi-body model of van Lopik and Acar [10]. The vertebrae were modelled as rigid bodies, interconnected by linear viscoelastic intervertebral disc elements, nonlinear viscoelastic ligaments and contractile muscle elements possessing both passive and active behaviour. The dynamic simulation package *MSC.visualNastran 4D 2001* is utilised as the computational medium.

The multi-body model of the whole human spine incorporates four essential elements: the vertebrae, the muscles, the ligaments and the intervertebral discs. The solid model of the upright erect human spine constituted the basis for the developed multi-body model, in which the geometrical surfaces that defined realistic anatomical dimensions of the spinal parts are entirely constructed from CT scans by Van Sint Jan [13] at the University of Brussels, Belgium, and stored into the software, Data Manager of Multimod project. These solid bodies not only include the essential parts of the vertebrae, but also accommodate other selected skeletal parts such as the head, the ribs, the clavicles, the scapulae, and the iliacs. The CT-scanned segments of the human skeletal parts are combined to form the whole solid model as shown in Figure 1.

Muscles are incorporated into the model as contractile muscle elements possessing both passive and active behaviour. The most essential muscle groups, such as fascicles of the erector spinae and multifidus, are integrated. Necessary geometric and morphologic features such as the origins, insertions and dimensions are taken from various studies in the literature [14-16]. In MSC.visualNastran 4D, linear actuator element is used to incorporate the muscles, governed by an external software, Virtual Muscle v.3.1.5 of Alfred E. Mann Institute at the University of Southern California [16] that runs within Matlab/Simulink and communicates with MSC.visualNastran 4D at each incremental step.

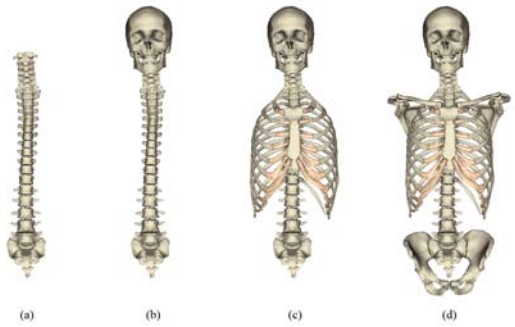

Figure 1. The solid model of the human spine as the basis of the multi-body model: (a) the entire spinal column, (b) with the head, (c) with the head and the ribs, and (d) with the head, the ribs, the clavicles, the scapulae, and the iliacs.

The ligaments in the present model are chosen as nonlinear viscoelastic ligaments. All six common types of ligaments are introduced to the model, which are ALL (anterior longitudinal ligament), PLL (posterior longitudinal ligament), LF (ligament flavum), JC (joint capsules), ISL (interspinous ligament) and SSL (supraspinous ligament) as depicted in Figure 2. The necessary biomechanical properties of human spine ligaments are taken from the literature [17, 18].

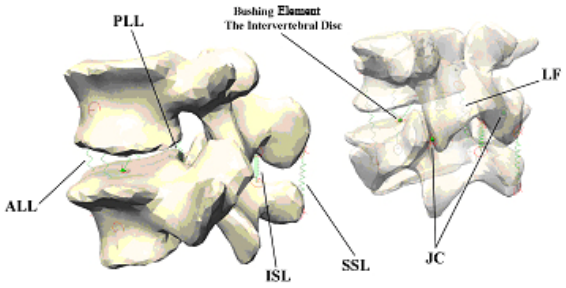

Figure 2. Ligaments and the intervertebral disc in the multi-body model.

Intervertebral discs are modelled as bushing elements in MSC.visualNastran 4D as illustrated in Figure 2. All translational and rotational degrees of freedom are allowed in a bushing element, but they are restricted through spring-damper relationships. The intervertebral discs are located at the centre of the space between the upper and lower end plates of adjacent vertebrae at a fixed distance relative to the centre of the upper vertebrae. There are no discs between the axis, atlas and occiput. Material properties of the disc for the model are collected from the studies in the literature [18-21].

All the constituting elements of the whole human spine are integrated to form the MB model as shown in Figure 3.

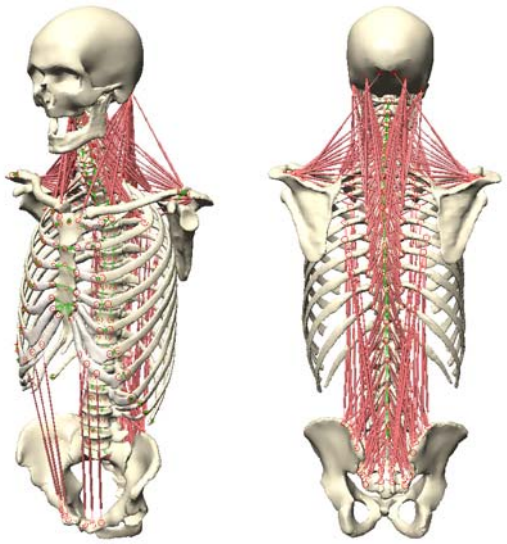

Figure 3. Oblique and rear views of the multi-body model of the whole human spine.

Multi-Body Model Validation

The validation of the multi-body model is conducted rigorously by comparing motion segment responses in the cervical spine, MB model responses in the cervical spine for frontal and lateral impacts, vertical loading for cervical spine, and MB model responses of thoracic and lumbar regions in rear-end impact. In 15g frontal and 7g lateral impact cases, the model is validated against well-known NBDL data [22]. In Figures 4 and 5, typical results from frontal and lateral impact cases are shown, respectively. C3C4 displacements and rotations under certain loading are provided in Figure 6 as an example for validation by using motion segment responses.

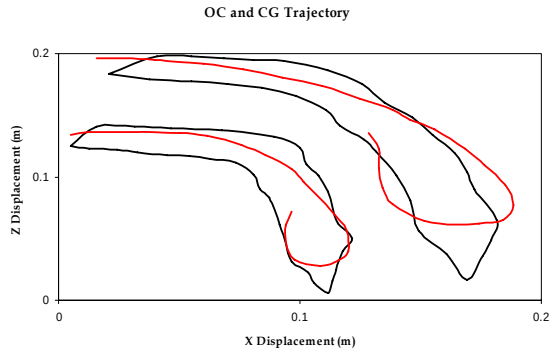

Figure 4. Head occiput and head centre of gravity trajectories in the horizontal (X) and vertical (Z) planes (OC lower, CG upper graph).

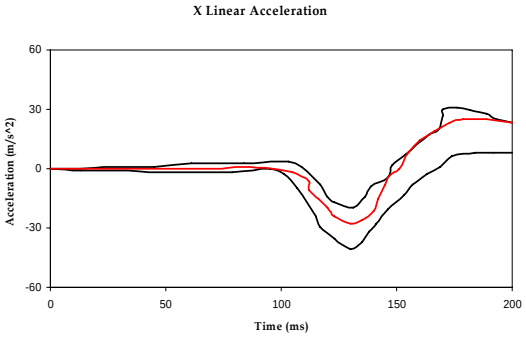

Figure 5. x linear acceleration of head centre of gravity vs. time in lateral impact.

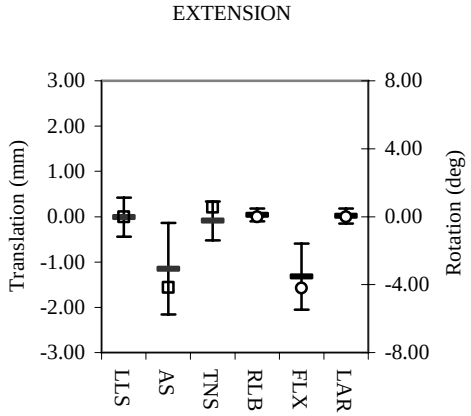

Figure 6. Displacements of model motion segment C3C4 in response to applied rotational load of 1.8 Nm for extension shown against the experimental results [23]. Resulting displacements are shown along the vertical axis, translations (□) on the left, rotations (○) on the right. Anterior shear (+AS), posterior shear (-AS), left lateral shear (+LLS), right lateral shear (-LLS), tension (+TNS), compression (-TNS), right lateral bending (+RLB), left lateral bending (-RLB), flexion (+FLX), extension (-FLX), left axial rotation (+LAR) and right axial rotation (-LAR).

ANALYSIS & RESULTS

The MB model is used to simulate the experimental conditions of Panjabi and co-workers [8, 9], who utilised a bench-top sled to simulate whiplash trauma on ligamentous human cadaveric cervical spine specimens which were without the muscle tissue and mounted to the sled at T1. The whiplash trauma input in the horizontal direction was introduced as the profile of the sled acceleration-time curve to the base of the specimen represented. The acceleration input was a triangular pulse with duration of 105ms and peak accelerations of 2.5g, 4.5g. 6.5g and 8.5g (1g = 9.8m/s^2).

In the MB simulation, all muscles are deactivated. The motion of T1 is constrained so only translation

along the x-axis was allowed. No gravitational effect is taken into consideration at this stage. The acceleration profiles are triangular with the same 105ms duration and corresponding peak accelerations as depicted in Figure 7.

The resulting head rotations and translations are compared against the results for the 8.5g trauma class.

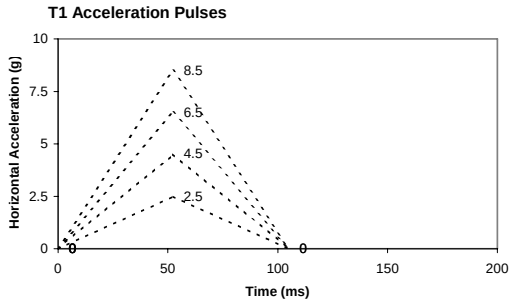

Figure 7. T1 acceleration profiles used as input to the cervical spine model.

The response of the ligamentous spine model to the 8.5g trauma acceleration is provided schematically in Figure 8. In the resulting head-neck motion a characteristic S-shaped curvature of the neck with lower level hyperextension and upper level flexion and subsequent C-shaped curvature with extension at all levels of the entire cervical spine are observed.

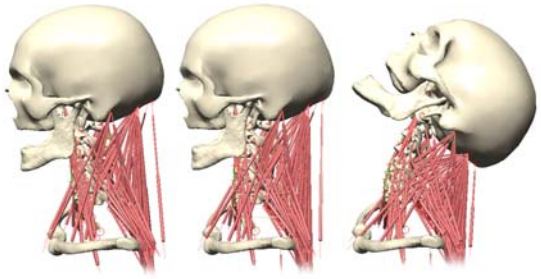

Figure 8. Response of the model to 8.5g whiplash acceleration for 0, 60, 120 ms (respectively, from left to right). Muscles were deactivated completely.

The head rotation, and head vertical and horizontal translations for the 8.5g case compared with the experimental results [24] is provided in Figure 9. The model shows a similar response to the cadaveric spine specimen, where head rotation follows a similar pattern but with a higher peak value. The MB model returns back slightly slower than is seen with the spine specimen soon after the maximum rotation and maximum posterior translation of the head. The vertical displacement of the head reaches a peak of around 6 cm below the initial height and shows good agreement with the experimental results.

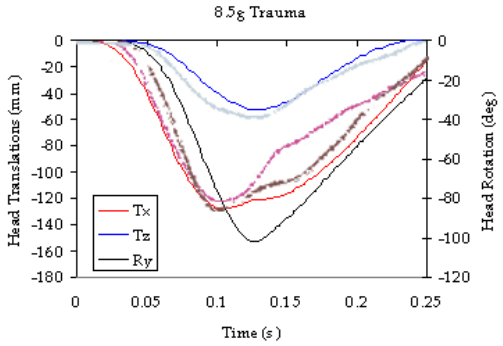

Figure 9. Model head translations and rotations for 8.5 g case compared to experimental values (which are shaded with similar colour).

During the acceleration part of the impulse, the head translates posteriorly and inferiorly with respect to T1 as the spine extends. Around 60 ms time period, the development of the characteristic S-shaped curvature of the cervical spine is observed. The vertebral rotation graphs in Figure 10 depicts that during this time period the upper levels of the spine (C0-C3) are flexed while the lower levels (C5-T1) are extended as observed from the experimental results. In the 75-100 ms time period, the upper vertebrae of the model change from flexion to extension as the whole model becomes more and more extended into a C-shaped curvature as also observed in the experiments. Maximum extension of the head and neck is reached at approximately 130 ms, slightly later than the experimental results. In the later stages of trauma the head rebounds almost completely to its initial starting configuration.

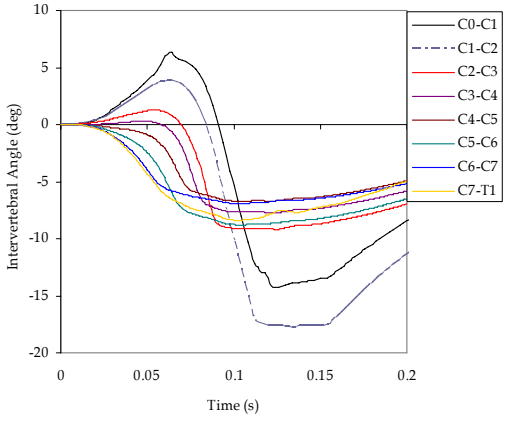

Figure 10. Intervertebral rotations at 8.5g impact.

Model predictions for head translations and rotations are provided in Figures 11-13, From which it can be observed that the more severe the

impact, the greater the rotations and translations are.

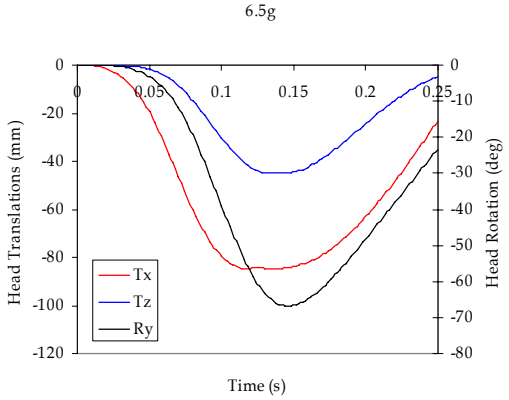

Figure 11. Model head translations and rotations for 6.5 g case.

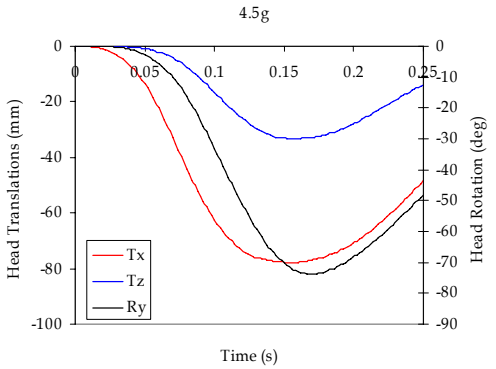

Figure 12. Model head translations and rotations for 4.5 g case.

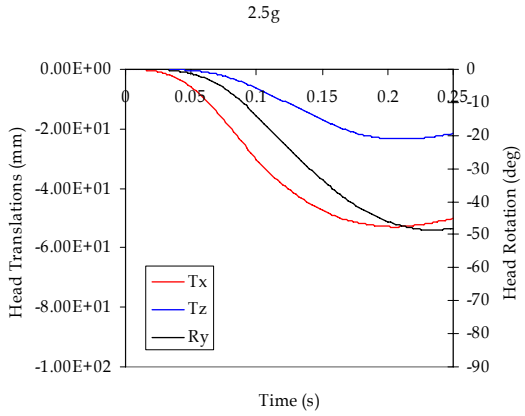

Figure 13. Model head translations and rotations for 2.5 g case.

The maximum intervertebral rotations of the model for the four cases simulated are presented in Figures 14-18. For the C2-C3 level of the cervical spine, the graph (Fig. 14) show that although the upper levels are initially forced into flexion in the model, the levels of flexion experienced are slightly smaller than the experimental values, which may be an indication of the model being slightly stiff in flexion in these areas. The levels of extension experienced in the later stages of impact show better agreement with the experimental data. Figures 15-18 show the maximum intervertebral extension rotations experienced by the lower five levels of the spine model. From the results, it seems that generally level C6-C7 appears to be too stiff when compared to the experimental results.

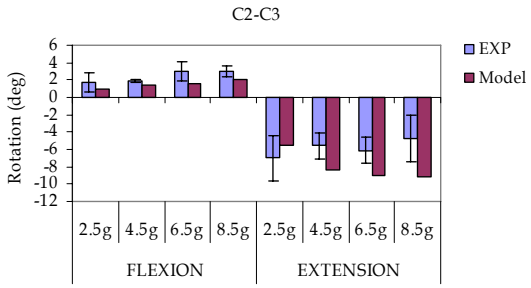

Figure 14. Maximum intervertebral angles achieved for C2-C3.

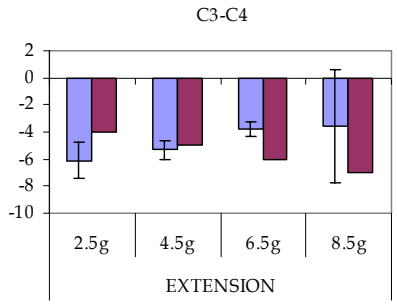

Figure 15. Maximum intervertebral angles achieved for C3-C4.

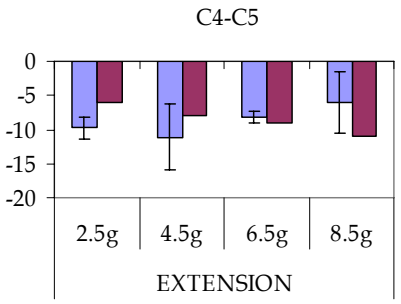

Figure 16. Maximum intervertebral angles achieved for C4-C5.

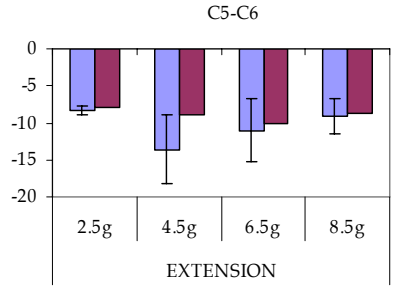

Figure 17. Maximum intervertebral angles achieved for C5-C6.

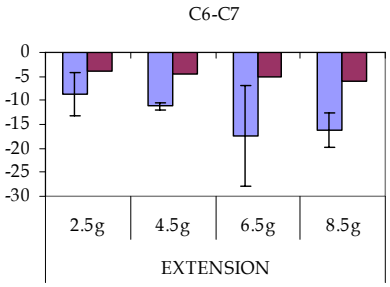

Figure 18. Maximum intervertebral angles achieved for C6-C7.

In order to investigate the effects of musculature, the muscles are incorporated into the model in two ways; as passive musculature and as active musculature. The comparison of model predictions for maximum intervertebral disc forces in tension and compression cases for 8.5g acceleration are tabulated in Table 1.

Table 1. Comparison of maximum disc forces in tension and compression for 8.5g acceleration case.

Force (N)	C2-C3	C3-C4	C4-C5	C5-C6	C6-C7
Maximum tension					
No muscles	95	62	25	2	0
Passive	223	132	64	31	0
Active	103	47	13	3	0
Maximum compression					
No muscles	224	273	281	279	265
Passive	257	303	294	310	289
Active	394	417	432	423	402

In maximum tension predictions for 8.5g case, the inclusion of passive musculature significantly increases the values at each level. Within each case, the forces decrease from C2-C3 to C6-C7. Inclusion of active musculature normalises the values towards no-muscle case, which appears to be more realistic in the light of the experimental data. In maximum compression predictions, active muscles seem to have a considerable effect on the maximum values with relatively higher magnitudes, whereas both no muscle and passive muscle cases exhibit similar values.

CONCLUSIONS

This study shows that the MB model of the whole human spine can be used to simulate a ligamentous cervical spine undergoing whiplash trauma. The MB model devoid of muscles is validated against test results, while most of the simulation results and model predictions showed good agreement with experiments. The model can successfully reproduce the characteristic motion of the head and neck when subjected to rear-end impact. The differential movement between the head and T1 causes initial flexion in the upper joints as the head translates backward, without rotation, relative to T1.

In the most severe impact case of 8.5g, the head rotations and displacements show reasonably good agreement with experimental data, particularly in following the trends of the empirical graphs. However, the model predictions yield slightly larger values than the experimental results.

The inclusion of the muscles into the model does not significantly alter the head and cervical spine rotations. However, the forces occurring at intervertebral levels are considerably affected due to muscle tensioning. It could be concluded from the model predictions with active musculature that an initially unaware occupant would not be affected in terms of cervical spine kinematics, but would be influenced via the varying loads within the soft tissues such as intervertebral discs.

REFERENCES

[1] Williams, J. L., and Belytschko, T. B. 1983. “A Three-Dimensional Model of the Human Cervical Spine for Impact Simulation” Journal of Biomechanical Engineering, Transactions of the ASME, 105, No. 4, 321-331.

[2] Van Lopik, D. W., and Acar, M. 2002. “The Development of a Multibody Head-Neck System for Impact Dynamics Using visualNastran 4D.” Proceedings of ESDA2002.

[3] Jaeger, M., and Luttmann, A. 1989. “Biomechanical Analysis and Assessment of Lumbar Stress During Load Lifting Using a Dynamic 19-Segment Human Model.” Ergonomics, 32, No. 1, 93-112.

[4] Monheit, G., and Badler, N. I. 1991. “A Kinematic Model of the Human Spine and Torso.” IEEE Computer Graphics and Applications, 11, No. 2, 29-38.

[5] Broman, H., Pope, M., and Hansson, T. 1996. “A Mathematical Model of the Impact Response of the Seated Subject.” Medical Engineering & Physics, 18, No. 5, 410-419.

[6] De Zee, M., Hansen, L., Andersen, T. B., Wong, C., Rasmussen, J., and Simonsen, E. 2003. “On the Development of a Detailed Rigid-Body Spine Model.” Proceedings of International Congress on Computational Bioengineering, Spain, 5pp.

[7] Ishikawa, Y., Shimada, Y., Iwami, T., Kamada, K., Matsunaga, T., Misawa, A., Aizawa, T., and Itoi, E. 2005. “Model Simulation for Restoration of

Trunk in Complete Paraplegia by Functional Electrical Simulation." Proceedings of IFESS05 Conference, Montreal, Canada.

[8] Panjabi, M. M., Crisco, J. J., Lydon, C., and Dvorak, J. 1998. "The Mechanical Properties of Human Alar and Transverse Ligaments at Slow and Fast Extension Rates." Clinical Biomechanics, 13, No. 2, 112-120.

[9] Panjabi, M. M., Dvorak, J., Duranceau, J., Yamamoto, I., Geber, M., Rausching, W., and Bueff, H. U. 1988. "Three-dimensional movements of the upper cervical spine." Spine, 13, 726-730.

[10] Van Lopik, D. W., and Acar, M. 2004. "A Computational Model of the Human Head and Neck System for the Analysis of Whiplash Motion." International Journal of Crashworthiness, 9, No. 5, 465-473.

[11] Esat, V., and Acar, M. 2005. "A Multi-Body Human Spine Model for Dynamic Analysis in Conjunction with the FE Analysis of Spinal Parts." Proceedings of 1st Annual Injury Biomechanics Symposium, The Ohio State University, Columbus, USA, 12 pp.

[12] Esat, V., and Acar, M., 2006. "A Multi-Body Model of the Whole Human Spine for Dynamic Analysis of Impact Situations." Proceedings of CMBBE06 International Symposium on Computer Methods in Biomechanics and Biomedical Engineering, Cote d'Azur, France, 6pp.

[13] Van Sint Jan, S. 2005. "Introducing Anatomical and Physiological Accuracy in Computerized Anthropometry for Increasing the Clinical Usefulness of Modeling Systems." Critical Reviews in Physical and Rehabilitation Medicine, 17, No. 4, 249-274.

[14] Bogduk, N., Macintosh, J. E., and Pearcy, M. J. A. 1992. "Universal Model of the Lumbar Back Muscles in the Upright Position." Spine, 17, No.8, 897-913.

[15] Winters, J. M., and Woo, S. L-Y. 1990. "Multiple Muscle Systems: Biomechanics and Movement Organization." Springer-Verlag.

[16] Cheng, E., Brown, I., and Loeb, J. 2001. "Virtual Muscle 3.1.5: Muscle Model For Matlab", Users Manual.

[17] Pintar, F. A., Yoganandan, N., Myers, T., Elhagediab, A., and Sances, A. Jr. 1992. "Biomechanical Properties of Human Lumbar Spine Ligaments." Journal of Biomechanics, 25, No.11, 1351-1356.

[18] Teo, E. C., and Ng, H. W. 2001. "Evaluation of the Role of Ligaments, Facets, and Disc Nucleus in Lower Cervical Spine Under Compression and Sagittal Moments Using Finite Element Method." Medical Engineering and Physics, 23, 155-164.

[19] Lavaste, F., Skalli, W., Robin, S., Roy-Camille, R., and Mazel, C. 1992. "Three-Dimensional Geometrical and Mechanical Modelling of the Lumbar Spine." Journal of Biomechanics, 25, No. 10, 1153-1164.

[20] Yang, K. H., Zhu, F., Luan, F., Zhao, L., and Begeman, P. C. 1998. "Development of a Finite Element Model of the Human Neck." Proceedings of the 42nd Stapp Car Crash Conference, Society of Automotive Engineers, SAE Paper No. 983157, 195-205.

[21] Wang, J.-L., Parnianpour, M., Shirazi-Adl, A. and Engin, A. E. 2000. "Viscoelastic Finite-Element Analysis of a Lumbar Motion Segment in Combined Compression and Sagittal Flexion: Effect of Loading Rate." Spine, 25, No.3, 310-318.

[22] Wismans, J., Van Oorshot, E., and Woltring, H. J. 1986. "Omni-directional human head-neck response." 30th Stapp Car Crash Proceedings, Society of Automotive Engineers, SAE Paper No. 861893, 313-331.

[23] Moroney, S. P., Schultz, A. B., Miller, J. A. A., and Andersson, G. B. J. 1988. "Load-Displacement Properties of Lower Cervical Spine Motion Segments." Journal of Biomechanics, 21, No. 9, 769-779.

[24] Grauer, J. N., Panjabi, M. M., Cholewicki, J., Nibu, K., and Dvorak, J. 1997. "Whiplash produces an S-shaped curvature of the neck with hyperextension at lower levels." Spine, 22, No. 21, 2489-2494.

THE EFFECT OF WHIPLASH PROTECTION SYSTEMS IN REAL-LIFE CRASHES AND THEIR CORRELATION TO CONSUMER CRASH TEST PROGRAMMES

Anders Kullgren
Maria Krafft
Folksam Research and Karolinska Institutet, Sweden
Anders Lie
Swedish Road Administration and Karolinska Institutet, Sweden
Claes Tingvall
Swedish Road Administration, Sweden and Monash University, Australia
Paper number: 07-0468

ABSTRACT

The objective was to study the influence of various types of car seats aimed at protecting whiplash injuries on real-life injury outcome. Furthermore, the aim was to study correlation between whiplash consumer crash tests and real-life injury outcome. In both cases the influence on long-term whiplash symptoms were studied.

Since 1997 various seats aimed at lowering the risk of whiplash injuries have been introduced in cars. The cars were divided into groups according to the safety technology used. Since 2003 consumer crash test programmes have been running. The correlation on group level between whiplash injury outcome in real-life crashes and the test results of consumer crash tests both in Sweden by Folksam and the Swedish Road Administration and by IIWPG were studied.

The results show that cars fitted with more advanced whiplash protection systems had 50% lower risk of whiplash injuries leading to long-term symptoms than cars launched since 1997 without whiplash systems. All three whiplash preventive technologies studied, RHR (Reactive Head Restraints), WhiPS (Whiplash Prevention System), and WIL (Whiplash Lessening System), showed lower risk of whiplash injury leading to long-term symptoms than cars fitted with standard seats.

A correlation was found between consumer whiplash crash tests and real-life outcome. It was found that cars rated in the worst group in the IIWPG and Folksam/SRA ratings had 43% and 60% higher risk of long-term symptoms in real-life crashes, respectively, than cars rated in the best group.

A limitation with the tests is that the consumer crash test programmes are conducted with the seat only, while the real-life injury outcome concerns the performance of the whole car.

It can be concluded that seats aimed at preventing whiplash injuries in general also lower the risk in real-life crashes. Furthermore it can be concluded that results from existing consumer crash test programmes for whiplash correlate with real-life injury outcome.

INTRODUCTION

In October 1997 the Swedish parliament decided upon the new road traffic safety policy in Sweden, the so-called Vision-Zero (Kommunikations-departementet 1997). An important part in the policy is to minimise health losses and not accidents or injuries in general. Health losses include fatal injuries and severe injuries where the person not is recovering within reasonable time, i.e. the focus is set on the public health problem.

Apart from fatalities, injuries leading to disability reported by insurance companies are a good indication of the number of serious road traffic injuries. They also give a good picture of both the typical injuries and the type of crashes that primarily should be in focus for road traffic safety actions. In Sweden more than 3,500 permanently disabled car occupants are reported every year (with a disability of at least 10% according to the classification used by Swedish insurance companies) (Försäkringsförbundet 1996). More than 50% of those are whiplash injuries. It is therefore important that the society focuses on reducing whiplash injuries.

In modern cars on the Swedish market, whiplash injuries account for approximately 70% of all injuries leading to disability (Folksam 2005). Most occupants reporting whiplash injuries recovers within a week, while between 5% and 10% will get more or less life lasting problems (Nygren 1984, Krafft 1998, Whiplashkommissionen 2003).

Whiplash prevention initiatives

Whiplash preventive measures have so far been focussed on developments of the seat. Since the 70s head restraints have been implemented more and more frequently. To date all seating positions in most car models are fitted with head restraints. The whiplash injury reducing effects of head restraints have been shown to be relatively low, between 5% and 15% (Nygren et al 1985, Morris and Thomas 1996). In order to increase the vehicle crashworthiness in high-speed rear end crashes, vehicle seats have become stiffer since the late 80s (Krafft 1998). Stiffer seats have probably increased

the whiplash injury risks in low-speed rear-end crashes.

Based on this knowledge more advanced whiplash protection devices have been introduced on the market. The better protection is achieved through improved geometry and dynamic properties of the head restraint or by active devices that move in a crash as the body loads the seat. The main ways to lower the whiplash injury risk are to minimise the relative motion between head and torso, to control energy transfer between the seat and the body and to absorb energy in the seat back.

To date several systems exist, for example RHR or AHR (Reactive Head Restraint or Active Head Restraint) in several car models, WhiPS (Whiplash Prevention System) in Volvo and Jaguar, WIL (Whiplash Injury Lessening) in Toyota. RHR was firstly introduced in Saab cars in 1998 (SAHR) (Wiklund and Larsson 1997), and is today the most common whiplash protection concept on the market. It exists in several models from for example Audi, Ford, Mercedes, Nissan, Opel, Skoda, Seat and VW. RHR is a mechanical system that actively moves the head restraint up and closer to the head and in a crash. Saab has apart from the head restraint also designed the seat back structure to better support the torso in a rear end crash. WhiPS was first introduced in Volvo cars in 1999 (Lundell et al 1998, Jakobsson 1998). The seat back is in a crash moved rearwards and yields in a controlled way to absorb energy. The Toyota system WIL (Sekizuka 1998) has no active parts and is only working with improved geometry and softer seat back. Ford has also introduced seats without active or reactive parts in the headrest, but with an improved design aimed at preventing whiplash injury.

Studies have been presented showing the effect of the Saab RHR and Volvo WhiPS indicating an injury reducing effect of approximately 40-50% (Viano and Olssén 2001, Insurance Institute for Highway Safety (IIHS) 2002, Jakobsson 2004, Krafft et al 2003). Apart from that the information of real-life performance of different systems is limited.

In recent years some consumer rating programs have been developed and introduced. In 2003 Folksam and the Swedish Road Administration (SRA) started crash testing of car seats, where each seat is exposed to three different tests. Also the German ADAC started crash testing of car seats using multiple tests for each seat (ADAC website). In 2004 the insurance initiative IIWPG (International Insurance Whiplash Prevention Group) started consumer crash testing in Europe and in the USA (IIHS and Thatcham websites). In those tests each seat was exposed to one test. Studies of the correlation between crash test results and real-life performance is rare.

Objectives of the study

The objective was to study the influence of various types of car seats aimed at protecting whiplash injuries on real-life injury outcome. Furthermore, the objective was to study correlation between whiplash consumer crash tests and real-life injury outcome. In both cases the influence on long-term whiplash symptoms were studied.

METHOD/MATERIAL

The study was based on two different data sources. To calculate the proportion of injuries leading to long-term symptoms all whiplash injuries in rear-end crashes reported to the insurance company Folksam between 1998 and 2006 were used. In total 6383 reported whiplash injuries were included. To calculate relative risk of an injury in rear-end crashes all two-car crashes reported by the police between 1998 and 2006 were used, in total 15587 crashes.

Injury classification

Claims reports including possible medical journals for all crashes with injured occupants between 1998 and 2006 were examined. Whiplash injuries reported in rear-end crashes within a range between +/-30 degrees from straight rear-end were noted.

Insurance claims were used to verify if the reported whiplash injuries led to long-term symptoms. Occupants with long-term symptoms were defined as those where a medical doctor examined the occupant and the occupant claimed injury symptoms for more than 4 weeks, which corresponds to a payment of at least 2000 SEK in the claims handling process used by Folksam. Out of the 6383 persons reporting a whiplash injury, 912 (13%) led to long-term symptoms according to that definition.

Calculation of relative injury risk

According to Evans (1986), when two cars collide with each other, the injury risk for Car 1 in relation to Car 2 can be expressed as the number of injured occupants in Car 1 in relation to the number in Car 2. This is equal to the risk of injury in car 1 in relation to the risk of injury in Car 2, which can be denoted as p_1 / p_2. Assuming that the probabilities p_1 and p_2 are independent, and that the injury risk in Car 2 can be expressed as the injury risk in Car 1 multiplied by a constant, four cases can be summed: x_1, x_2, x_3 and x_4. The relative injury risk in the whole range of impact severity is equal to equation (1). In this study the relative

injury risk for the sum of all cars in each group studied was calculated.

In a similar way the relative risk of injury in rear-end crashes can be calculated with the same technique, where the number of crashes with injured drivers in the struck car in rear-end crashes in relation to the number of crashes with injured drivers in the striking car are summed, see Table 1. The method used in this study to calculate relative injury risk has been further described by Hägg et al. (1992) and Hägg et al (1999).

The initially presented method is relevant for cars of similar mass. If Car 1 and Car 2 have unequal mass, the exposure to impact severity will be unequal as well. While crashworthiness rating based on real-life experience should preferably show the benefit or dis-benefit of mass, the current method would give too much attention to mass, as it would also include the benefit or dis-benefit for the colliding partner. When calculating the injury risk for car models relative to the average car, it is important that the relative injury risk for all car models can be compared with the identical average car. This is not the case if the influence of mass differences on the exposure for the collision partner is not compensated. The initial estimate, equation (1), must therefore be modified to take mass relations into account. The factor *m* was calculated for the car models in each group under study, and thus used to compensate the relative injury risk for the models in each group, see equation (2).

Table 1. Classification of combinations of injured drivers in the struck and striking car in rear-end crashes.

		Drivers in the striking car		Total
		driver injured	driver not injured	
Drivers in the struck car	driver injured	x_1	x_2	$x_1 + x_2$
	driver not injured	x_3	x_4	
Total		$x_1 + x_3$		

x_1 = number of crashes with injured drivers in both cars
x_2 = number of crashes with injured drivers in struck car and not in the striking car
x_3= number of crashes with injured drivers in striking car and not in struck car
x_4= number of crashes without injured drivers in both cars

$$R = (x_1 + x_2) / (x_1 + x_3) \quad (1).$$

$$R_{modified} = R * m^{((M-Maverage)/100)} = (x_1 + x_2) / (x_1 + x_3) * m^{((M-Maverage)/100)} \quad (2).$$

M is the mass of the studied vehicle and $M_{average}$ is the average mass of all vehicles. In these calculations the factor *m* was set as 1.035, see Hägg et al. (1992), which means that the mass effect used to control for the exposure on impact severity was 3.5% per 100 kg. The relative risk of sustaining an injury with long-term symptom was calculated as the product of the relative injury risk and the proportion of occupants with long-term symptoms in relation to the number of reported whiplash injuries.

Categories of cars studied

The whiplash injury and disability risks were calculated for some different categories;

- If the car was fitted with a specially designed whiplash protection system. Those not fitted with whiplash protection system were divided in cars launched before and after 1997.
- Kind of whiplash protection system in cars launched after 1997.
- Performance in the IIWPG ratings.
- Performance in the Folksam/SRA ratings.

The whiplash protections systems defined are RHR-Reactive Head Restraint, WhiPS (Volvo) and WIL (Toyota). Cars with seats fitted with RHR were divided into Saab RHR and RHR in the other manufacturers. Standard seats were defined as those not fitted with any of the systems mentioned above. A group with standard seats tested in consumer ratings was also compared.

RESULTS

A summary of the results is presented in Table 2. Detailed number of crashes and injured for the calculation of relative injury risk is presented in Table 3 in the Appendix.

Cars fitted with more advanced whiplash protection systems had approximately 50% lower proportion of whiplash injuries leading to long-term symptoms as cars with standard seats launched after 1997. Also, the relative risk of a sustaining a whiplash injury leading to long-term symptoms was approximately 50% lower in cars fitted with more advanced whiplash protection systems than in cars

with standard seats launched after 1997. Compared with cars launched before 1997 with standard seats the difference was even higher.

It was also found that cars with RHR, WhiPS or WIL, all had lower risk of whiplash injuries leading to long-term symptoms compared with cars with standard seats. Saab cars with RHR showed lower whiplash injury risk than the group of cars with RHR seats from other manufacturers.

Standard seats tested in consumer ratings had lower whiplash injury risk than other standard seats.

A correlation was found between both IIWPG and Folksam/SRA ratings and proportion of injuries leading to long-term symptoms as well as for relative risk of sustaining a whiplash injury leading to long-term symptoms. Car seats rated in the worst group (Red) in the Folksam/SRA crash tests had 60% higher risk of long-term whiplash injury risk than car seats rated in the best group (Green+). Cars rated in the worst group (Poor) in the IIWPG crash tests had 43% higher risk compared with cars seats rated in the best group (Good).

Table 2. Proportions of injuries with long-term symptoms, relative injury risk in rear-end crashes and relative risk of a whiplash injury with long-term symptoms.

		Whiplash injuries leading to long-term symptoms			Relative injury risk in rear-end crashes		Relative risk of long-term symptoms
Type of study		Reported whiplash injuries (n)	Injuries leading to disability (n)	Proportion of injuries leading to disability (p_{dis})	Number of crashes	Relative injury risk (R)	Relative risk of disability (R* p_{dis})
Special whiplash protection system	Cars with a system	534	40	7,5%	1216	0,977	0,073
	Standard seats 97-	1571	213	13,6%	2488	1,051	0,143
	Standard seats -97	4109	635	15,5%	11883	0,970	0,150
Kind of whiplash protection system (Car models from model year 1997)	RHR	165	10	6,1%	433	1,11	0,067
	Saab RHR	114	6	5,3%	341	0,98	0,052
	Other RHR	51	4	7,8%	92	1,04	0,081
	WhiPS	89	6	6,7%	631	0,95	0,064
	WIL	264	20	7,6%	125	1,10	0,083
	Std seats tested in consumer ratings	196	20	10,2%	368	1,06	0,108
	Other std seats	1366	194	14,2%	2125	1,04	0,148
IIWPG rating	Good	253	17	6,7%	1083	0,95	0,064
	Acceptable	52	3	5,8%	49	1,24	0,071
	Marginal	86	5	5,8%	105	1,21	0,070
	Poor	205	18	8,8%	235	1,04	0,092
	Not tested seats	5615	836	14,9%	14107	0,98	0,146
Folksam/SRA rating	Green+	140	8	5,7%	729	0,98	0,056
	Green	314	21	6,7%	1089	0,98	0,066
	Yellow	77	4	5,2%	60	1,30	0,068
	Red	23	2	8,7%	40	1,03	0,089
	Not tested seats	5798	857	14,9%	14392	0,99	0,147

DISCUSSION

Whiplash injuries leading to permanent disability are serious and account for the vast majority of injuries leading to permanent disability (Nygren 1984, Krafft 1998). Many initiatives to reduce the problem have been taken, where most car manufacturers also include whiplash protection in their designs of new models (Lundell et al 1998, Wiklund and Larsson 1998). Many are also introducing more advanced whiplash protection systems in their models. Measuring the performance of recent introduced whiplash prevention technology is very important for future activities in legislation and consumer testing, such as EuroNCAP. In recent years many initiatives of consumer rating system aimed at measuring neck injury risk in rear-end crashes have been launched. But the correlation between real-life whiplash injury outcome and results from these consumer rating programmes has to date not been presented.

Existing consumer crash testing is focussed the seat performance since the seat plays a major role in protecting the occupants from whiplash injury. This approach is probably relevant in today's situation, where the seat plays a major role for the

whiplash injury risk, but since real-life outcome concerns the performance of the whole car, the results could be influenced by the difference.

The definition of long-term symptoms used in this study was chosen because it takes several years, sometimes up to 6 years, until a degree of permanent disability can be finally set and verified according to the system used by the insurance companies in Sweden (Försäkringsförbundet 1996). To be able to use this definition crashes older than 6 years can only be used, which is not applicable to study whiplash preventive systems introduced the latest 6 years.

Due to the limited number of crashes and injured it was not possible to study the performance of single car models, only groups of cars. All various car models fitted with reactive head restraints (RHR) may have different performance in real-life crashes. In this study it was only possible to study the difference between Saab RHR and RHR for other manufacturers, such as Audi, Ford, Nissan, Opel and VW. No major difference between these could be verified.

The results from this study is very positive and show that efforts made by car manufacturers to reduce whiplash injury risks has been successful, although there are still potential improvements to make. It is also positive that test results from consumer test programmes correlate with real-life performance. Also in this case there are still potential improvements to make to better mirror real-life injury risks. There is always a need to verify crash test results with results from real-world crashes.

Results from existing consumer crash test programmes indicate a large variation in protection. Some seats perform well even without more advanced whiplash protection systems, while some seats fitted with for example RHR received poor rating results. Identifying that a seat has a whiplash protection device is not enough. It stresses the need for consumer test programmes to be used as guidance for consumers in picking the best cars and it also stresses the need for validation of their performance in real-life crashes.

Finally, it is important to stress that further efforts should be made to improve car seats and also other safety technology to reduce whiplash injuries leading to permanent disability. Although the attempts made so far reduces the whiplash injury risk a lot, there is still a long way to go. In modern cars, whiplash injury accounts for approximately 70 % of all injuries leading to disability (Folksam 2005). Even if half of the whiplash injuries in rear-end crashes could be avoided, whiplash is still the most dominating injury leading to permanent disability.

CONCLUSIONS

- Cars fitted with advanced whiplash protection systems had 50% lower risk of whiplash injuries leading to long-term symptoms compared with standard seats launched after 1997.
- The whiplash prevention systems, RHR (Reactive Head Restrains), WhiPS or WIL, had lower risk of whiplash injuries leading to long-term symptoms compared with standard seats launched after 1997.
- A correlation was found between consumer crash test programmes and real-life whiplash injury outcome. Cars with seats rated as good in the consumer crash tests had lower risk of whiplash injuries leading to long-term symptoms compared with seats with poor results.

REFERENCES

ADAC website: www.adac.de

Evans L (1986) Double pair comparison – a new method to determine how occupant characteristics affect fatality risk in traffic crashes. *Accid. Anal. and Prev*., Vol. 18, No. 3:pp 217-227.

Folksam (2005) How safe is your car? 2005. www.folksam.se or Folksam Research 10660 Stockholm Sweden.

Försäkringsförbundet (1996) Gadering av medicinsk invaliditet –96 (only in Swedish). IFU Utbildning AB, Stockholm Sweden.

Hägg A, v Koch M, Kullgren A, Lie A, Nygren Å, Tingvall C (1992) Folksam Car Model Safety Rating 1991-92, Folksam Research 106 60, Stockholm, Sweden.

Hägg A, Krafft M, Kullgren A, Lie A, Malm S, Tingvall C, Ydenius A (1999) Folksam Car Model Safety Ratings 1999, Folksam Research 106 60, Stockholm, Sweden.

IIHS website: www.iihs.org

Jakobsson L (1998) Automobile Design and Whiplash Prevention. In: Whiplash Injuries: Current Concepts in Prevention, Diagnoses and Treatment of the Cervical Whiplash Syndrome. Edited by Robert Gunzberg, Maerk Szpalski, Lippincott-Raven Publishers, pp. 299-306, Philadelphia.

Jakobsson L. Whiplash Associated Disorders in Frontal and Rear-End Car Impacts. Biomechanical. Thesis for the degree o doctor of philosophy. Crash Safety Dividson , Dep of Machine and Vehicle Systems. Chalmers University of Technology, Sweden 2004.

Kommunkationsdepartementet (1997) På väg mot det trafiksäkra samhället, DS 1997:13, (English short version: En Route to a Society with Safe Road Traffic, Selected extract from Memorandum prepared by the Ministry of Transport and Communications, DS 1997:13), Stockholm.

Kraftt M (1998) Non-Fatal Injuries to Car Occupants - Injury assessment and analysis of impacts causing short- and long-term consequences with special reference to neck injuries, Thesis, Karolinska Institutet, Stockholm, Sweden.

Krafft M, Kullgren A, Lie A, Tingvall C (2003) Utvärdering av whiplashskydd vid påkörning bakifrån – verkliga olyckor och krockprov. ("Evaluation of whiplshprotection systems in rear-end collisions – real-life crashes and crash tests"). Folksam and SRA, Folksam research 10660 Stockholm, Sweden.

Lundell B, Jakobson L, Alfredsson B, Lindström M, Simonsson L (1998) The WHIPS seat – A car seat for improved protection against neck injuries in rear end impacts. Paper No 98-S7-O-08, Proc. 16th ESV Conf, 1998, pp. 1586-1596.

Nygren Å (1984) Injuries to car occupants – some aspects of the interior safety of cars. Akta Oto-Laryngologica, Supplement 395. Almqvist & Wiksell, Stockholm. Sweden. ISSN 0365-5237.

Nygren Å, Gustavsson H, Tingvall C (1985) Effects of Different Types of Headrests in Rear-end Collisions. Proc. of the 9th ESV conf. Oxford, UK. pp85-90

Sekizuka M (1998) Seat Designs for Whiplash Injury Lessening, Proc. 16th Int. Techn. Conf. on ESV, Windsor, Canada.

Thatcham website: www.thatcham.org

Viano D and Olsen S (2001) The Effectiveness of Active Head Restraint in Preventing Whiplash. The Journal of TRAUMA Vol 51:pp959-969.

Whiplashkommissionen (2003) (Swedish whiplash commission) www.whiplashkommissionen.se.

Wiklund K, Larsson H (1997) SAAB Active Head Restraint (SAHR) - Seat Design to Reduce the Risk of Neck Injuries in Rear Impacts, SAE Paper 980297, Warrendale.

APPENDIX

Table 3. Numbers of crashes with different combinations of injured occupants and relative injury risks in rear-end crashes.

		No. crashes	X_1	X_2	X_3	R	m	$R_{modified}$
Cars with and without whiplash protection	Seats with whiplash system	1216	351	461	501	0,95	1,03	0,98
	Standard seats from MY 1997	2488	711	1075	952	1,07	0,98	1,05
	Standard seats until MY 1997	11883	3093	5013	4986	1,00	0,97	0,97
Type of whiplash device	RHR	433	140	157	172	0,95	1,17	1,11
	Saab RHR	341	117	116	133	0,93	1,05	0,98
	Other RHR	92	23	41	39	1,03	1,00	1,04
	WHIPS	631	160	238	273	0,92	1,03	0,95
	WIL	125	43	53	39	1,17	0,94	1,10
	Standard seats tested 97-	368	96	170	149	1,09	0,98	1,06
	Other standard seats 97-	2125	618	912	807	1,07	0,97	1,04
IIWPG rating	Good	1083	306	400	459	0,92	1,03	0,95
	Acceptable	49	13	25	17	1,27	0,97	1,24
	Marginal	105	24	56	41	1,23	0,98	1,21
	Poor	235	76	97	86	1,07	0,98	1,04
	Good+Acc	1132	319	425	476	0,94	1,03	0,97
	Marg+Poor	340	100	153	127	1,11	0,98	1,09
	Not tested	14107	3724	5969	5830	1,02	0,97	0,98
Folksam/SRA rating	Green+	729	181	193	226	0,92	1,06	0,98
	Green	1089	293	279	332	0,92	1,07	0,98
	Yellow	60	17	22	12	1,34	0,97	1,30
	Red	40	16	9	9	1,00	1,03	1,03
	Above average	1099	295	285	333	0,92	1,03	0,95
	Below average	90	31	25	19	1,12	0,95	1,07
	Not tested	14392	3800	6115	5942	1,02	0,97	0,99
Total		15587	4155	6549	6438	1,01	0,99	1,00

REVIEW OF EXISTING INJURY CRITERIA AND THEIR TOLERANCE LIMITS FOR WHIPLASH INJURIES WITH RESPECT TO TESTING EXPERIENCE AND RATING SYSTEMS

Klaus Bortenschlager
PDB – Partnership for Dummy Technology and Biomechanics, Germany
Markus Hartlieb
DaimlerChrysler AG, Germany
Karl Barnsteiner
BMW AG, Germany
Leonhard Ferdinand
Dr. Ing. h.c. F. Porsche AG, Germany
David Kramberger
Audi AG, Germany
Sven Siems
Volkswagen AG, Germany
Markus Muser
AGU Zürich, Switzerland
Kai-Uwe Schmitt
AGU Zürich, Switzerland, and
University and ETH Zürich, Switzerland
Paper Number 07-0486

ABSTRACT

In the recent years, a large effort has been directed towards the investigation of injury mechanisms and injury tolerance criteria related to whiplash associated disorders (WAD). Nevertheless, many questions, especially related to injury criteria and their respective biomechanical tolerance levels, remain unresolved. With the introduction of consumer tests in which the protection potential of seats against WAD is evaluated, a discussion of the criteria used for these ratings is needed, since for most proposed WAD injury criteria, e.g. NIC, Nkm, no widely accepted tolerance levels or even accurate injury risk curves are available today. One of the often disregarded points in the tolerance limit discussions is the fact that most injury criteria values have a non-linear relation to injury risk. Many tolerance levels for criteria related to injuries other than WAD (such as HIC, Nij, TTI, TI etc.) were derived using highly non-linear logistic regression curves. The biomechanical loads discussed in conjunction with WAD, e.g. accelerations, forces, torque, are generally very low in comparison to loads acting in other crash situations. Therefore, even minor changes in a test set-up may result in significant changes in the loads measured. Furthermore, issues of repeatability and reproducibility become more important in these low-load test conditions.
A series of sled tests was conducted to assess the influence of several test parameters on the repeatability of results obtained with the BioRID-IIg Dummy. The sled tests were performed according to the test procedure proposed by EuroNCAP. The results show that some criteria like the neck shear force exhibit variations up to 30%. The influence of such deviations has to be considered when introducing a reliable rating system for WAD.

INTRODUCTION

Soft tissue neck injuries as sustained in rear-end collisions are still a major concern in road traffic safety. Despite the various research that was undertaken in the last years the underlying injury mechanism is biomechanically not yet fully understood. Nevertheless, several injury predictors are proposed. Some of these show good correlations with real world accident studies and therefore seem suited to assess the injury risk. However, due to the complex nature of the injury, even for those criteria uncertainties remain with respect to the threshold values suggested. Since accurate injury risk curves are often not available, it is difficult to clearly define a threshold value which can reliably be regarded as a limit for injury.
Despite these uncertainties, there are indications that an improved seat design reduces WAD. Therefore, attempts are made to encourage manufactures to improve seat design. One way to achieve this, is the adoption of seat tests in consumer rating-programs. Consequently, evaluating the performance of seats with regard to WAD is currently widely discussed. Several studies showed that sled tests seem a suitable method to investigate the behaviour of a seat in low speed rear-impact [e.g. 1, 2]. Additionally, static measurements (geometric head-restraint assessment) as defined by several organizations aim in improving head restraint geometry.
In this study the repeatability of seat assessment using static and dynamic tests is investigated. Furthermore, by applying a rating scheme, the influence of data variations on rating results is demonstrated.

MATERIALS & METHODS

To evaluate different injury criteria, a series of tests consisting of static as well as dynamic tests (i.e. sled tests) were performed. One current car seat model from a high volume car manufacturer was chosen. All tests were conducted by using this seat model. This seat does not feature any (re-)active system to prevent WAD. For each sled test, a new seat was used, i.e. no seat was loaded twice. The head restraint was positioned identically for all tests (head restraint was locked in mid-height position) and the seat back angle was always adjusted to a 25° ±0.2° torso line measured by SAE-J826 H-Point Manikin.
A BioRID-IIg dummy of the latest build level was used throughout this study and certified prior and after the test series. The dummy was seated according to IIWPG procedure [3].

Static tests

Prior to each sled test, static measurements were taken to determine the head restraint height and the backset (i.e. the horizontal head to head restraint distance). The data was acquired and recorded as described in the IIWPG geometry measurement technique [3] using a SAE H-Point machine according to SAE-J826 equipped with the Head Restraint Measuring Device (HRMD).

Sled tests

Dynamic testing was performed using a HyperG220 acceleration-sled on which the seats were rigidly mounted. All seats were adjusted in the same way. The BioRID-IIg was instrumented according to IIWPG [3].

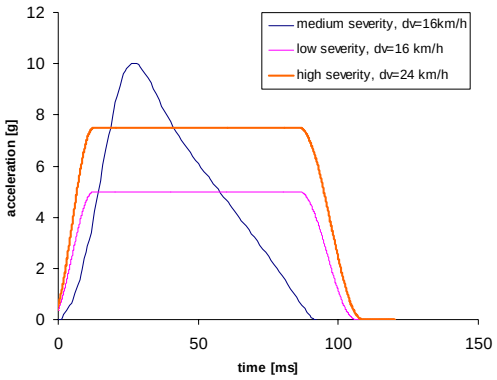

Figure 1. Crash pulses used in the sled tests.

A total of 18 sled tests were conducted using three different crash pulses (Figure 1).

- Pulse 1: low severity pulse, trapezoid, 16 km/h delta-v
- Pulse 2: medium severity pulse, triangular, 16 km/h delta-v
- Pulse 3: high severity, trapezoid-pulse, 24 km/h delta-v

The 18 tests were performed as 6 series whereas each series uses each pulse once (Table 1).

Table 1. Test matix. A total of 18 tests grouped in 6 series were performed.

Test No.	Pulse severity	Series No.
PDB07002	low	1
PDB07001	medium	1
PDB07003	high	1
PDB07004	low	2
PDB07005	medium	2
PDB07006	high	2
PDB07007	low	3
PDB07008	medium	3
PDB07009	high	3
PDB07010	low	4
PDB07011	medium	4
PDB07012	high	4
PDB07017	low	5
PDB07018	medium	5
PDB07019	high	5
PDB07020	low	6
PDB07021	medium	6
PDB07022	high	6

The following measures and neck injury predictors, respectively, were evaluated: NIC [5], Nkm [6], time until dummy head first contacts head restraint (time to head restraint contact), T1-acceleration in x-direction (T1x), rebound velocity, neck shear force (Fx), and neck axial force (Fz).
NIC considers the relative acceleration between head and torso and is derived as shown below.

$$NIC(t) = 0.2m \cdot a_{rel}(t) + (v_{rel}(t))^2 \quad (1)$$

Nkm is calculated by taking into account the neck shear force (Fx) as well as the flexion/extension moment (My).

$$N_{km}(t) = \frac{F_x(t)}{F_{\text{int}}} + \frac{M_y(t)}{M_{\text{int}}} \qquad (2)$$

Head restraint contact time was measured by using contact foils. The rebound velocity was derived by film analysis. The maximum rebound-velocity was determined starting at the point in time when the head motion is changing its direction from the rearward to a forward movement. The maximum values of the other criteria were considered from time T0 until the head leaves the head restraint.

Rating system

In general a rating system for assessing the risk of injury for car occupants should be based on biomechanical facts. It should be able to differentiate between high and low injury risk. To obtain usable as well as comparable results it is important to gain robust data with a high level of repeatability and reproducibility. Several rating systems for assessing WAD in low speed rear-impact are already introduced (e.g. IIHS, Thatcham, Folksam, ADAC). EuroNCAP is also planing to implement a new WAD test procedure in their existing occupant rating [4, 7].

This study is based on this proposed EuroNCAP WAD rating system. It consists of two parts, static (geometric) measurements and dynamic sled tests.
For the static tests, the backset and head restraint height were rated according to the limits given in Table 3. Scores range from -1 to +1; a sliding scale was used.
As for the results of the sled tests, Table 4 illustrates the higher and lower performance limits used for the rating. For results in between the higher and lower limits, a sliding scale was used to obtain the score. Each parameter in the dynamic tests can reach a maximum score of 0.5 points. The overall score of a single dynamic test is the sum of the score of NIC, Nkm, rebound velocity, Fx, Fz plus the highest score from either T1x or head contact time i.e. for one pulse a maximum of 3 points is possible.
For the final rating, the worst score of all 3 static measurements (i.e. 3 seats) of one series is added to the points received for all 3 pulses in the dynamic part.

RESULTS

The static evaluation measured by the SAE-Manikin with HRMD of all 18 tests showed a x-value of 45.4 mm (min. 42 mm / max. 52 mm) and a z-value of 37.0 mm (min. 35 mm / max. 39 mm) on average. The BioRID-IIg backset for these tests was 59.0 mm on average (min. 57 mm / max. 60 mm).
The repeatability of the delta-v values reached in the dynamic tests is presented in Table 4. It shows that the delta-v values were generally achieved with high accuracy which results in a low standard deviation.
The results obtained for the parameters determined in the sled tests are summarized in Figures 2 to 9 and Table 6. A repeatability analysis was conducted using the coefficient of variation (CV) method. The CV is defined as the standard deviation (SD) of the measured values divided by the sample mean, and is expressed as a percentage [10]. The repeated responses were assessed by applying the rating scale according Table 2 [11].

Table 2. Rating scale to assess repeatability.

CV = 3%	3% < CV = 7%	7% < CV = 10%	CV > 10
good	acceptable	marginal	not acceptable

It can be seen that T1 acceleration (T1x), head contact time, axial neck force (Fz) and rebound velocity show good to acceptable coefficient of variations (CV). NIC and Nkm, which are derived from basic measures by calculation show a larger CV (marginal to not acceptable). The largest CV, however, was found for the neck shear force (Fx) (not acceptable). This findings corresponds to previous studies [9].

Table 3. Threshold values used for evaluating the static tests.

	Lower performance limit	Higher performance limit
Backset [mm]	30	90
Height [mm]	0	80

Table 4. Preliminary threshold values used for evaluating the dynamic tests [7].

	Lower performance limit	Higher performance limit
Low severity pulse		
NIC [m2/s2]	9	15
Nkm [-]	0.12	0.35
Rebound velocity [m/s]	3.00	4.40
Fx (upper neck shear) [N]	30	110
Fz (neck axial) [N]	270	610
T1 x-acceleration [g]	9.4	12.0
Time head restraint contact [ms]	55	77
Medium severity pulse		
NIC [m2/s2]	11	24
Nkm [-]	0.15	0.55
Rebound velocity [m/s]	3.2	4.8
Fx (upper neck shear) [N]	30	190
Fz (neck axial) [N]	360	750
T1 x-acceleration [g]	9.3	13.1
Time head restraint contact [ms]	51	76
High severity pulse		
NIC [m2/s2]	13	23
Nkm [-]	0.22	0.47
Rebound velocity [m/s]	4.1	5.5
Fx (upper neck shear) [N]	30	210
Fz (neck axial) [N]	470	770
T1 x-acceleration [g]	12.5	15.9
Time head restraint contact [ms]	48	75

Table 5. Delta-v values produced. For each pulse 6 tests were performed.

Pulse	Average delta-v [km/h]	SD [km/h]	CV [%]
1 (low)	15.9	0.3	1.8
2 (medium)	15.7	0.3	2.2
3 (high)	24.1	0.2	0.9

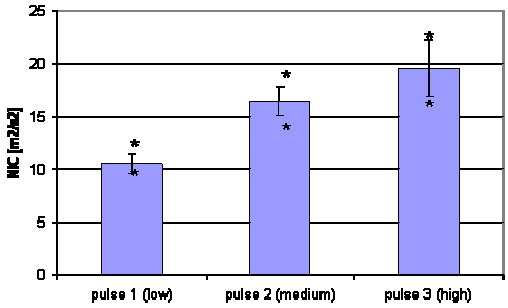

Figure 2. NIC values. Error bars denote one standard deviation (SD). Stars represent the minimum and maximum value. For each pulse 6 tests were performed.

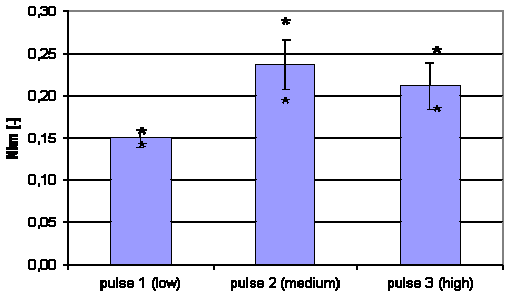

Figure 3. Nkm values. Error bars denote one standard deviation (SD). Stars represent the minimum and maximum value. For each pulse 6 tests were performed

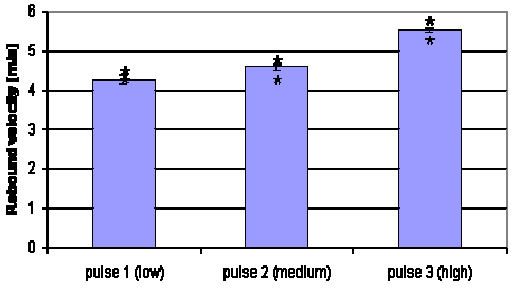

Figure 4. Rebound velocities. Error bars denote one standard deviation (SD). Stars represent the minimum and maximum value. For each pulse 6 tests were performed

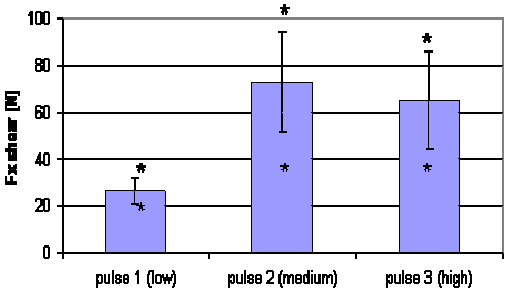

Figure 5. Neck shear forces. Error bars denote one standard deviation (SD). Stars represent the minimum and maximum value. For each pulse 6 tests were performed

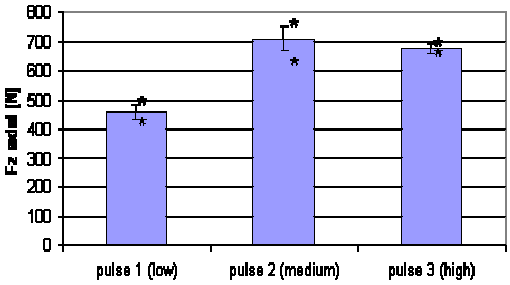

Figure 6. Neck axial forces. Error bars denote one standard deviation (SD). Stars represent the minimum and maximum value. For each pulse 6 tests were performed

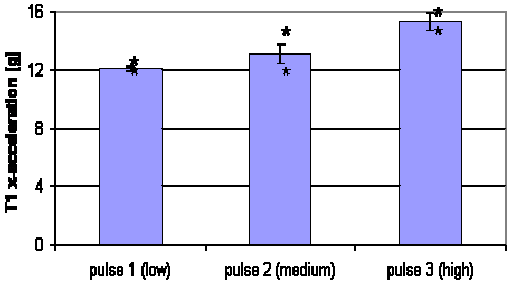

Figure 7. T1 x-acceleration. Error bars denote one standard deviation (SD). Stars represent the minimum and maximum value. For each pulse 6 tests were performed

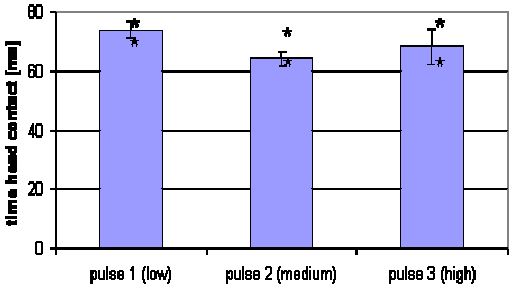

Figure 8. Time to head restraint contact. Error bars denote one standard deviation (SD). Stars represent the minimum and maximum value. For each pulse 6 tests were performed

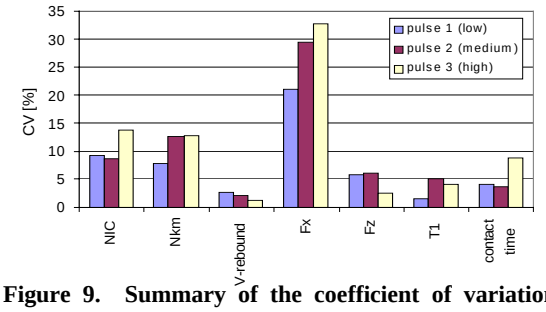

Figure 9. Summary of the coefficient of variation (CV) for all parameters and all pulses.

Table 6. Sled test results. For each pulse 6 tests were conducted.

	Average	Min. Max.	SD	CV [%]
Low severity pulse				
NIC [m2/s2]	10.52	9.73 12.05	0.97	9.18
Nkm [-]	0.15	0.14 0.16	0.01	7.68
Rebound velocity [m/s]	4.28	4.12 4.48	0.12	2.76
Fx (upper neck shear) [N]	26.37	19.17 35.24	5.55	21.04
Fz (neck axial) [N]	456.50	427.00 497.00	26.33	5.77
T1 x-acceleration [g]	12.13	11.82 12.31	0.18	1.45
Time head restraint contact [ms]	73.95	70.0 77.9	2.99	4.05
Medium severity pulse				
NIC [m2/s2]	16.38	14.31 18.52	1.72	10.50
Nkm [-]	0.23	0.19 0.28	0.03	14.02
Rebound velocity [m/s]	4.56	4.45 4.67	0.08	1.83
Fx (upper neck shear) [N]	69.13	36.80 82.30	19.26	27.86
Fz (neck axial) [N]	703.33	622.00 753.00	46.06	6.55
T1 x-acceleration [g]	12.91	11.90 13.65	0.61	4.69
Time head restraint contact [ms]	64.23	61.00 69.00	2.89	4.49
High severity pulse				
NIC [m2/s2]	19.56	15.95 23.36	2.70	13.83
Nkm [-]	0.21	0.18 0.25	0.03	12.73
Rebound velocity [m/s]	5.52	5.44 5.62	0.07	1.23
Fx (upper neck shear) [N]	65.12	35.97 92.30	21.21	32.57
Fz (neck axial) [N]	675.00	644.00 694.00	17.23	2.55
T1 x-acceleration [g]	15.33	14.52 16.10	0.62	4.08
Time head restraint contact [ms]	68.42	62.0 76.0	6.02	8.80

Finally the results were rated according to the scoring system described above. Table 7 summarizes the scores obtained for the static as well as the dynamic tests. The results of the final scores, i.e. adding the worst static and all three dynamic scores for each series, are presented in Table 8.

As an example the final score of series 1 was obtained by adding the scores of the dynamic tests for the 3 different pulses (right column in Table 7) and the worst value of the corresponding static test (middle column in Table 7):

Score dyn. test 1 – low severity pulse	1.80
+ Score dyn. test 1 – medium severity pulse	1.84
+ Score dyn. test 1 – high severity pulse	1.48
+ Score static test 1 – worst value	0.05
Final score series 1	5.17

Table 7. Scores according to the proposed rating system for the static and dynamic tests.

Number of series	Score static test	Score dynamic test
Low severity pulse		
1	0.05	1.80
2	0.10	1.63
3	0.08	1.67
4	0.10	1.48
5	0.05	1.63
6	0.08	1.71
Average	*0.08*	*1.66*
CV %		*6.36*
Medium severity pulse		
1	0.10	1.84
2	0.05	1.62
3	0.05	1.41
4	0.08	1.08
5	0.08	1.33
6	0.08	1.38
Average	*0.07*	*1.44*
CV %		*18.50*
High severity pulse		
1	0.05	1.48
2	0.10	1.44
3	0.10	1.76
4	0.02	1.38
5	0.08	1.24
6	0.10	1.05
Average	*0.08*	*1.39*
CV %		*17.06*

Table 8. Final scores of the 6 test series.

	Final score
series 1	5.17
series 2	4.74
series 3	4.89
series 4	3.96
series 5	4.25
series 6	4.22
Maximum	*5.17*
Minimum	*3.96*
Average	*4.57*
SD	*0.47*
CV [%]	*10.27*

DISCUSSION

In order to investigate the repeatability of the seat assessment procedure according the EuroNCAP proposal [4, 7], a series of sled tests were performed. All tests of this study were conducted with the same seat model whereas for each test a new seat was used. A 3-pulse approach according to the EuroNCAP proposal was applied. Different delta-v values (16 km/h and 24 km/h) as well as different pulse shapes (trapezoid and triangular) were used. This means, that for this kind of WAD assessment of a vehicle seat, a test series of 3 single tests with 3 different pulses is needed. In our study we repeated this complete assessment procedure 6 times, i.e. 18 sled tests were performed (cf. Table 1).
Similarly to the work by Adalian et al. (2005), it could be shown that all crash pulses can be reproduced with sufficient accuracy. The delta-v values for all pulses of this study were achieved with small deviations only.
An important condition was to ensure, that all 18 tests were performed in a very accurate way. Particularly the seat adjustment and the positioning of the BioRID-IIg dummy were set only with less tolerances. The seat back angle was adjusted within a range of 25° +/-0.2° (torso angle of SAE-Manikin). The accuracy in pelvis angle was 26.5° +/-0.3° and the H-Point of the BioRID-IIg was also in a small range of +/-0.3 mm relative to a fixed reference-point. The static measurements (head rest geometry) performed with the HRMD result in a range for the x-value from 42 mm to 52 mm. This was in line with previous studies [9]. The z-values measured by HRMD were within 35 mm to 39 mm. It is well-known, that the backset of the BioRID head has an important influence on the measurements in sled testing. Therefore, we kept this backset as constant as possible. In all of the 18 tests the BioRID-IIg backset was within 57 mm to 60 mm.
All these conditions were important and necessary for this study. To detect changes in the dummy performance, particularly due to tests with the high severity pulse, the dummy was calibrated after the complete test series. Comparing these results with the pre-test calibration did not indicate any changes in the dummy properties.

In a first step the measurements were analysed. In a second step the repeatability of the complete seat assessment method according to the EuroNCAP proposal [4, 7] was investigated.

By comparing the test results between the 3 pulses in detail, it was found that the head-contact time measured in the medium an high severity pulse are almost in the same range whereas the contact time in the low severity pulse is slightly higher on average.
T1x and the rebound velocity show for the low and medium pulse similar values whereas for the high severity pulse the measurements were about 10% to 20% increased.
A significant difference was found in the neck tension force (Fz). The results from medium pulse show the largest deviations (622 N to 753 N) with an average value of 703 N. A surprising result was, that the average value of the high severity pulse (675 N) is lower compared to the medium pulse. Whereas the average in neck tension in low severity pulse tests is remarkable lower (457 N) as expected.

The neck-shear force (Fx) shows the worst result in repeatability. The average values of medium and high severity pulse are almost in the same range (69 N / 65 N). Due to the large deviation of the measurements obtained from the medium and the high severity pulse, the ranges are largely overlapping. This demonstrates that the discriminatory power of such a rating system is limited. The values from low severity pulse clearly indicate a less loading, also with a not negligible deviation from 19 N to 35 N.
The deviation of Nkm, which depends on Fx, shows a less deviation compared to Fx. But due to the overlapping range of measurements (0.19 to 0.28 and 0.18 to 0.25 for medium and high), this criteria is also not able to discriminate between medium and high severity pulse. The average Nkm values for medium and high severity pulse are almost the same, whereas the average value for low severity pulse is lower and shows also a reduced deviation (0.14 to 0.16).
The NIC value on average increases with increasing of loading. (10.5 / 16.4 / 19.6 respectively for low- / medium- / high-severity pulse). Also the deviations increase (CV: 9.2% / 10.5% / 13.8%).
Summarizing it was found, that T1 acceleration (T1x), head contact time, axial neck force (Fz) and rebound velocity show good to acceptable

coefficient of variation [CV]. NIC and Nkm which are derived from basic measures by calculation show a larger standard deviation (marginal to not acceptable). The neck shear force (Fx) showed the largest (not acceptable) spread for all pulses. Depending on the type of pulse (low, medium, high), the differences in CV ranged between 20 % to 30%. Particularly with regard to the very accurate way how the test were prepared and performed this poor repeatability especially for Fx is surprising. An obvious reason could not be found.
Furthermore, the deviation in test results can increase even more by conducting tests in different test labs.

In the next step the single measurements were compared according to the proposed sliding scales [Table 4]. This study investigated only one single seat model. Therefore, an assessment of the sliding scales is not possible. By comparing the measured values with the range of the sliding scale, we assume, that the sliding scale for the head contact time in the low severity pulse is too low compared to medium and high severity pulse and should therefore be moved to higher values. But much more important is the fact, that for most of the criteria the ratio of the range of the sliding scale compared to the range of measured values is questionable, i.e. the deviation of the measured values are too large compared to the sliding scales. The range of measured Fx in medium severity pulse test is 37 N to 92 N, whereas the range for the corresponding sliding scale is 30 N to 190 N [Table 4], that means, the range of measured values spread almost over half of the sliding scale. For NIC and Nkm the spread of the measured values is also not sufficient high compared to the range of the corresponding sliding scales.

Finally we investigated and determined the influence of the measured values on the entire rating scheme [4, 7]
By calculation the rating points for the 3 different pulses we achieved an average of 1.66 points (low severity pulse), 1.44 points (medium severity pulse), 1.39 points (high severity pulse). The coefficient of variation for the low severity pulse is good (CV = 6.36%), whereas for the medium pulse (CV = 18.5%) and the high severity pulse (CV = 17.06%) is not acceptable. The total points for the entire seat assessment including the static measurement are on average 4.57 points with a CV of 10%. Even this deviation does not seem to be remarkable, however, the difference between minimum and maximum score is remarkable. The lowest score of the 6 test series was 3.96 points, the highest 5.17 points; which is about +/-13 % deviation to the calculated mean score, or with other words 26 % from the best to the worst result.

There are legitimate questions if with a rating system which offers such a poor repeatability, an objective seat assessment can be made at all. However, a rating system needs a certain robustness in terms of repeatability otherwise it appears unreliable.
Also there are some concerns about the discriminating power, i.e. to rate a seat against an injury related scale in an objective way.
Each rating system for assessing the occupant safety should be related to a biomechanical scale. But even in the field of WAD this biomechanical knowledge is not complete and therefore derived sliding scales are missed. Nevertheless, at this point we will briefly discuss the biomechanical background. The use of different threshold values for lower and higher performance limits and sliding scales is difficult to understand from a biomechanical point of view. If a criterion is regarded as a predictor for injury, it is assumed that a certain loading results in a corresponding injury risk. Usually biomechanical experiments are the basis on which injury criteria and injury risk curves are defined. In most cases these curves are non-linear and the injury criteria are derived by statistical means (e.g. non-linear regression). Goldsmith and Ommaya (1984), for example, performed several volunteer experiments and derived corresponding threshold diagrams for neck extension/flexion moments as well as for neck shear and axial forces. None of their diagrams shows a linear correlation. Therefore doubts arise with respect to the use of (linear) sliding scales since an evaluation based thereon has hardly any relation to the biomechanical basis of an injury risk.
Similarly, the absolute values chosen in the rating scheme can be criticized. While Goldsmith and Ommaya (1984) found a threshold value for voluntarily tolerated neck shear forces of 845 N the rating system sets an upper limit for the severe pulse of 210 N which is rather low. In contrast, the values for NIC with which a test would be passed go up to 24 m2/s2 in den medium severity pulse. This is not just a value higher than the most often citied injury threshold of 15 m2/s2 but also not logical since the highest values would be expected for the high severity pulse.
Despite the fact that the lower and higher performance limits might lack a biomechanical foundation, adjusting such limits to different crash pulses by means of scaling is fundamentally wrong. From a biomechanical perspective, changing the limits means shifting the threshold on the underlying injury risk curve. In other words, a rating system with different injury threshold values accepts that the occupant is subjected to a different injury risk at a different pulse. Due to the lack of accurate injury risk curves today, the effect of such a shift can not be assessed.

In our paper we criticized the poor repeatability of Fx, at this point we will give an example from the biomechanical perspective. If a person lies on his back on a table such that the head is not supported, an estimated shear force of 48 N (4.8 kg head mass) and a moment of torque of 4.8 Nm (10 cm lever, 4.8 kg) acts on the neck. This already gives a roughly estimated Nkm of 0.15. This opens the question if the proposed sliding scales of these criteria are too low in a region far away where WAD related injuries could occur.

CONCLUSIONS

Performing sled tests representing rear-end collisions revealed that the accuracy with which currently discussed neck injury criteria can be obtained varies between 1.2% and 33%. Since the biomechanical loads discussed in the field of WAD are generally very low in comparison to loads acting in other crash situations, even minor changes in a test set-up may result in significant changes in the loads measured. Consequently, the spread of data increases.

Main Findings

- The neck shear force (Fx) exhibits a “not acceptable” repeatability score for all 3 pulses conducted.

- NIC and Nkm show a “marginal coefficient of variation (CV) in the low severity pulse. However, in the medium and the high severity pulse the CV for NIC and Nkm turn into the “not acceptable” range.

- Although the deviations of most of the single criteria of all 3 pulses are similar. The scoring of the low severity pulse (CV = 6.36%) show less deviation in contrast to the medium (CV = 18.5%) and the high severity pulse (CV = 17.06%).

Rating systems are necessarily based on such test results. Therefore the scoring system used must be robust enough to account for the spread of the input data. Only a comprehensible and repeatable scoring together with a biomechanical relevance will yield to a strong test procedure. The discriminatory power of the scoring system used here, however, seems to be unsatisfactory. The minimum and maximum scores obtained for testing the same seat varied considerably. Consequently, depending on the definition of the final minimum score requirements, the same seat can fail or pass. This finding illustrates a lack of robustness of the scoring system as it is proposed today.

REFERENCES

[1] Adalin C, Sferco R, Ray P (2005) The repeatibility and reproducibility of proposed test procedures and injury criteria for assessing neck injuries in rear impact, Proc. ESV Conf., Paper No. 05-0340

[2] Bortenschlager K, Kramberger D, Barnsteiner K, Hartlieb M, Ferdinand L, Leyer H, Muser M, Schmitt K-U (2003) Comparison tests of BioRID II and RID 2 with regard to repeatability, reproducibility and sensitivity for assessment of car seat protection potential in rear-end impacts, Stapp Car Crash Journal, 47:473-488

[3] RCAR-IIWPG Seat-Head Restraint Evaluation Protocol (Version 2.5 – Sept. 2006)

[4] EuroNCAP-Dynamic Assessment of Car Seats for Neck Injury Protection (Version 2.3 Final Draft)

[5] Boström O, Svensson M, Aldman B, Hansson H, Håland Y, Lövsund P, Seeman T, Suneson A, Säljö A, Örtengren T (1996) A new neck injury criterion candidate based on injury findings in the cervical spinal ganglia after experimental neck extension trauma, Proc. IRCOBI Conf., pp. 123-136

[6] Schmitt K-U, Muser M, Walz F, Niederer P (2002) Nkm - a proposal for a neck protection criterion for low speed rear-end impacts, Traffic Injury Prevention, Vol. 3 (2), pp. 117-126

[7] Klanner W, ADAC, Presentation given on November 14, 2006 at the EuroNCAP Industry Liaison Meeting

[8] Goldsmith W, and Ommaya A. K, (1984) Head and Neck Injury Criteria and Tolerance Levels, The Biomechanics of Impact Trauma. Eds. B. Aldman and A. Chapon, Amsterdam, The Netherlands, Elsevier Science Publishers, 149–187.

[9] Hartlieb M. on behalf of PDB, Study on Repeatability and Reproducibility of BioRID-Dummy Measurements for Whiplash Assessment, ISO/TC22/SC10/WG1 Document-No. N579

[10] Mertz H, (2004), Calculation Methods & Acceptance Levels for Assessing Repeatability and Reproducibility (R & R), ISO/TC22/SC12/WG5 Document-No. N751

[11] Edmund Hautmann, Risa Scherer, Akihiko Akiyama, Martin Page, Lan Xu, Greg Kostyniuk, Minoru Sakurai, Klaus Bortenschlager, Takeshi Harigae, Suzanne Tylko (2003), Updated Biofidelity Rating of the revised WorldSID Prototype Dummy, ESV Conf., Paper No. 388